Exploring the Binding of Small Guest Molecules in Sodium Deoxycholate Hydrogels

by

Mehraveh Seyedalikhani
B.Sc, University of Tehran, 2006
M.Sc, Iran University of Science and Technology, 2008

A Dissertation Submitted in Partial Fulfillment
of the Requirements for the Degree of

DOCTOR OF PHILOSOPHY

in the Department of Chemistry

Supervisory Committee

Exploring the Binding of Small Guest Molecules in Sodium Deoxycholate Hydrogels

by

Mehraveh Seyedalikhani
B.Sc, University of Tehran, 2006
M.Sc, Iran University of Science and Technology, 2008

Supervisory Committee

Dr. Cornelia Bohne (Department of Chemistry)
Supervisor

Dr. Irina Paci (Department of Chemistry)
Departmental Member

Dr. Matthew Moffitt (Department of Chemistry)
Departmental Member

Dr. Richard Keeler (Department of Physics and Astronomy)
Outside Member

Abstract

Supervisory Committee
Dr. Cornelia Bohne (Department of Chemistry)
Supervisor
Dr. Irina Paci (Department of Chemistry)
Departmental Member
Dr. Matthew Moffitt (Department of Chemistry)
Departmental Member
Dr. Richard Keeler (Department of Physics and Astronomy)
Outside Member

Bile salts are supramolecules with amphiphilic properties. Bile salts form aggregates in aqueous solutions. The primary aggregates of bile salts are hydrophobic and the secondary aggregates which form at higher concentrations are relatively hydrophilic. Among bile salts, sodium deoxycholate (NaDC) has been known to form hydrogels at pHs close to the neutral pH and within a certain concentration range.

The aim of this work was to provide insight into the properties of a NaDC hydrogel as a supramolecular gel system through three different projects. Pyrene is a hydrophobic polycyclic aromatic compound which was used as a fluorescent probe and the guest for these projects. 1,1'-dioctadecyl-3,3,3',3'-tetramethylindodicarbocyanine perchlorate (DiD) is another fluorescent compound which was used as another guest.

The objective of the first project was to understand the mobility of a small guest molecule in NaDC gel in the presence of cucurbit[6]uril (CB[6]) compound as an additive for the gel. Cucurbit[n]urils are macrocyclic compounds with a hydrophobic cavity and two hydrophilic portals. The presence of CB[6] provides another binding site for pyrene in addition to the primary aggregates of the bile salts. The results showed that

the mobility of the guest from water and CB[6] to the bile salts network happens when the temperature is raised. The release of the guest back into the water happens when the gel is cooled.

The objective of the second project was to investigate the effect of surfaces with different hydrophilicity on the NaDC gel properties. The results of fluorescence correlation spectroscopy (FCS) experiments revealed that either the hydrophilicity of the surface does not affect the NaDC gel network or the FCS is insensitive to the structural changes induced by the hydrophilicity of the surface. These experiments depicted that the aggregates involved in the gel's network are the same as those formed in the aqueous solutions. Moreover, results of the steady-state and time-resolved fluorescence experiments showed that the bulk gel properties are not affected by the hydrophilicity of the surface.

The objective of the last project was to determine the effect of ions on NaDC gel properties. The results showed that cations with different charge density have different effects on the gel formation and properties. The presence of inorganic salts with a monovalent cation leads to the formation of a kinetically favored gel sample within a few hours after sample preparation. The extension of the network occurs overtime and a thermodynamically stable gel forms a couple of days after sample preparation.

Table of contents

List of Tables

List of Figures

List of Schemes

List of Abbreviations

Å	angstrom
A_i	pre-exponential factors for species *i*
AFM	atomic force microscopy
API	N-(4-aminophenyl)imidazole
BINOL-terpy-Cu(II)	1,1'-bi-2-naphthol-terpyridine-copper(II)
χ^2	reduced chi-squared parameter
°C	degree Celsius
cmc	critical micellar concentration
cP	centipoise
CB[n]	cucurbit[n]uril
CB[6]	cucurbit[6]uril
CB[7]	cucurbit[7]uril
CB[8]	cucurbit[8]uril
cm	centimeter
Cy5	3H-Indolium, 2-[5-[1-[6-[(2,5-dioxo-1-pyrrolidinyl)oxy]-6-oxohexyl]-1,3-dihydro-3,3-dimethyl-5-sulfo-2H-indol-2-ylidene]-1,3-pentadien-1-yl]-1-ethyl-3,3-dimethyl-5-sulfo-, potassium salt
D	diffusion constant
DAH	1,6-Diaminohexane
demic	demicellization
diethylphosphato	diethylphosphatoethyltriethoxysilane
DiD	1,1'-dioctadecyl-3,3,3',3'-tetramethylindodicarbocyanine perchlorate
ΔH	change in enthalpy
ΔS	change in entropy
ΔG	change in Gibbs free energy
ΔC_p	change in heat capacity
eq	equivalent
FCS	fluorescence correlation spectroscopy
F_i	fractional intensity of emissive species *i*
<*F*>	Mean fluorescence intensity
f	frequency or isomerization fraction
γ_c	critical strain
g	gram
G'	storage modulus
G"	loss modulus
G(0)	initial correlation function
G(τ)	correlation function
Hz	hertz
h	hour

I_0	initial intensity
I	fluorescence intensity
IRF	instrument response function
in	inch
ISO	isomerization
iodo	3-iodopropyltrimethoxysilane
K	association constant or Kelvin
kJ	kilojoule
k_q	quenching rate constant
κ	structure parameter
LED	light emitting diode
LVR	linear viscoelastic regime
LMWG	low molecular weight gelators
M	molar
min	minute
mL	milliliter
mM	millimolar
mm	millimeter
ms	millisecond
MΩ	megaohm
MHz	megahertz
µL	microliter
µM	micromolar
µs	microsecond
µW	microwatt
nm	nanometer
ns	nanosecond
n-decyl	n-decyltriethoxysilane
obs	observed
Osc	oscillatory
ω_{xy}	width of the observation volume
ω_z	height of the observation volume
Pa	pascal
pK_a	acid dissociation constant
Pn	1-pyrenesulfonyl derivatives
RT	room temperature
SAFiN	self-assembled fibrillary network
SDS	sodium dodecyl sulfate
SPC	single photon counter
σ	yield stress
THF	tertrahydrofuran
T_{gs}	gel to sol transition temperature
T_{sg}	sol to gel transition temperature
T	triplet excited state

τ_i	lifetime of emissive species *i*
τ_D	translational diffusion time
τ_T	tripled excited state lifetime
τ_{ISO}	isomerization time
UV	ultra-violet
v	volume
w	weight

Acknowledgments

I would like to express my sincere appreciation to my supervisor Dr. Cornelia Bohne for giving me the opportunity to be a member of her research group and for all her support, motivation and guidance. My gratitude for what I have learned from her can't be expressed in words, not only in the scientific arena but also on the personal level. My deepest gratefulness and humblest respect goes to Luis Netter for all his technical assistance, kindness and support. I am extremely thankful to Suma Susan Thomas for being a fantastic co-worker and for all the joyful moments I experienced with her as a friend.

I would like to thank Dr. Julian Zhu at the University of Montreal for the opportunities to perform rheology measurements in his lab and Dr. Satu Strandman for all her valuable inputs regarding the rheological experiments. I also would like to thank Dr. Robert Godin and Dr. Gonzalo Cosa at McGill University and Regivaldo Gomes and Dr. Alex Brolo at the University of Victoria for their productive collaboration. I also would like to thank my committee members Dr. Irina Paci, Dr. Matthew Moffitt and Dr. Richard Keeler for sharing the knowledge of their area of expertise with me to expand my perspective on my research.

I would like to thank Dr. Denis Fuentealba for helping me to enter the wonderful world of the gels at the beginning of my work. I am also thankful to the current and former members of Bohne's research group for creating a fabulous working environment. I am so thankful to Jenna Erwin for proofreading of my thesis.

My special gratitude goes to my dad and my sisters, Mahkameh and Mahara. Their endless love, support and belief in me are undoubtedly the most valuable gift I have had throughout my life. I also would like to thank my dear uncle, Kazem, and his family for all their support since the moment I landed in Canada.

Finally, I would like to thank Xerox, NSERC and UVic for financial support of my research.

Dedication

To my Mom

For teaching me

RESPECT and PATIENCE

1 Introduction

1.1 Gels

Gels are solid-like materials which do not flow, although they contain a significant amount of liquids in their composition. The liquid component of the gel is normally entrapped in a three dimensional network formed by the assembly of a compound called the gelator. The resulting material shows viscoelastic properties. Viscoelastic behavior of the gels is perhaps the most important property which makes gels into materials that are applied in our daily lives, such as soap and toothpaste, as well as in advanced technologies, such as drug delivery and tissue engineering.[1]

1.2 Gel classifications

Gels can be categorized in different ways. Depending on the size of the gelator molecules, gels could be classified into macromolecular (polymer) gels or supramolecular gels. The building blocks in supramolecular gels normally have a low molecular weight and are known as low molecular weight gelators (LMWG). The gel network can be formed either through physical or chemical interactions when the gelator is a polymer. However, in the case of supramolecular gels only the physical (non-covalent) interactions are involved in the self-assembled fibrillary network (SAFiN). Although, the term SAFiN is widely used for molecular gelators, the network of these gels is not necessarily fibrillar,[2] but the interactions are always non-covalent. The interactions involved in supramolecular gel formation are namely hydrogen bonding, ion-

ion interactions and hydrophobic/solvophobic effects. These interactions are naturally weak. As a result, supramolecular gels are normally weak gels where their formation and deformation can show a high degree of reversibility. In contrast, in the case of polymer gels where the network is formed by covalent bonds, the gel formation is not a reversible process. However, for those polymer gels where the network forms by physical interactions, reversibility can be observed.

A significant percent weight of gels is liquid.[3] Gels can also be classified as hydrogels or organogels based on the solvent that is entrapped in the gel's network. Sometimes a combination of water and an organic solvent[4] is required for the solubilization of the gelator and then the gel formation occurs. For example, Weiss et al. studied the gelation of 1-pyrenesulfonyl derivatives (Pn, where n is the number of methylene units separating the amino groups (Scheme 1.1) in water-THF mixtures. Pn (n is 2, 3, 4, 6, 7 and 8) at 2% w/v is not soluble in either water or THF at room temperature. However, Pn is totally soluble in the mixture of water and THF. The volume ratio between water and THF at which each Pn is entirely soluble is dependent on the number of units n. On the other hand, the gelation of these compounds happens at volume ratios of water and THF for which the compounds are partially soluble. [4]

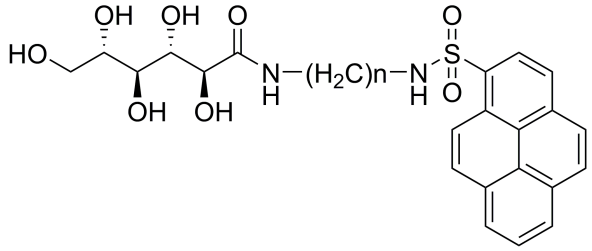

Scheme 1.1. Chemical structure of 1-pyrenesulfonyl derivatives which can form a gel in the mixture of water-THF.

1.3 Effect of additives on the properties of gels

For some gels a third component needs to be added to the solution of the main building block for gel formation to happen. In this case, the compound present in a higher mole fraction is normally considered as the gelator and the one present in a lower mole fraction is called the co-gelator or additive. For these gel systems neither the gelator nor the co-gelator has the ability to form the network when they are used individually. However, a gel forms by using a certain range of molar ratios between the two molecular components.[1] Scheme 1.2.A illustrates this category of the gels.

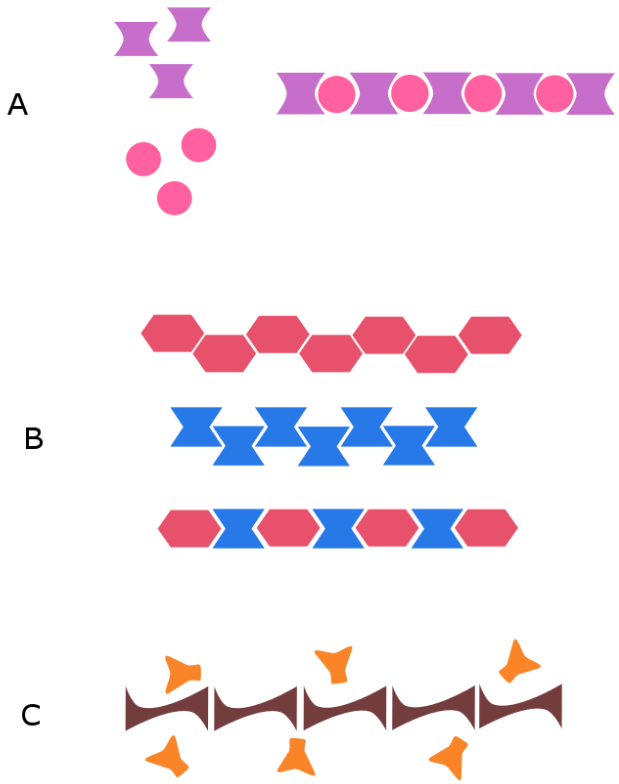

Scheme 1.2. Illustration of the different classes of additives used in surpramolecular gels.

As an example, lithocholic acid (Scheme 1.3, left) is a bile acid with amphiphilic properties. This compound does not form a gel when dissolved in water. Dimeric and oligomeric amines, which are shown in Scheme 1.3 (middle and right), also are not gelators in aqueous solutions. However, addition of lithocholic acid to the aqueous solution of any of these amines and within a certain concentration ratio leads to gel formation.[5] It is interesting that the more polar analogs of lithocholic acid such as cholic acid or deoxycholic acid are not able to gelatinize aqueous solutions of any of the amines shown in Scheme 1.3 and many other amines tested by Bhattacharya and co-workers.[5]

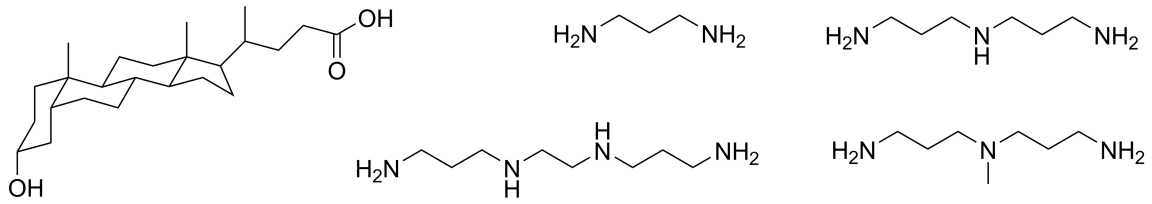

Scheme 1.3. Chemical structures of lithocholic acid (left), 1,3-propanediamine (middle, top), 1,2-bis(3-aminopropylamino)ethane (middle, bottom), 3,3'-aminobispropylamine (right, top) and 3,3'-methyliminobispropylamine.

A different type of additive comprises compounds that are used to change some properties of the gel. In these cases, the additive may or may not be able to gelatinize the solvent individually. Scheme 1.2.B presents schematically a gel where both components are able to form gels individually, while the combination of these two gelators leads to the gel formation as well. The changes induced in the gel system are either due to specific interactions between the gelator and additive or between the additive and the solvent, and in some cases changes to both types of interactions occur. For example, Steed et al. introduced a gel system for crystal-growing of non-gelling molecules.[6] The bisurea compound (Scheme 1.4, left) has the ability to form a gel. Carbamazepine (Scheme 1.4, right) is an anticonvulsant drug. A solution of 1% wt of bisurea and 1% wt of carbamazepine in hot toluene forms a gel when cooled. The crystals of carbamazepine appear in the gel after 8-12 h. Comparison of the mechanical properties of the bisurea gel in the presence and absence of carbamazepine illustrates that the disruption of the gels happen at higher yield stress value when carbamazepine is added to the gel. The authors

suggest that the formation of carbamazepine crystals leads to strengthening of the bisurea network.

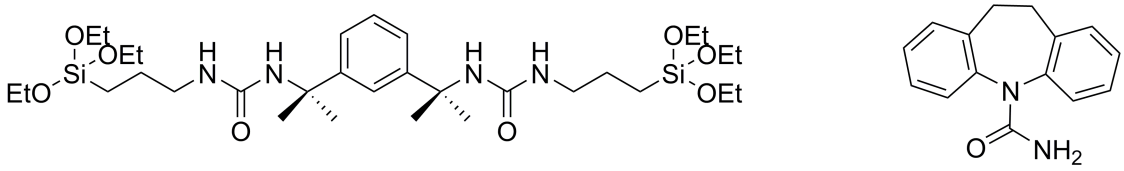

Scheme 1.4. Chemical structure of a bisurea gelator (left) and carbamazepine (right).

There are also cases where a compound with specific properties is added to the gel system to make the gel suitable for particular applications (Scheme 1.2.C). One interesting example of this type of gel is a light sensitive organogel reported by Shinkai et al.[7] Photodimerization of anthracene may happen when two anthracene molecules are in appropriate arrangement with respect to each other. Shinkai and co-workers found that an equivalent mixture of alkylamine (alkyl chain with 8, 9 or 10 carbons) and anthracene-9-carboxylates forms a gel in cyclohexane. The gel converts to the solution when it is irradiated by UV-light. Gradual disappearance of fibrillary bundles was observed on dark-field optical microscope during the photoirradiation. Heating the obtained solution to the boiling point of the solvent followed by cooling to 15 °C led to the reformation of the gel.

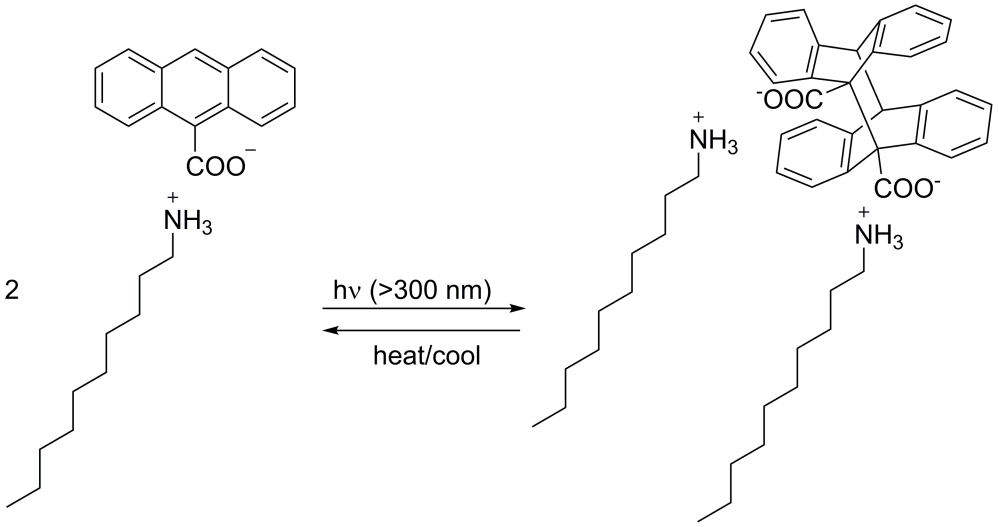

Scheme 1.5. Alkylammonium and anthracene-9-carboxylate organogel converts to the solution upon light irradiation.

1.4 Supramolecular gels as host systems

Supramolecular gels can be loaded with guest molecules. Depending on the affinity of the guest molecules for the network or solvent, different interactions may happen in the system. Although there are examples where covalent bonds are involved in host-guest interactions, herein I will provide some examples where host-guest interactions are noncovalent, because the guest molecules I used in this thesis are interacting with the gel through noncovalent interactions.

In general, there are three categories where the gel system acts as a host.[8] i) Noncovalent interactions between small guest molecules and the gel that can be used for molecular recognition events. For example, 1,1'-bi-2-naphthol-terpyridine-Cu(II) (BINOL-terpy-Cu(II), (Scheme 1.6) forms a gel after being sonicated in $CHCl_3$.[9] Pu and

coworkers showed that the R and S enantiomers of BINOL-terpy-Cu(II) can be used as host gel systems for recognition of chirality of small chiral guest molecules. For example, addition of 0.1 eq of (S)-phenylglycinol to the (R)- BINOL-terpy-Cu(II) leads to gel disruption after 2 min of sonication. However, the (R)- BINOL-terpy-Cu(II) gel remained stable when 0.1 eq of (R)-phenylglycinol was added. A minimum of 2 eq was required from the (R)-phenylglycinol to cause the gel to collapse.

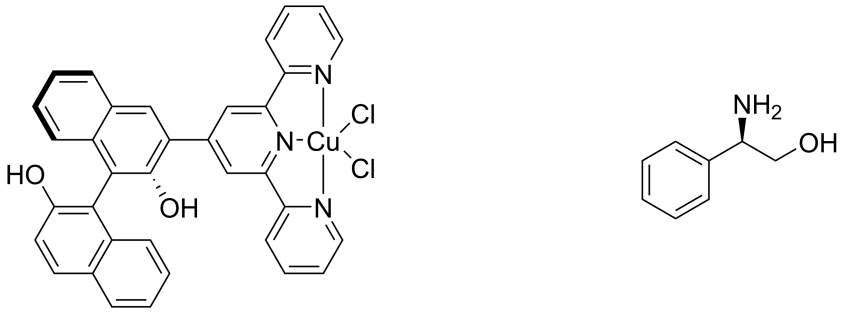

Scheme 1.6. Chemical structure of (R)-BINOL-terpy-Cu(II) (left) and (R)-phenylglycinol (right).

ii) Supramolecular gels can be used as the host system for stabilization/activation of certain compounds. For example, Shumburo and Biewer introduced an organogel of 4-*tert*-butyl-1-phenylcyclohexanol that can stabilize the photomerocyanine species of spiropyran photochromic switches (Scheme 1.7).[10] The half-life for the photomerocyanine species is 2.6 times higher in the 4-*tert*-butyl-1-phenylcyclohexanol/mineral oil gel in comparison to the half-life in solution. For a succinyl-ester-substituted spiropyran, the lifetime of the photomerocyanine isomer can

increase about 195 fold. The authors suggest that this stabilization effect is due to the interactions between the photomerocyanines and the gel fibers.

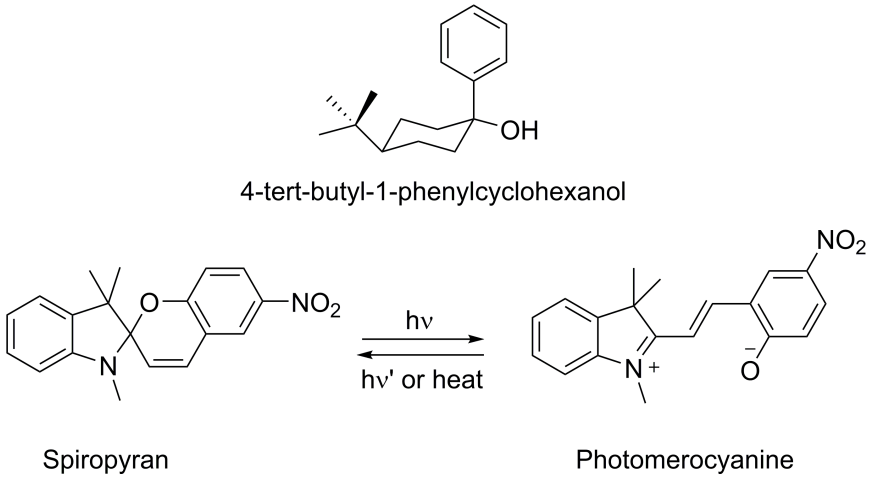

Scheme 1.7. Chemical structure of 4-*tert*-butyl-1-phenylcyclohexanol and the photochromic switch of spiropyran to photomerocyanine.

iii) Gels also can be used as templates for some reactions such as polymer imprinting. For example, Weiss and coworkers reported the polymerization of methyl methacrylate and styrene in an alkylammonium bromide gel.[11] Tetraoctadecylammonium bromide (Scheme 1.8) forms a gel in styrene or methyl methacrylate. After polymerization of the solvent, the gelator can be removed from the polymer matrix. The obtained material has submicron cross-sectional channels.

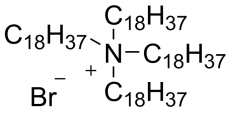

Scheme 1.8. Chemical structure of tetraoctadecylammonium bromide.

1.5 Bile salts

Bile salts such as sodium deoxycholate (Scheme 1.9) are biosurfactants that are naturally synthesized in the liver and stored in the gallbladder. They have an important role in digestion of compounds such as cholesterol and fatty acids.[12] Bile salts are amphiphilic compounds with a hydrophobic convex surface due to presence of alkyl groups and a hydrophilic concave surface due to presence of hydroxyl groups.

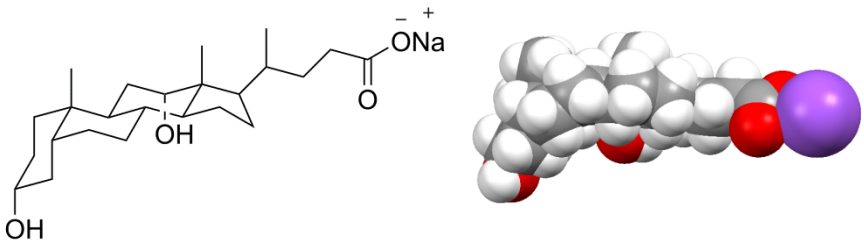

Scheme 1.9. Chemical structure (left) and space filled model (right) of sodium deoxycholate.

1.5.1 Bile salt aggregates

The amphiphilicity of bile salts makes them form aggregates in aqueous media. Aggregation of bile salts is different from that observed for conventional micelles because in the case of bile salts a very well-defined polar head group attached to a hydrophobic tail group does not exist. Several models have been proposed to describe the aggregation of bile salts.[13-18]

Some researchers suggest that the aggregation of bile salts is a continuous process.[18,19] They propose that the size of the aggregates continuously increases when the concentration of bile salt increases. In this multiequilibrium model the aggregation is

explained by sequential equilibria (Equation 1.1). A critical micellar concentration cannot be defined in this model.

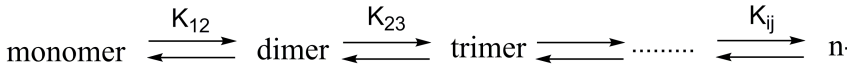

Equation 1.1

$$K_{12} = K_{23} = ...= K_{ij}$$

Equation 1.2

On the other hand, there are reports where authors determine the critical micellar concentrations and estimate the number of monomers involved in the aggregates.[12,17,20] This model assumes that aggregation requires a certain concentration of bile salt monomers before the aggregation process starts.

The primary/secondary aggregation model which originally was proposed by Small et al. in 1969 is still the most accepted model among all.[16] In this model, the primary aggregates of bile salts form due to hydrophobic interactions. One year earlier, Small had shown that the size of the bile salt aggregates, which he called micelles, depends on various parameters such as the temperature, the pH and the concentration of counter ions.[15] At lower concentrations of bile salts and counter ions, the aggregates are small and the aggregation number is around 2-6 for both trihydroxy and dihyroxy bile salts. Dihydroxy bile salts such as sodium deoxycholate form larger aggregates (aggregation number of 12-100) at higher concentrations[15,16] In the next step of the

aggregation process, secondary aggregates form through hydrogen bond formation between hydroxyl groups on the surface of the primary aggregates.

Presence of both hydrophobic and hydrophilic binding sites for guest molecules in bile salt systems makes them suitable as hosts for various types of guest molecules. For example, bile salts facilitate the solubilization of insoluble or partially water soluble lipids such as cholesterol, fatty acids, phospholipids and monoglycerides.[12] Besides, bile salts can be considered as flexible hosts, since the aggregate formation is influenced by the shape and size of the guest molecules.[21] This flexibility makes bile salt aggregates advantageous with respect to accommodating guest molecules with different sizes when compared to rigid host systems, such as cyclodextrins and cucurbit[n]urils.

Many studies have been dedicated to aggregation and micellization of bile salts using different techniques. However, parameters such as aggregation number and critical micellar concentration are not very well quantified even in those papers where the authors used the same techniques.[13,14,18,22-24] Even more, there are disagreements among researchers on the sign and values of thermodynamic parameters such enthalpy and entropy for the aggregation of bile salts.[14,23-25] Nonetheless, there are some common aspects on which there is agreement. It is established that addition of salts, variation of temperature and pH and the type of bile salt can change the aggregation behavior of bile salts.

1.5.2 Bile salt gels

Sodium deoxycholate (NaDC) is the most widely reported bile salt for the ability of gel formation. The sodium deoxycholate gel has been known for quite a long time.[26] NaDC is a LMWG which can form gel in aqueous solutions if its concentration is sufficiently high for the SAFiN formation within a narrow pH range. Solutions at a close to neutral pH lead to gel formation and phosphate buffers are normally used to adjust the pH. NaDC gel formation is a reversible process where the transition between the gel and sol phases can be induced by heat. In addition, NaDC gels are known to be thixotropic.[27] Thixotropic gels convert to liquid when an external mechanical force is applied on them.[28] Stirring or shaking liquefies the thixotropic gel. The system returns to the original gel state if the external force is removed and the gel is allowed to remain undisturbed. The NaDC hydrogel is formed based on physical interactions such as hydrogen bonds and the hydrophobic effect. Through a comprehensive rheological study, Tato et al. showed that the hydrogen bonds are the main forces involved in the formation and strength of the NaDC gel.[29] Blow and Rich proposed that NaDC gel fibers have helical configuration.[27] NaDC hydrogels are shown to have applications in different fields of chemistry and material sciences such as drug delivery[30,31] and nanoscience.[31,32]

Other bile salts also can form gels under specific experimental conditions. For example, Maitra and coworkers showed that sodium cholate can form a gel in the presence of metal ions like Ca^{2+}, Cu^{2+}, Co^{2+}, etc.[33] The authors illustrated that the helical framework of the calcium cholate hydrogel is suitable for preparation of gold and silver nanoparticles.[33]

Some bile acid derivatives form gels which have specific applications or responses. For example, Maitra and coworkers developed a thermochromic hydrogel using a tripodal cholic acid derivate as the gelator (Scheme 1.10). They doped the sodium salt of bromophenol blue into the gel. Bromophenol blue is a pH sensitive dye which is blue at pH > 4.6 and yellow at pH < 3. The gel color was observed to be green, while it switched to yellow when the gel was converted to solution by heating. The authors suggested that the observed color change is due to preferential incorporation of the blue form in the hydrophobic pocket of the gelator in the gel phase.[34]

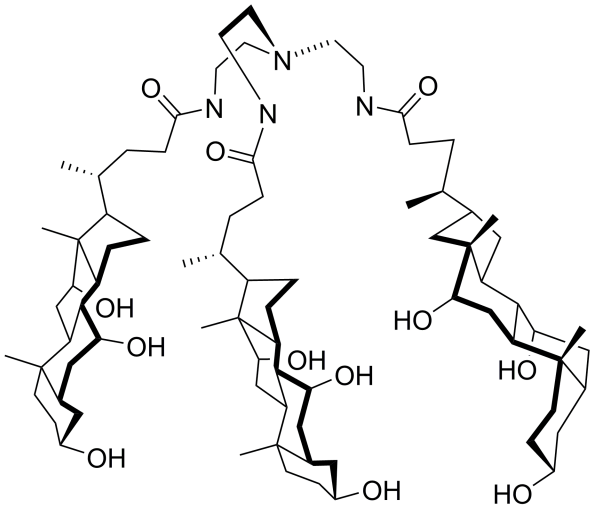

Scheme 1.10. A tripodal cholic acid derivative used as the gelator in a thermochromic hydrogel.

1.6 Effect of surfaces on the properties of gels

Chemical reactions and physical interactions at the interface are different from those in bulk solutions or solids. For this reason, surface chemistry has been a point of

interest for many researchers. The effect of surface chemistry needs to be understood for many purposes, such as the design of heterogeneous catalysts or the prevention of corrosion. Somorjai and Li reviewed some of the applications of surface chemistry in heterogeneous catalysis, semiconductors, medical technology, anticorrosion and lubricants.[35]

Many researchers are interested in understanding the lubrication properties of hydrogels due to their potential applications in tissue engineering.[36-38] Biological tissues are not only strong materials (elastic modulus of 10^4-10^7 Pa) but also show low surface sliding friction between cartilages and strong adhesion between hard bones and tendons.[36] Therefore, understanding the gel-surface interactions is important to be able to design materials which display the surface sliding friction properties similar or close to those in biological tissues.

There are more reports on the effect of surfaces for polymer gels than for supramolecular gels. Polymer gels are normally strong enough to be prepared in a mold with different surface properties. These gels can then be taken to other equipments for characterization purposes. For example, Gong et al. showed that the poly(N,N-dimethyl acrylamide) hydrogel prepared on hydrophilic silicon substrates has different topolographical and elastic properties as measured by AFM compared to gels prepared on hydrophobic polystyrene substrates. The surface of the gel prepared on the silicon substrate was smoother than the gel prepared on hydrophobic polystyrene. Moreover, gels prepared on polystyrene have a lower surface friction than those prepared on silicon

substrates.[39] In a separate report, Tran et al. showed that the mold used for the polymerization of a chemical gel of poly(N,N-dimethyl acrylamide) has an influence on the surface of the gel. They illustrated that the surface of the obtained gel is less cross-linked in comparison to the bulk.[40]

It is not unreasonable to think that the formation of SAFiNs also can be affected by the surface at which the nucleation and growth of the fibers occurs. Surface properties not only could be influential on gel formation, but also may play a role in the shape and size of the fibers as well as the type of connection between fibers.[2]

The number of studies on the effect of the nature of the surface on the formation of supramolecular gels is limited. The only work which describes the effect of surface in a supramolecular gel system was published recently by Zelzer et al.[41] They used a cytidine derivative (C14-cytidine, Scheme 1.11) as the gelator and showed that the presence of different functional groups on the surface affects the fiber structure and mechanical properties of the C14-cytidine gel film. They used piranha cleaned glass as a polar surface covered by hydroxyl groups and a trimethoxyphenylsilanized glass as a hydrophobic surface bearing phenyl groups. Atomic force microscope experiments illustrated that the fiber diameters are 61.7 ± 4.4 nm and 47 ± 9 nm for the surfaces bearing phenyl and hydroxyl groups respectively. No significant difference in fiber diameters was observed for the bulk gel prepared in vials bearing the same functional groups suggesting that the effect of the properties of the surface on the gel has a limited range. These authors were also able to measure the Young's moduli using atomic force

microscope experiments. The qualitative results suggested that the gel film formed on the hydrophobic surface was stiffer than the one prepared on the hydrophilic surface.[41]

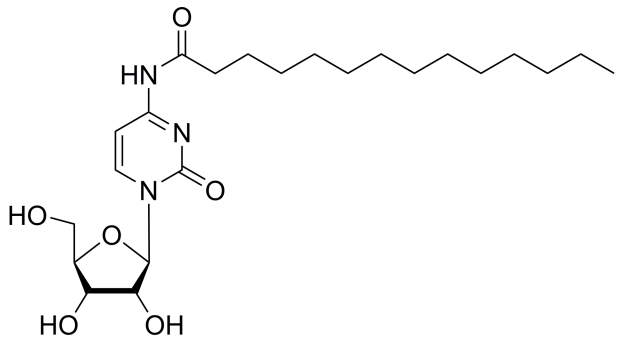

Scheme 1.11. Chemical structure of C14-cytidine.

It is not only the surface that can influence the gel formation, but it is also possible to design the gels that have an impact on the properties of surfaces. In an interesting work, Nakano et al. reported a superhydrophobic surface prepared using perfluoroalkyl chains as an organogelator.[42] The removal of the solvent from the organogel prepared on the glass surfaces provided a xerogel coated surface with very high hydrophobicity. The measured water contact angle for this sample is reported to be 150°. The term aerogel is used for the solid material which is obtained by removal of solvent from a gel sample without fibers being collapsed. Aerogels are normally obtained from gels with mechanically strong fibers like polymers. If the gel fibers are not strong

enough, they will collapse under the force of the gravity after solvent removal. These gels are called as xerogels.[11]

One obstacle to study the effect of surface chemistry on supramolecular gels is their mechanical strength that precludes removing the sample from the surface. Therefore, investigation of the effect of surface chemistry on supramolecular gels requires the use of techniques which can provide "in situ" information on the properties of the gel.

1.7 Effect of ions on the properties of supramolecular systems

1.7.1 Effect of ions on the properties of supramolecular systems in solution

Supramolecular systems are based on weak interactions which include ion-ion and ion-dipole interactions. Thus, it is not surprising to see alterations of supramolecular systems when ions are added or removed from the supramolecular solutions. Ions of mineral and organic salts with different charges, charge density and shape can influence the structure and dynamics of supramolecular systems. A classic example of the effect of salts on supramolecular systems is the micellization of sodium dodecyl sulfate (SDS). The average size of the SDS micelles increases when the concentration of monomer is increased.[43] It has been shown that the average weight of the large micelles is dependent on the salt that is added to the solution. These larger micelles have a rodlike shape and their molecular weight in the salt solution is related to the salts with the following order: NaSCN < NaF < NaCl < NaBr < NaI.[43]

The addition of salts also can change the aggregation of bile salts.[12,17,44] O'Connor and coworkers proposed that the addition of electrolytes leads to the destabilization of the small bile salt aggregates,[17] which then leads to the formation of the larger aggregates. Zana and coworkers studied the effect of NaCl on the aggregation of sodium deoxycholate. They showed that at NaDC concentrations ≤ 4% (ca. 96 mM) and at NaCl concentrations below 0.6 M only primary aggregates of NaDC exist in solution. The secondary aggregates form in 10% solution of NaDC and 0.6 M NaCl.[44]

One further consideration is that the aggregation of bile salts can change depending on the counter ion that is present in the solution. For example, addition of 2.5-35 mM $CaCl_2$ to the 0.1 M NaDC solution leads to the formation of precipitates.[45]

1.7.2 Effect of ions on supramolecular gels

Ions can impact supramolecular gel systems in two different ways. There are cases in which the presence of ions is necessary for the gel to form and/or for tuning the gel's properties.[33,46-49] On the other hand, ions can have a role as stimuli, and the gel system is designed to be responsive to one or more ions.[50,51]

For example, the calix[4]arene carboxylate derivative shown in Scheme 1.12 is a nongelator. Park et al. showed that this compound can gelatinize in a 1:1 mixture of methanol-water if K^+ or Rb^+ are added to the solution. Addition of Li^+, Na^+, Cs^+, Cd^+, Cu^{2+}, Ag^+ and Cu^+ did not lead to gel formation. Higher mechanical stability was observed for the gel with Rb^+. Based on the crystals derived from the gel with K^+ or Rb^+,

the authors suggest that the gel with K^+ was formed by hydrogen bonds, while for the Rb^+ gel coordination bonds were also involved in the gel formation in addition to the hydrogen bonds.[49]

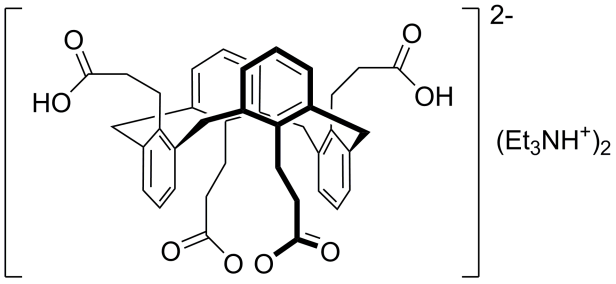

Scheme 1.12. Chemical structure of triethylammonium salt of calix[4]arene tetraacetate (deprotonated form).

In another example, Maitra et al. showed that the gelation of nongelator sodium cholate can occur in the presence of ions such as Ca^{2+}, Cu^{2+}, Co^{2+}, Zn^{2+}, Cd^{2+}, Hg^{2+} and Ag^+. The morphology of the dried gels was observed to be different for each of the metal ions according to the scanning electron microscopy measurements.[33]

Some of the examples of ion sensitive gels were reviewed by Escuder et al.[50] and Xiong et al.[52] Steed and coworkers have been studying the anion tuning of gels based on ureas.[6,53,54] They have shown that the gelation of the bisurea system is based on hydrogen bond formation. Addition of anions inhibits the gelation due to the interaction of anions with hydrogen-bonding donor groups. This interaction competes with hydrogen bond

formation in the gel. The degree to which the anion prevents the gelation is correlated to the affinity of the anion for the gelator.[55]

There are a few reports in the literature that describe the effect of salts on NaDC gels. It has been shown that addition of salts such as NaCl and NaBr can change the mechanical properties of sodium deoxycholate gels.[29,56,57] Although addition of salts leads to stiffer gels, the enhancement of mechanical strength is not very significant. Moreover, according to transmission electron microscopy experiments, addition of NaBr to NaDC gels leads to the formation of thicker fibers in the gel network.[57] Although, these reports provide good insight regarding the macroscopic changes in NaDC gels upon addition of salts, there is a lack of understanding about the effect of salts at the microscopic level.

1.8 Techniques

Fluoresce-based techniques are very popular to investigate supramolecular systems. In general, fluorescence is a sensitive technique which allows the monitoring of changes in the system even at low concentrations of fluorophores. Many of the organic molecules used in supramolecular systems are fluorophores or can be attached to a fluorophore by physical interactions or chemical bonds. Therefore, it is possible to use fluorescence in a wide range of supramolecular systems.

Fluorescence techniques are widely used to investigate gel systems. In general, there are two ways that one can choose to study the gel by using fluorescence: i) The

gelator (or the co-gelator) has fluorescence properties which can be monitored at different conditions. As an example, Kim et al. synthesized a low molecular-weight organogelator containing azobenzene moieties (Scheme 1.13). They demonstrated that the gel-to-sol transition occurred by irradiation of the sample with UV light. Irradiation of UV light leads to the trans-to-cis isomerization of the azobenzene. The reverse process occurs when the irradiation is stopped, and therefore, the solution converts to the gel. Although this paper is not based on the fluorescence properties on the azobenzene, it is an interesting example of a photo-responsive supramolecular gel system in which the chromophore is part of the gelator.

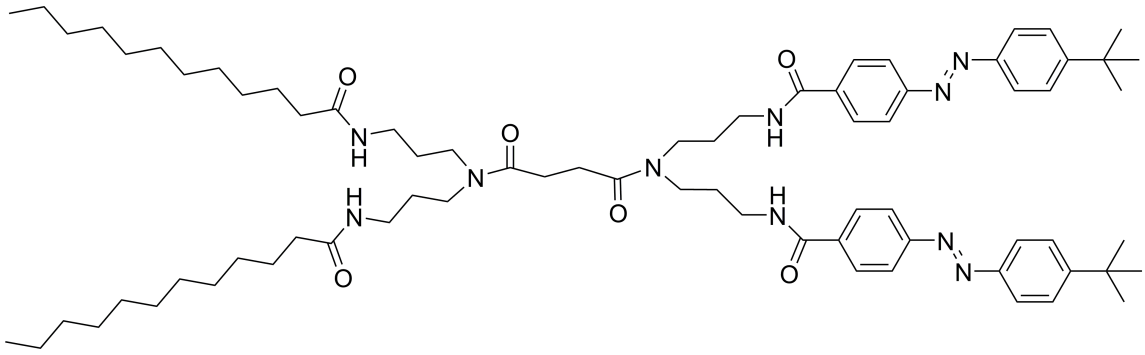

Scheme 1.13. Chemical structure of a bis-dendritic, light-responsive organo-gelator containing azobenzene moieties.

ii) A fluorescence probe is added to the system. For example, Tato et al. used pyrene as the fluorescence probe to follow the gelation of sodium deoxycholate. They showed that the combination of two aggregates, each one carrying a pyrene molecule, happens during the gelation process. Therefore, the interaction of two pyrene molecules,

one in its ground state and the other as an excited state, becomes probable and as a result excimer emission is observed during gelation.[22] In another example, Adams and coworkers used a series of fluorescence molecules to monitor the gelation of peptide-based gelators.[58] They showed that Tioflavin T can act as a molecular rotor. Fluorescence molecular rotors are molecules that can twist upon photo-excitation. This twist leads to the increase of non-radiative processes, decreasing the fluorescence quantum yield. It is expected that the fluorescence intensity increases when the twisting is prevented. In a viscous solution or during gelation the fluorescence intensity of Tioflavin T increases.

The main difference between these two methods is the concentration of the fluorophore in the gel. When the fluorophore is part of the gelator its concentration is much higher than when the fluorophore is added as the probe. When the fluorophore is part of gelator it can be involved in the interactions within the system and play a role in the structural properties of the gel.

1.8.1 Steady-state fluorescence

In a steady-state fluorescence measurement, the fluorophore is excited by a light beam at a certain wavelength. The emission spectra are plotted as the fluorescence intensity versus wavelength of the emitted light. The shape of the spectra, the position of the peaks and the fluorescence intensity in an emission spectrum are informative about the emissive species in a system and their surrounding environment.

Pyrene (Scheme 1.14) was selected as the probe in the current work because of its photophysical properties. Pyrene emission spectra (Figure 1.1) have five distinguished bands where the intensity of band I is sensitive to the polarity of the environment while the intensity of band III is not. Therefore, the I/III ratio of the pyrene emission is a criterion to probe the polarity of the surrounding environment. The higher the I/III ratio value, the more polar the environment. The I/III ratio of pyrene in water is measured to be 1.6-1.9 in polar solvent such as water and 0.5-0.6 in hydrophobic nonpolar solvents such as hexane.[59]

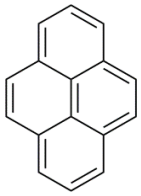

Scheme 1.14. Chemical structure of pyrene.

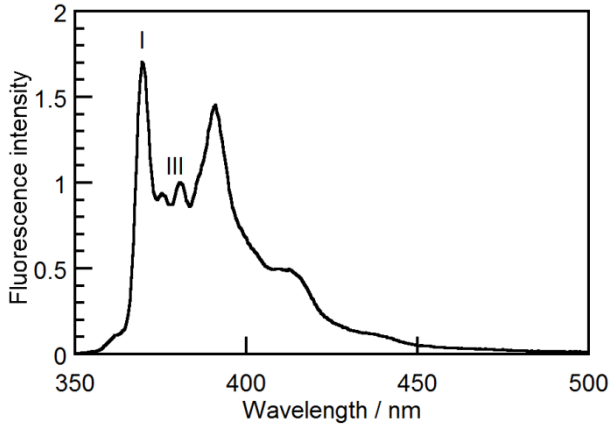

Figure 1.1. Normalized fluorescence intensity of pyrene in 50 mM phosphate buffer. The I/III is 1.73 ± 0.04.

1.8.2 Time-resolved fluorescence

Time-resolved fluorescence is an informative technique that is widely used in studying supramolecular systems. Among time-resolved fluorescence experiments, single photon counting (SPC) measurements are very popular. In this technique, a light source (a light emitting diode or a laser) is used to create the fluorophore excited state. The time taken for the detection of a single photon is measured and a histogram of the number photons detected as a function of time is constructed. This histogram of the fluorescence decay can be fitted with Equation 1.3 to determine the excited state lifetime. In Equation 1.3, the parameter A_i is the pre-exponential factor for the each emissive species with the lifetime of τ_i. In this equation i is the number of species involved in the fluorescence decay and the sum of A_i values is unity.

$$I(t) = I_0 \sum_{1}^{i} A_i \, e^{-t/\tau_i} \qquad \text{Equation 1.3}$$

In this work, the fluorescence decays of pyrene excited states were recorded on a single photon counter (SPC). Overall, the fit of the decays with the Equation 1.3 provides information about three different aspects of pyrene molecules in the gel. Equation 1.3 corresponds to a sum of exponentials functions. For example, if a fraction of pyrene molecules are free in water and some are bound to bile salt aggregates in the gel network, the value for "i" is 2. Parameter τ_i is the lifetime of each of the species and A_i provides information regarding the percentage of each species. For example, pyrene excited state in phosphate buffer has a mono-exponential decay with the lifetime of 138 ns at RT (Figure 1.2).

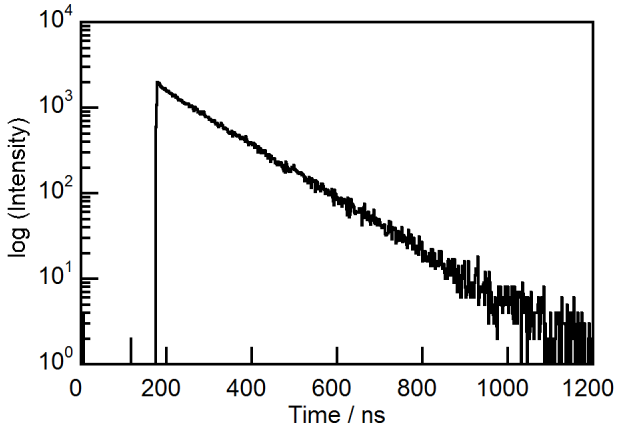

Figure 1.2. Fluorescence decay of pyrene in 50 mM phosphate buffer.

1.8.3 Fluorescence correlation spectroscopy (FCS)

Fluorescence correlation spectroscopy (FCS) is a powerful technique to study dynamic processes in various environments.[60,61] The combination of FCS and confocal microscopy in the 1990s enabled the technique to have the sensitivity of single-molecule detection and therefore broadened its use to studies in different fields.[60] This technique is frequently used to determine the hydrodynamic radii of small fluorescent molecules, polymers or nanoparticles. FCS experiments also provide useful information regarding the diffusion of fluorescent molecules in heterogeneous media such as polymer melts, porous materials, colloids and gels. It is also possible to use FCS to investigate the aggregation of molecules at solid-liquid interfaces.[61] This method is based on monitoring the fluorescence fluctuations due to the diffusion of fluorescent molecules or fluorescently tagged species in a very small volume. The correlation analysis of the fluorescence fluctuation provides information related to any process that leads to change

in the fluorescence intensity such as the translational and rotational diffusion coefficient of fluorophores, kinetic rate constants that lead to non-fluorescent molecules and association constants between fluorophores and other components that change the emission intensity of the fluorophore.

1.9 Objectives

The general goal for this thesis is to shed some light on different aspects of a supramolecular hydrogel system. Understanding the mobility of a guest in a complex gel, investigating the effects of temperature and ionic strength as well as the effect of surfaces on the properties of the sodium deoxycholate gel are some of the aspects that are addressed in this thesis. The objectives of the projects described in the following chapters are:

1.9.1 Investigation of the mobility of a small guest molecule in the NaDC gel

Understanding the mobility of a small guest molecule in a gel system is interesting from many points of view. Gels can be considered as host systems that can accommodate small guest molecules. This capability of the gels is in particular important for their potential applications including drug delivery. As was mentioned above gels have a minimum of two components involved in their structure: a gelator and a solvent. It is important to understand the distribution of guest molecules between the different phases of the gel. It is reasonable to expect that the guest molecules incorporated into the

gel show different affinities for different environments within the gel. The hypothesis for this work is that the distribution of the guest molecules between the network and the solvent is dependent on different factors. Physical properties of the guest such as polarity, size and shape are influential in its distribution in the gel. The hydrophobicity/hydrophilicity of the guest can lead to different affinities for the water phase or the network in hydrogels.

It is also important to understand how the relocation of a guest molecule from one site to another within the gel happens when an external stimulus such as temperature is applied to the gel. These data are potentially informative in the cases where release or recovery of a guest molecule in the gel system happens with the application of stimuli.

1.9.2 Effect of surface on the gel formation and gel properties

There is a lack of studies in the literature regarding the effect of different surfaces on the property of gels in general and on supramolecular gels in particular. The mechanical properties of the supramolecular gels are perhaps the biggest drawback in investigating the effect of properties of the surface on the gel. When the gel is mechanically weak, it is harder to prepare the sample on surfaces with certain properties and to then remove the gel in order to perform measurements on another equipment. Therefore, it is necessary to design the experiments where measurements can be performed “in situ”.

In my work, we tried to investigate the effect of surfaces bearing different functional groups on NaDC aggregation and gel formation with the hypothesis that different surfaces could affect the properties of the gel. Fluorescence correlation spectroscopy experiments were used to provide information regarding the gel close to the surface, while steady-state and time-resolved experiments were informative about the bulk gel prepared on different surfaces.

1.9.3 Effect of salts on NaDC gel properties

Understanding the effect of ions on the properties of the NaDC gel is important for potential applications of the gel, such as in drug delivery. Concentrations of cations such as Na^+, K^+, Ca^{2+} and anions like phosphate are not the same in different parts of the human body. Therefore, it is crucial to understand the properties of the gel at different concentrations of ions.

It is also expected that ions with different charge and charge density will influence the gel in different ways. The NaDC gel is formed based on weak interactions. Therefore, all the interactions such as attraction between the ions with opposite charge and ion-dipole interactions can play a role in altering the gel's properties. Although it is almost impossible to investigate a particular ion-ion or ion-dipole interaction in a complex system like the NaDC gel, it is important to understand how addition of salts affects the gel.

2 Guest shuttling within a supramolecular hydrogel of sodium deoxycholate with cucurbit[6]uril as an additive

2.1 Introduction

Additives are compounds which are added to gels to facilitate gel formation or to tune specific gel properties. The effect of additives on the properties of gels can be generally classified into three categories: i) The additive has a role of co-gelator. In this case, the presence of the additive is necessary for the formation of the gel. The main component present at higher molar fraction does not form the gel for the experimental conditions used unless the additive is present. ii) The additive and the gelator both form gels separately for specific experimental conditions, but the mixture of them forms a gel with different properties from the gels containing only the individual components. iii) The additive does not have an impact on gel formation, but leads to the change in some of the gel's properties.

Macrocycles have been used as additives to gels. Linkage between "n" number of glycoluril monomers leads to the formation of macrocyclic compounds known as cucurbit[n]urils (CB[n]s). These macrocycles have a hydrophobic cavity and two

hydrophilic portals due to the presence of carbonyl groups. The size of the cavity is dependent on the number of glycoluril units of the macrocyclic structure (Scheme 2.1).

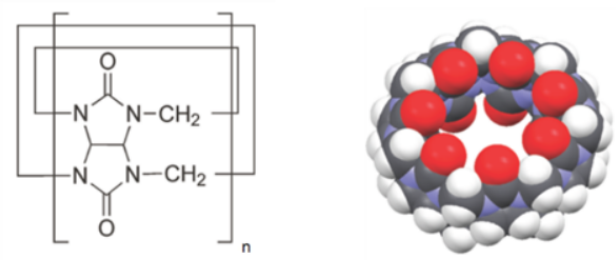

Scheme 2.1. Chemical structure of CB[n]s (left) and the space filling structure of CB[7] (right).

CB[n]s are interesting supermolecules because these hosts can form complexes with hydrophobic guests with high binding constants in comparison to other macrocyclic molecules.[62] For example, association binding constant of methylene blue with CB[7] is 1.3×10^7 M^{-1} while the binding constant for this guest with β-cyclodextrin, which is a host with a similar cavity size as CB[7], is 4.1×10^2 M^{-1} (Scheme 2.2).[63] One of the strongest host-guest non-covalent interactions was reported by Isaacs et al. for the complex of CB[7] and the diamantane diammonium ion (Scheme 2.2) where the complex has the association equilibrium constant of 7.2×10^{17} M^{-1} in pure D_2O.[64]

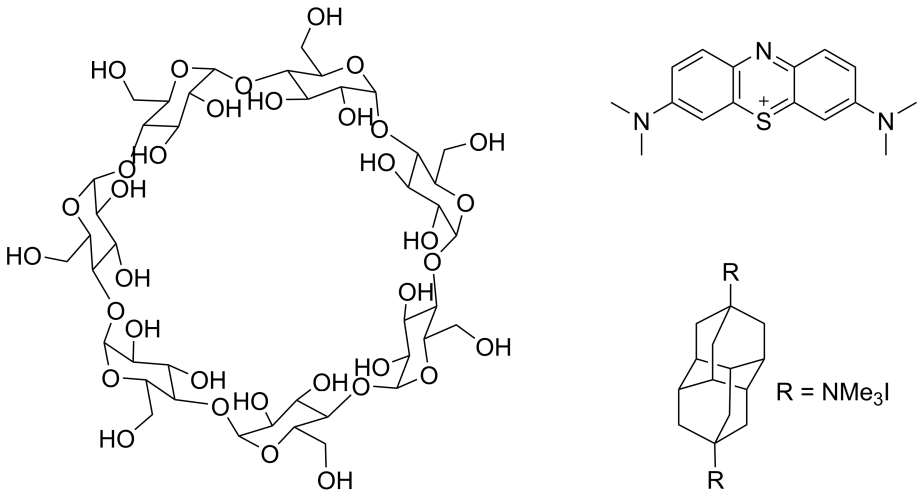

Scheme 2.2. Chemical structures of β-cyclodexterin (left), methylene blue (right, top) and diamantine diammonium iodide (right, bottom).

Within the CB[n] family, CB[7] on its own can form hydrogels at low pHs (0 to 2).[65] CB[6] was used as a co-gelator for butan-1-aminium 4-methylbenzenesulfinate to make a thermo-responsive hydrogel.[66] CB[6] or CB[8] can facilitate gel formation when they are covalently bound to natural[64,67-69] or artificial polymers.[70,71] In these cases, guest molecules with high affinity for the cavity of CB[6] or CB[8] are attached to one polymer strand while the CB[n] is connected to a different polymer strand. Host-guest complexation leads to the cross-linking between the polymer strands, which forms the network with the capability of solvent entrapment leading to gel formation. Scheme 2.3 illustrates schematically the formation of 1:2 complexes between CB[8] and phenylalanine moieties attached to a polysaccharide chain.[68]

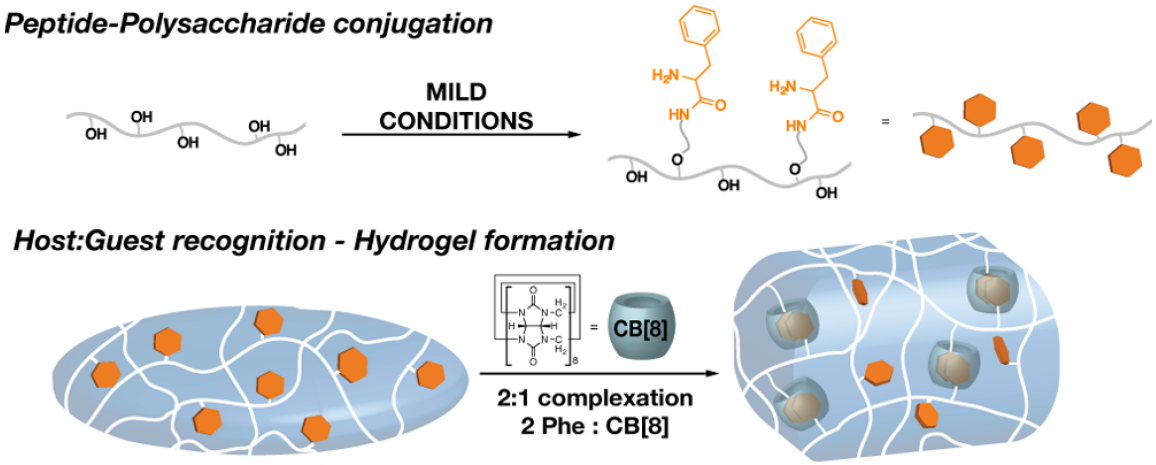

Scheme 2.3. Complexation of the phenyl group of phenylalanine attached to polysaccharide chain and CB[8], leading to the formation of a hydrogel. Reprinted with permission from reference 68. Copyright © 2015, American Chemical Society.

Gels are stable within a certain temperature range. Transition to the sol phase or precipitation of the components occurs outside of this temperature range. Nonetheless, the alteration of properties of the gel can happen when the temperature varies within the range of temperatures for which the material is a gel. This chapter will show that the location of a guest in a gel changes with temperature.

Besides the thermal stability of the gels, their mechanical stability is important for their applications. Rheological measurements are the most popular experiments in the gel literature which provide information regarding the mechanical properties of gels.[1,54,72,73] The strength of the gel with respect to time, application of external forces such as shear stress or strain and temperature can be determined on a rheometer by monitoring the

storage modulus (G') and loss modulus (G"). G' and G" represent the elastic and viscous behavior of the material, respectively.[72]

Pyrene was used to characterize the binding of a guest to the gel network and the additive. Pyrene forms a weak complex with the additive CB[6]. The association constant between pyrene and CB[6] in solution is reported to be $(3.1 \pm 0.9) \times 10^2$ M^{-1}.[74] The nature of the complexation of pyrene and CB[6] is not very well known. Pyrene is larger than the size of the cavity of CB[6]. Therefore, the complete inclusion of pyrene into CB[6] is not possible. Viglia et al. proposed that pyrene is partially bound to CB[6]. The network of the gels I studied were formed from sodium deoxycholate aggregates, which is a bile salt. Pyrene was previously used to study the aggregation of bile salts in solution. These studies were based on steady-state and time-resolved fluorescence measurements.[23,44]

The objective of the studies presented in this chapter was to understand the mobility of a small guest molecule in a complex supramolecular gel system. CB[6] with different concentrations was used as an additive for the NaDC gel. The NaDC-CB[6] gel has multiple binding sites available for pyrene as a small guest molecule. Pyrene can interact with CB[6], bind to the hydrophobic site of bile salts in the gel network or remain free in the aqueous phase of the gel. The mobility of the guest between these binding environments was studied by variation of temperature.

2.2 Experimental section

2.2.1 Materials

NaDC (Fluka, > 98%), Na_2HPO_4 (Anachemia, anhydrous, > 99%), $NaH_2PO_4•H_2O$ (Anachemia, > 99%), methanol (Fisher, spectral grade, > 99.9%), HCl (4.00 N Anachemia) were used as received. Pyrene (Fluka, 99%) was recrystallized from ethanol twice and its purity was established by the observation of a mono-exponential fluorescence decay in aerated water (127 ns).[75,76] 1,6-Diaminohexane (DAH, Aldrich, 98%) and N-(4-aminophenyl)imidazole (API, Aldrich 98%) (Scheme 2.4) were used without further purification. Deionized water (Barnstead NANOpure deionizing systems ≥ 17.8 MΩ cm) was used for the preparation of all solutions.

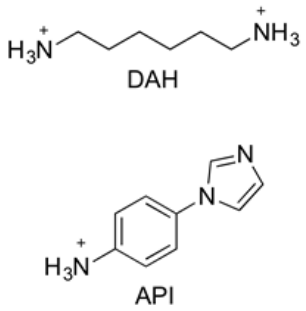

Scheme 2.4. Chemical structures for 1,6-diammoniumhexane (DAH) and N-(4-aminophenyl)imidazolium (API) cations.

2.2.2 Sample preparation

The final NaDC concentration was 30 mM (1.25 % w/v). A pyrene stock solution (5 mM in methanol) was employed and the final pyrene concentrations were 2 or 5 μM. The phosphate buffer stock solution was 0.5 M at pH 6.6 and the final phosphate buffer concentrations for the gels was 50 mM.

For NaDC gels, 1.8 mL of the aqueous NaDC solution (33.3 mM) was heated for 15 min at 60 ºC followed by the addition of 0.8 or 2.0 μL pyrene and 0.2 mL of the phosphate stock solutions. This mixture was left at 60 ºC for another 15 min before being transferred to cells and cooled. The samples were left undisturbed for at least 1 h before experiments were performed. For shorter times the gels showed some flow upon inversion. For NaDC-CB[6] gels, the CB[6] solid was suspended in 1.8 mL water to which 0.2 mL phosphate buffer was added. Addition of phosphate buffer led to the solubilization of CB[6] at RT. This solution was heated at 60 ºC for 15 min and the required amount of pyrene was injected as a methanolic stock solution followed by the addition of solid NaDC (24.8 mg). The solution was maintained at 60 ºC for a further 15 min before being transferred to cells and cooled. Samples containing CB[6] also were kept undisturbed for a minimum of 1 h before any measurements were performed. The final CB[6] concentrations were 1.5, 3.0 or 6.0 mM.

For rheology experiments the gels were prepared as described above without the addition of pyrene and were transferred to the plate in the rheometer while hot.

2.2.3 Equipment

Rheology experiments were performed using a TA Instrument AR2000 stress-controlled rheometer with a Peltier plate for temperature control using a plate and cone geometry (60 mm 2º acrylic cone) and a solvent trap filled with paraffin oil to prevent evaporation or condensation. The hot solutions were poured onto the rheometer plate using a pipette. The gap between the plate and the cone was immediately closed and the edges of the cone were sealed using 1 mL paraffin oil to avoid evaporation of water. The temperature was set to 15 ºC. Preliminary experiments where the gel was transferred to the plate showed that 20 h equilibration time was required to reach a stable gel. For this reason, all gels formed within the rheometer set-up were left to equilibrate for 20 h and were monitored during equilibration under a 0.5 Hz oscillation frequency and 0.1% strain to assure that the G' and G" values were constant before any further experiments were done. Oscillatory stress sweeps between 0.1 and 100 Pa were performed using a 0.5 Hz frequency and 0.1% strain. Frequency sweeps were performed between 0.1 and 100 Hz at 0.1% strain. The frequency sweeps were performed after the sample was slowly heated (0.4 ºC/min) to 55 ºC, when an abrupt decrease in G' and G" was observed, and was then slowly cooled to 15 ºC (0.4 ºC/min).

Fluorescence emission spectra between 350 and 550 nm were collected with a PTI QM-2 fluorimeter using an excitation wavelength of 331 nm. The bandwidth for the monochromators was 1 nm and the wavelengths step size was 0.5 nm. The analysis of the spectra were performed using Felix32 (version 1.2) software. Fluorescence decays at 390 nm were recorded using an Edinburgh Instruments OB920 single photon counter (SPC)

where samples were excited with a 335 nm light emitting diode (EPLED-330, Edinburgh Instruments). The bandwidth for the emission monochromator was 16 nm. Data for gels were accumulated until 100,000 counts were reached in the channel of maximum intensity. Gel samples are scattering and a large number of counts were accumulated to ensure at least 5,000 counts for the maximum intensity of the pyrene emission. Decays measured for pyrene in solutions were accumulated until 2,000 counts were reached in the maximum intensity channel. The kinetics was analyzed with a function corresponding to a sum of exponentials using the FAST software from Edinburgh Instruments. This analysis took into account the contribution from light scattering due to the use of the triangular cell. Fits were considered adequate when the residuals between the data and fit were random and the χ^2 values were between 0.9 and 1.3.

The temperature in the cell holders of the QM-2 and SPC was controlled with an external water bath. Samples were held at each temperature for ca. 10 min before measuring the spectra or decays. The temperature annealing experiments started with samples at 15-20 $^{\circ}$C and the temperature was raised incrementally up to ca. 50 °C before being cooled with similar temperature intervals. Gels for the temperature variation studies were formed in triangular cells, which were placed in the sample holder that could be thermostatized. This cell led to a 45° arrangement between the excitation beam and the surface of the cell. The emission was collected from the front face of the cell. Gels formed in an absorption cell were used for experiments performed at RT, where the emission was collected in a front-face arrangement using a sample holder that minimizes specular reflections, detection of scattered light and anisotropy effects by tilting the cell

backwards and having the optics set at a magic angle.[77] Solution experiments were measured in 10 × 10 mm fluorescence cells.

2.2.4 CB[6] synthesis and purification

Synthesis: This synthesis was developed by Dr. Palani Natarajan by modifying established methods.[78,79] Reagent grade chemicals were used for the synthesis. Glycoluril (10.0 g, 70.04 mmol) was dissolved under sonication in 80-90 mL of 9 M H_2SO_4 at RT and inside a 100 mL two-necked round bottom flask. Solid paraformaldehyde (4.2 g, 140.08 mmol) was added to the solution while stirring. The mixture was heated at 100 ºC for 10-12 h and was then cooled to RT. Addition of 100 mL of methanol led to the precipitation of white solid. The obtained solid, which contains CB[6], was filtered and washed with water to remove CB[5] and CB[7]. Purification of CB[6] was performed by dissolving 10 g of solid into 130-150 mL of formic acid with the aid of sonication. Insoluble solid was removed by filtration. Saturated filtrate was kept undisturbed for 48 h at RT which led to the crystallization of CB[6]. Crystals were isolated by filtration and were added into a beaker containing 200 mL water. This suspension was stirred overnight, filtered and the solid CB[6] was then dried. Its purity was tested by ESI-MS.

Titration: CB[n]s adsorb water over time. For this reason stock solutions of CB[6] were titrated. The titration is based on the competitive binding of 1,6-diammoniumhexane (DAH) and N-(4-aminophenyl)imidazolium (API) cations (Scheme 2.1). The binding constant for DAH of $(2.9 \pm 0.2) \times 10^8$ M^{-1} (0.05 M NaCl)[80] is much higher than the binding constant for API (8×10^4 M^{-1}, pH ~ 5.7).[81] The fluorescence of

API is increased when bound to CB[6]. The fluorescence of API decreases as DAH is added until a constant value is reached (Figure 2.1, left). Both guests are protonated in this assay since the pK_a value for imidazole, aniline and DAH are ca. 7, 4.6 and 9.8 respectively.[82] The experimental pK_a value for the API is not reported. However, at the 1 mM HCl concentration (pH=3) all the species are protonated.

The stock solutions for the titration were the following: (i) 500 μM CB[6]/0.1 M NaCl aqueous solution. The CB[6] concentration stated assumes a 100% pure sample. (ii) 1 mM neutral DAH in water (diluted from an initial 10 mM solution) and (iii) 10 mM neutral API in water. The analyte solution was prepared by adding 200 μL of the CB[6] stock and 20 μL of the API stock to a 10 mL volumetric flask which was diluted to 10 mL with a 1 mM aqueous HCl solution. The final concentrations of CB[6], Na^+ cations and API in the analyte solution were 10 μM, 2 mM and 20 μM, respectively. The fluorescence spectra for a CB[6] (10 μM)/NaCl (2 mM) and for the CB[6] (10 μM)/NaCl (2 mM) solutions with the maximum concentration of DAH used in the titration were recorded. The latter spectrum was subtracted as the baseline spectrum from the spectra of the sample containing API.

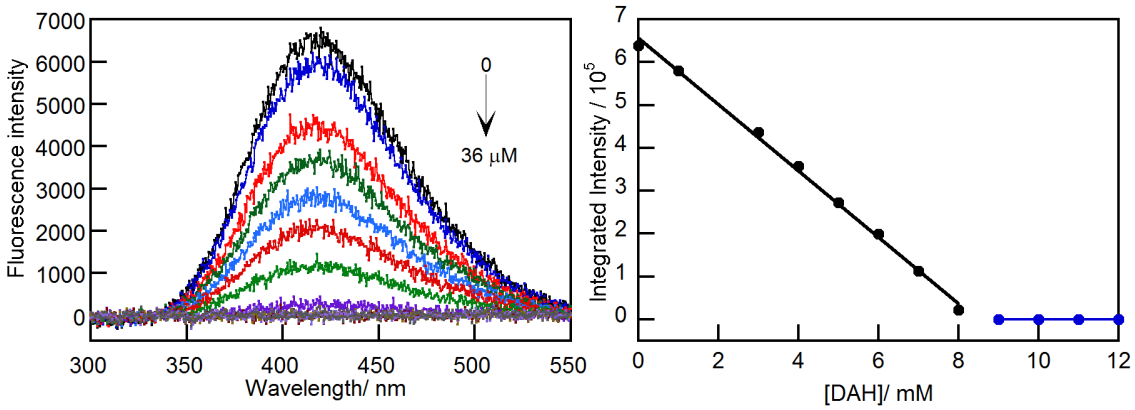

Figure 2.1. Decrease in the fluorescence intensity of API complexed to CB[6] upon addition of DAH (3 μL additions of a 1 mM DAH stock solution into 3 mL of the API/CB[6] solution) and the dependence of the fluorescence intensity on the CB[6] concentration (right), where the fit of the data in black was used to determine the equivalence point (intercept with the X-axis).

A PTI QM-2 fluorimeter was used to collect the emission spectra and the samples were excited at 280 nm. The monochromators slits were set to achieve 2 nm bandwidths. The emission spectra (0.5 nm step size, 0.25 s integration time) were collected between 295 and 550 nm. The samples contained in 10 × 10 mm fluorescence cells were kept at 20 ºC using a circulating water bath.

The titration was performed by subsequently adding 3 μL of the DAH stock solution to the analyte solution and recording the API emission spectra until the fluorescence intensity did not change for 3 additions (Figure 2.1, right). The corrected fluorescence spectra were integrated between 330 and 550 nm, and the intensities from this integration were plotted against the concentration of DAH. The intercept with the X-axis corresponds to the actual CB[6] concentration. In the example of Figure 2.1, the total

volume of DAH added was 36 μL and the purity of CB[6] was 84%. Concentrations were not corrected for the dilution, since the dilution was around 1%.

2.2.5 Setup for inversion test

A home built set-up was used to determine the gel-to-sol transition temperatures (T_{gs}) by measuring the temperature at which the gel was liquefied in an inverted vial placed in a water bath. Samples were prepared in cylindrical glass vials with an inner diameter of ca. 1.5 cm. A 2 mL volume was added to the vials and the gels were prepared as described above without the addition of pyrene. Samples were cooled from 60 ºC to RT and were kept undisturbed on the bench for at least 1 h. The closed sample vials were then inverted and immersed in a water bath that was stirred. Figure 2.2 shows the set-up for the inversion test showing NaDC gels with incorporated dyes of different color for presentation purposes. The gel on the right in blue shows the gel before any changes at the interface. The gels on the left (red) and middle (yellow) show changes at the interface because the NaDC gels were inverted before the resting time of 1 h. The temperature was raised from 21 °C to 55 °C over a period of 150 min. The gels before the heating started had the shape of the sample containing the blue dye (Figure 2.2, right) and the temperatures were recorded when the first drop fell from the gel/air interface (T_1) and when the gel fell due to the action of gravity (T_{gs}).

Inversion experiments were also performed for samples that were heated and cooled in the fluorimeter. Samples were prepared in triangular cells and were cooled to

RT on the bench. The cell was heated in the fluorimeter and the sample was removed at each temperature and was inverted to check if the material was flowing.

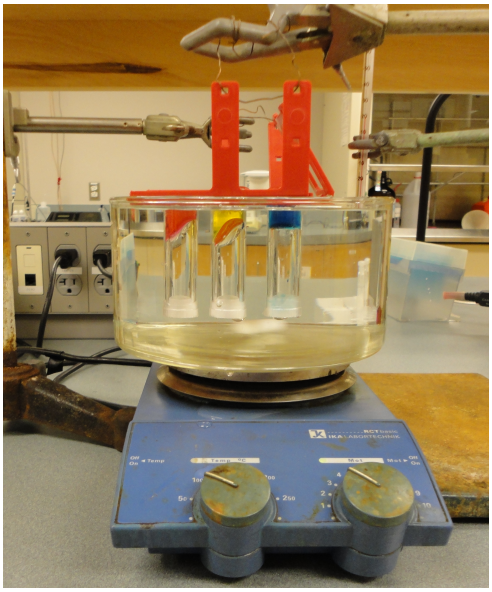

Figure 2.2. Set-up for the inversion test showing gels with incorporated dyes of different colors. The gel on the right in blue shows the gel before any changes at the interface. The gels on the left (red) and middle (yellow) show changes at the interface because the gels were inverted before the resting time of 1 h.

2.3 Results

2.3.1 Vial inversion test

The vial inversion test is widely used for the determination of the gel-to-sol transition temperature (T_{gs}).[83] T_{gs} is defined as the temperature at which the gel material falls down due to gravity. I will use the term "freshly prepared gel" for the gel which is prepared by uncontrolled cooling of the solutions at 60 °C to RT followed by a resting period of at least 1h. T_{gs} values were determined for freshly prepared gels with different

concentrations of CB[6] (Table 2.1). T_1 values are the temperatures at which some change at the gel-to-air interface was observed and a drop of liquid was developed and fell down. As shown in Table 2.1 addition of CB[6] to the NaDC gel leads to an increase of T_1 and T_{gs} of around 6-7 °C. These results indicate that addition of CB[6] leads to increased resistance of the gels to the increase in temperature. However, the T_{gs} did not change much when the concentration of CB[6] was varied from 1.5 to 6 mM.

Table 2.1**.** Temperatures when the first drop developed (T_1) and when the gel fell due to gravity (T_{gs})

[CB[6]]/[NaDC][a]	T_1 / °C[b]	T_{gs} / °C[b]
0	40.5 ± 0.7	43 ± 1
0.05	48 ± 1	49.2 ± 0.4
0.1	49 ± 1	50.5 ± 0.7
0.2	49.2 ± 0.3	53 ± 3

[a], [NaDC] = 30 mM; [b], average of two independent experiments; errors correspond to average deviations.

The inversion method was also performed by heating the samples inside the fluorimeter chamber. During heating the same T_{gs} values (48 ºC for CB[6]]/[NaDC] = 0.05; 51 ºC for CB[6]]/[NaDC] = 0.2) were obtained by this method as determined for the inversion test in a water bath (Table 2.1), indicating that the method using the fluorimeter led to comparable values with those obtained in the inversion method in the water bath. The same method using the fluorimeter was used during cooling in order to determine the sol-to-gel transition temperature (T_{sg}) that cannot be measured using the inversion test in

the water bath. The T_{sg} was 40 and 42 ºC for the gels with [CB[6]]/[NaDC] ratios of 0.05 and 0.2, respectively.

2.3.2 Rheology measurements

Studies on the mechanical properties of NaDC gels showed that this gel belongs to the category of "weak" gels and the mechanical properties of the gel were shown to depend on the concentration of NaDC, pH of the solution, and ionic strength.[29] In the current work, the concentrations of the gel components, NaDC and phosphate buffer were chosen in a way to ensure that the gel is transparent and that pyrene excimer formation is minimized. The viscoelastic properties of the gels are normally investigated by measuring the storage (G') and loss (G") moduli, which describe the elastic and viscous behavior of the material.[84]

In my thesis the quantitative analysis of the results of rheology experiments was difficult because the NaDC gels with or without CB[6] are weak. For these weak gels, poor contact between the plates and inhomogeneities or bubbles in the sample are the source of errors which makes it difficult to obtain reproducible data. However, the rheology experiments provide useful qualitative information regarding the mechanical strength of the gels.

All rheological experiments were performed in the linear viscoelastic regime (LVR) to ensure that the response of the gel to the external forces is independent of the applied stress or strain. The LVR was determined by an oscillatory stress sweep experiment shown in Figure 2.3. The samples were left undisturbed to equilibrate for 20 h

followed by a 30 min time sweep experiment to ensure that the G' and G'' values were stable (Figure 2.4). The absolute values for G' and G" vary between sample preparations. However in the case of NaDC gels, G' was always lower than G", while for NaDC-CB[6] gels G' was always higher than G". In addition, the G' value for the NaDC-CB[6] gel was always higher than for the NaDC gel.

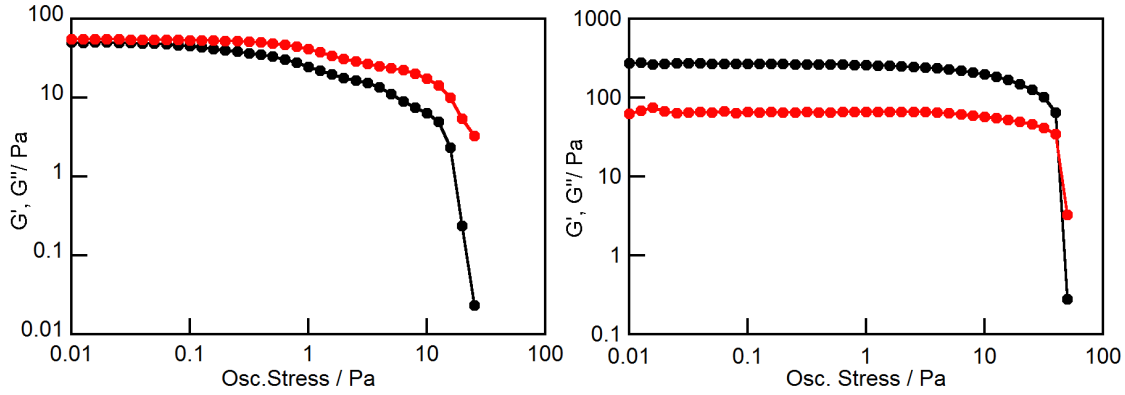

Figure 2.3. Oscillatory stress dependence of G' (black) and G" (red) for freshly prepared NaDC (left) and CB[6]-NaDC gels (right, [CB[6]]/[NaDC] = 0.2) measured after 20 h of equilibration and a 30 min time sweep experiment. Temperature (15 ºC), frequency (0.5 Hz) and strain (0.1 %) were kept constant.

The NaDC gel was shear thinning both in the absence and presence of CB[6], but the critical stress where the breakdown of the self-assembled structures of the gel occurred, determined from the onset of the abrupt decrease of G' and G" during stress sweeps, was slightly higher for NaDC-CB[6] (40 Pa vs. 16 Pa of NaDC, Figure 2.3). The G' and G" values for the NaDC-CB[6] gel are constant over a wide range of oscillatory stress values before the sharp decrease in moduli occurs. In contrast, for the NaDC gel

the moduli remain constant only between 0.01 to ~ 0.1 Pa and a gradual decrease was observed before the abrupt decrease in the moduli.

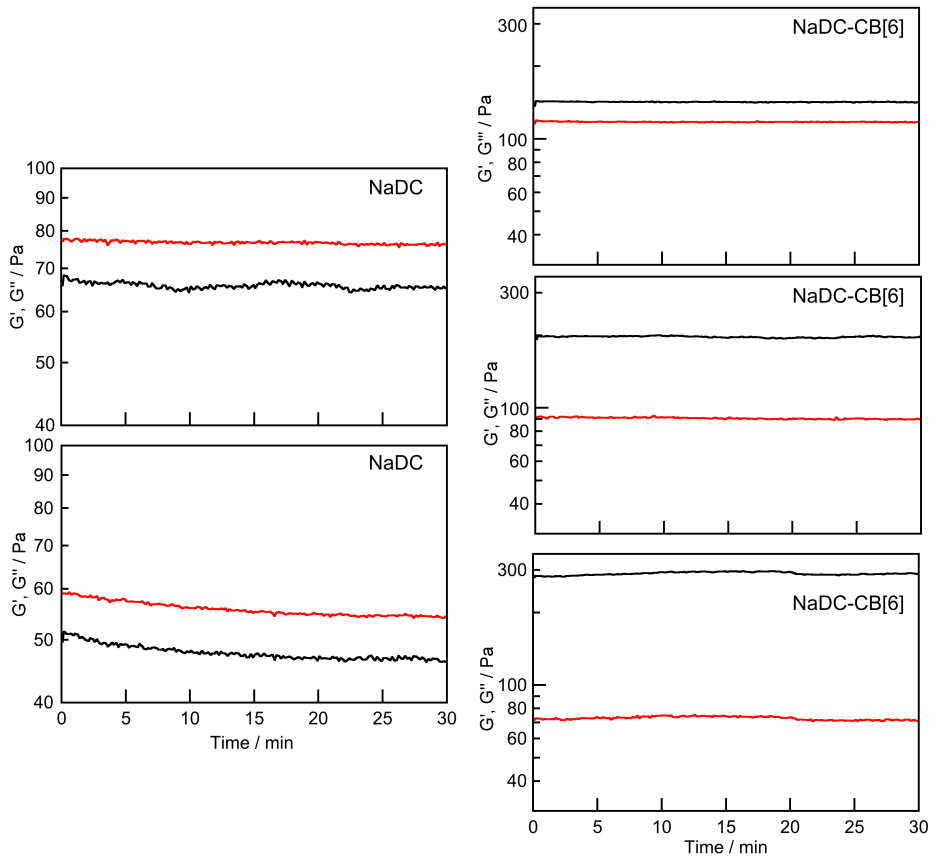

Figure 2.4. Time sweep (T = 15 ºC, frequency = 0.5 Hz, strain = 0.1 %) for individual gels (right - NaDC; left-NaDC-CB[6], [CB[6]]/[NaDC] = 0.2) after equilibrating the sample in the rheometer for 20 h.

For both type of gels, G' was higher than G" when samples went through a temperature annealing cycle (Figure 2.5). One of the main characteristics for a material to be called a gel is that G' should be higher than G". Although for freshly prepared NaDC samples this criterion is not fulfilled, I still consider the NaDC sample a gel since it

fulfills other criteria of gels.[2] For example, the NaDC sample does not flow upon inversion of its sample vial for ca. 1 h. The higher moduli for the gels with CB[6] indicates that addition of CB[6] led to the stiffening of the gel.

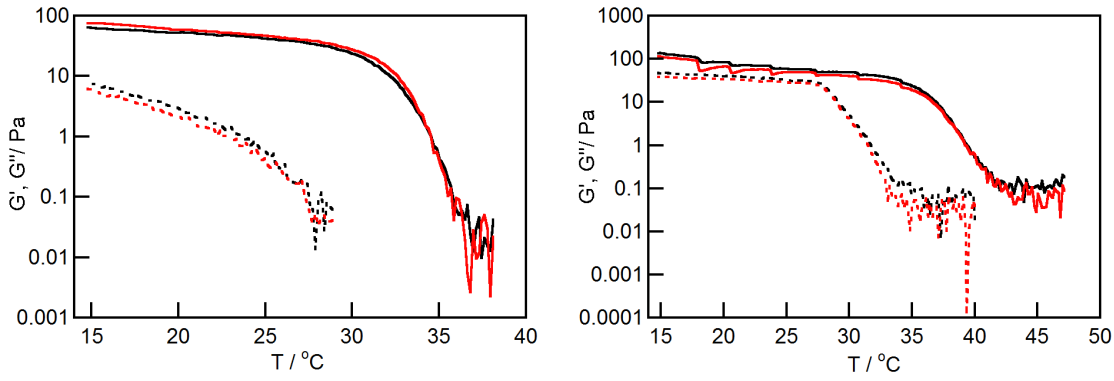

Figure 2.5. Temperature dependence of G' (black) and G" (red) for NaDC gel (left plot) and NaDC-CB[6] gel (right plot, [CB[6]]/[NaDC] = 0.2). Solid and dashed lines represent the heating and cooling cycle respectively. The experiments were performed under a constant frequency of 0.5 Hz and a 0.1% strain.

In the case of the frequency sweep experiments, samples underwent a heating-cooling cycle after the 20 h equilibration time. Frequency sweep experiments are important from two perspectives: first, to evaluate if the "solid-like" material is a gel and second, to determine the strength of the gel. To call a material a "gel" the G' value must be larger than the G" value over a large range of frequencies especially at lower frequencies.[72,83,85] There are reports in the literature where G" increases at lower frequencies while the G' values remain constant. The explanation for this observation is that in an oscillatory measurement the frequency has a reverse relationship with time.

Experiments performed at lower frequencies provide enough time for those processes which need to occur with longer relaxation times to proceed.[72] Frequency sweep experiments on NaDC and NaDC-CB[6] gels that underwent temperature annealing showed that G' remained higher than G" for a wide range of frequencies (Figure 2.6). However, the moduli for both gels showed a strong dependence on the frequency, indicating that these gels are weak as for example in comparison to chemically crosslinked polymer gels where no strong dependence on the frequency is observed. This result was expected since most of the supramolecular gels form due to weak and reversible interactions.

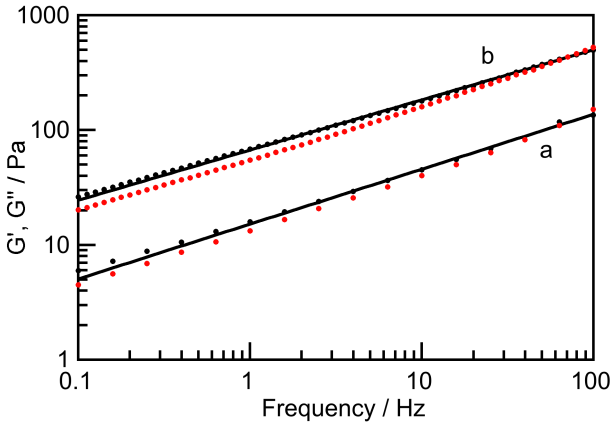

Figure 2.6. Frequency dependence (T = 15 ºC, strain = 0.1%) of G' (black) and G'' (red) for the temperature-annealed gels of NaDC (a, 30 mM) and NaDC-CB[6] (b, [CB[6]]/[NaDC] = 0.2). The solid lines correspond to the fit of the data for G' to Equation 2.1.

The frequency dependence of G' follows a power law (Equation 2.1). The NaDC gel showed slightly stronger frequency dependence (n = 0.48 ± 0.01) than the NaDC-

CB[6] gel (n = 0.437 ± 0.001). This result again indicates stiffening of the gel in the presence of CB[6], as strong gels would show frequency-independent behavior (n = 0), while a high-viscosity liquid would exhibit n = 2.[85]

$$G' \propto f^n \qquad \text{Equation 2.1}$$

2.3.3 Steady-state and time-resolved experiments for pyrene in NaDC gels

Pyrene was chosen as the fluorescence guest molecule, because of its unique photophysical properties which makes this molecule a suitable probe for investigation of the different microenvironments in the gels. The ratio between the intensity of the first (I) and third (III) vibronic bands of the fluorescence emission spectrum of pyrene is a criterion for the polarity of the environment in which pyrene is located.[86] The I/III ratio of pyrene in a 50 mM aqueous solution of phosphate buffer was measured to be 1.73 ± 0.04 (inset of Figure 2.7, 2 independent experiments). For the freshly prepared NaDC gel and CB[6]-NaDC gels at molar ratios of 0.05, 0.1 and 0.2, the I/III ratio of pyrene was 0.94 ± 0.03, 1.17 ± 0.02, 1.29 ± 0.04 and 1.4 ± 0.1 respectively (Figure 2.7, 3 independent experiments).

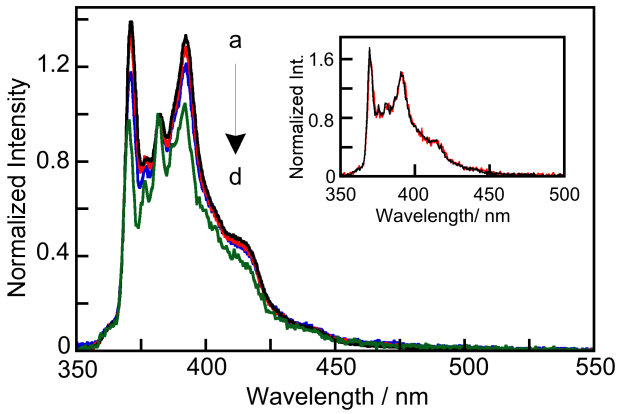

Figure 2.7. Emission spectra normalized at peak III (~ 383 nm) for pyrene (2.0 μM) in freshly prepared NaDC gels (30 mM) with [CB[6]]/[NaDC] ratios of: a - 0.2 (black), b - 0.1 (red), c - 0.05 (blue) and d - 0 (green). The inset shows the normalized spectra at peak III for pyrene (0.5 μM) in 50 mM phosphate buffer in the absence of CB[6] (black) and in the presence of 3 mM CB[6] (red).

The observed I/III ratio value for pyrene is a weighted average of the I/III ratio of pyrene located in different environments within the gel. For example, the measured I/III ratio value for pyrene in the freshly prepared NaDC gel was 0.94. This value is in between the measured I/III ratio of pyrene in 50 mM phosphate buffer (1.73 ± 0.04) and in a 30 mM NaDC solution in the presence of 0.2 M NaCl (0.69 ± 0.01). This result shows that in a freshly prepared gel sample either pyrene is distributed between bile salts aggregates and water or there are binding sites for pyrene in the gel network which are different from the binding sites of primary aggregates of bile salts. Moreover, time-resolved fluorescence experiments described below support the partitioning of pyrene between the aqueous phase of the gel and primary aggregates of the bile salt network.

Variation of the I/III ratio values for the pyrene emission was monitored when the gel sample underwent a heating and cooling cycle. A decrease in the I/III ratios was observed when a freshly prepared NaDC gel sample was heated (Figure 2.8).

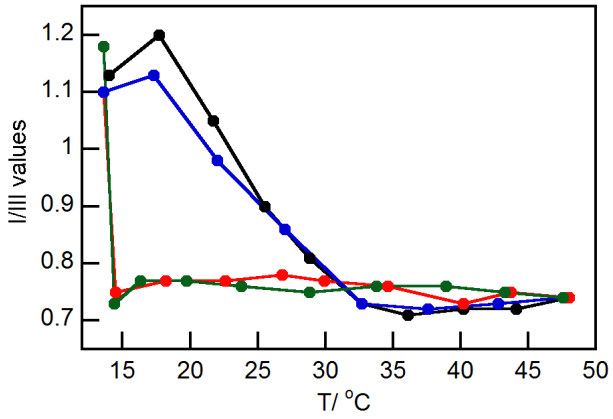

Figure 2.8. Dependence of the I/III ratio for the pyrene emission (2 μM) in a NaDC gel on temperature for subsequent heating (black and then blue) and cooling cycles (red and then green). The lines are included to guide the eye.

The I/III ratio at 48 ºC was 0.74 ± 0.01 (Figure 2.9, 4 independent experiments). This value is close to the value observed for NaDC aggregates in solution (0.69 ± 0.01 for 30 mM NaDC in 0.2 M NaCl). This result suggests that at high temperatures pyrene is located in a hydrophobic environment, namely the primary aggregates of bile salts.[44,87] As depicted in Figure 2.8, the relocation of pyrene into bile salt aggregates is a gradual process which occurs at temperatures well below the T_{gs} for the NaDC gel of 43 °C. During the cooling process, the I/III ratio value remained constant around 0.75 until ca. 13-15 °C was reached when a sharp enhancement of the I/III ratio was observed. This

result indicates that during cooling pyrene is located in the NaDC network until the lowest temperature is reached. The hysteresis for the change in I/III ratio values is a reversible process since the same dependencies were observed for a second heating and cooling cycle (Figure 2.8).

Pyrene excimer emission was observed in the NaDC gel at low temperatures with a very low intensity (<8%) in comparison to the monomer emission (Figure 2.9). Pyrene excimer normally forms when a pyrene molecule in its ground state encounters another pyrene molecule in its excited state which leads to a broad fluorescence emission at wavelengths centered at 470 nm. When a sample of freshly prepared NaDC gel was heated gradually, the excimer emission was observed at temperatures below 36 °C. At around 36 °C, where the material is still a gel, the excimer emission disappeared. The excimer emission was not observed for temperatures above 36 ºC in the gel and for the sol phase. During cooling the excimer emission reappeared at 14 ºC and had the same intensity as before the heating cycle (Figure 2.9). The same trends were observed when the NaDC gel went through the second heating and cooling cycle. Formation of pyrene excimer was used previously to monitor the gelation of NaDC.[22] However, the experimental conditions (20 mM phosphate buffer concentration and pH 6.8) for the previous work were different from the conditions I used. In contrast to the NaDC gel, no excimer emission was observed for the NaDC-CB[6] gels.

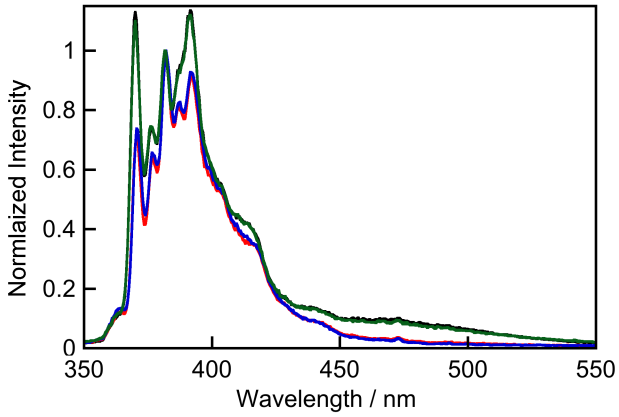

Figure 2.9. Emission spectra for pyrene (2.0 μM) in a freshly prepared NaDC gel at 15 ºC (black), heated to 36 ºC (red) and then 48 ºC (blue), followed by slow cooling to 14 ºC (green).

Time-resolved fluorescence is used for the characterization of supramolecular systems when fluorophores bound to different binding sites in the system have different excited state lifetimes.[88] A monoexponential decay can be recorded when the fluorophore is placed in just one environment, while the decay can be fitted to a sum of exponential terms when the fluorophore is bound to different environments (Equation 2.2). In this equation I is the fluorescence intensity, A_i and τ_i are the pre-exponential factor and the lifetime of the emissive species "i". The A_i value is related to the amount of species i in the environment. The sum of the A_i values is equal to 1 by definition.

$$I(t) = I_0 \sum_{1}^{i} A_i \, e^{-t/\tau_i} \qquad \text{Equation 2.2}$$

The emission from excited pyrene in water has a monoexponential decay with a lifetime around 130 ns.[75,76] The lifetime of pyrene in 30 mM NaDC in the presence of 0.2 M NaCl was measured as 386 ± 6 ns. Fluorescence decays of the pyrene emission in NaDC gels were collected over a 5 μs time window. Therefore, the time increment for each channe1 is 4.7 ns. The use of the triangular cell and the orthogonal geometry between excitation and emission optics for the SPC measurements led to the observation of light scattering. The time profile of the scattered light has the time profile of the excitation source and is very sharp (Figure 2.10). The emission decays were recorded for 100,000 counts in the channel of maximum intensity to ensure that sufficient numbers of counts (5,000-12,000) were collected for the maximum pyrene emission intensity. Moreover, there was a short-lived component from the emission of a bile salt impurity (<10 ns). The lifetime of the impurity in a sodium cholate sample was determined to be around 2-5 ns.[87] The light scattering and impurity emission were eliminated by starting the fit for the analysis of the data 3-10 channels (14-47 ns) after the maximum peak of the decay. A tail fit was used for the analysis because the excitation source is narrow and recovolution of the excitation time profile with the decay was not required.

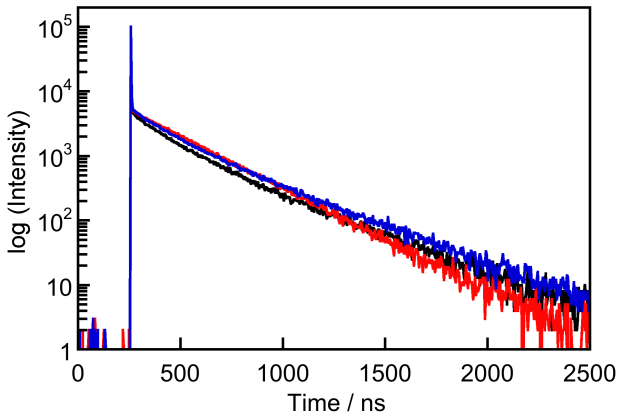

Figure 2.10. Decays for the emission of pyrene (2 μM) in a NaDC gel for the freshly prepared sample at 14 ºC (black), at 50 ºC (red) and after slow cooling at 15 ºC (blue). For lifetimes and pre-exponential values see Table 2.2.

For a freshly prepared NaDC gel at RT, the fluorescence decays of pyrene could be fitted with a sum of two exponentials using Equation 2.3. The obtained lifetimes were 131 and 342 ns, which are the same as the lifetime for pyrene in water and in the primary aggregates of bile salt in solution. This result indicates that a portion of pyrene molecules are located in the aqueous phase of the gel while the rest are trapped in the hydrophobic sites of the network.

$$I(t) = A_w e^{-t/\tau_w} + A_{BS} e^{-t/\tau_{BS}} \qquad \text{Equation 2.3}$$

In an independent experiment the lifetime of pyrene in water was measured at different temperatures (Figure 2.11). The data were fit empirically to a quadratic equation ($\tau = 0.0235T^2 - 2.41T + 169$), which was used to calculate the value of the pyrene lifetimes in water at different temperatures. The values for the pyrene lifetimes in water were then fixed for the analysis of the pyrene decays in the NaDC gel (Table 2.2) for the

purpose of increasing the precision of the pre-exponential A_w values. For a freshly prepared NaDC gel at the low temperature of 14-15 ºC, around 55% of pyrene molecules were in water and around 45% were in the bile salt network. Gradual heating of the sample led to the relocation of pyrene from water into the network. At temperatures higher than 40 °C almost all the pyrene molecules were placed in the hydrophobic sites of the network. The gel-to-sol transition was examined by inverting the triangular cell and it was determined to be around 50 °C. The fluorescence decays of pyrene at 50 °C and in the sol phase were mono-exponential which showed that all the pyrene molecules were in the aggregates, although the phase change occurred (Figure 2.12 top plot and Table 2.2). When the temperature was gradually reduced the pyrene molecules remained in the bile salt aggregates and network for a wide range of temperatures. However, at the lowest temperature around 15 °C a significant portion (47%) of pyrene molecules were released from the network into the water (Figure 2.12 bottom plot and Table 2.2).

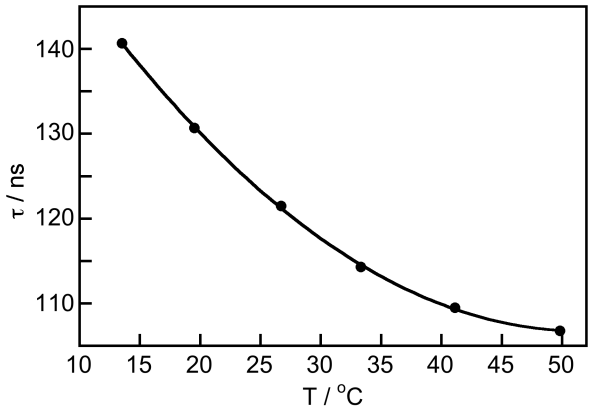

Figure 2.11. Dependence of the singlet excited state lifetime of pyrene (1 μM) in water with temperature.

Table 2.2. Lifetimes and pre-exponential factors for pyrene in water[a] (τ_w, A_w) and in the bile salt network/aggregate (τ_{BS}, A_{BS}) of a NaDC gel.[b]

T / °C	τ_w / ns	A_w	τ_{BS} / ns	A_{BS}	χ^2
14	140	0.55 ± 0.01	343	0.45 ± 0.01	1.210
18	134	0.54 ± 0.01	344	0.46 ± 0.01	1.127
21	129	0.45 ± 0.01	334	0.55 ± 0.01	0.967
25	124	0.35 ± 0.01	330	0.65 ± 0.01	0.903
29	119	0.22 ± 0.01	324	0.78 ± 0.01	1.145
32	115	0.13 ± 0.01	316	0.87 ± 0.01	1.034
36	112	0.08 ± 0.01	307	0.92 ± 0.01	1.005
40	110	0.02 ± 0.01	293	0.98 ± 0.02	1.061
46			283	1	1.001
47			273	1	1.107
50			267	1	1.000
46			286	1	0.968
42			304	1	1.006
38			324	1	1.121
34			342	1	1.126
29			360	1	1.071
25			374	1	1.093
21			388	1	1.045
18			390	1	1.104
15	139	0.47 ± 0.01	348	0.53 ± 0.01	1.106

[a], the lifetimes for pyrene in water were fixed to the values calculated from the data in Figure 2.11; [b], the errors for the A values are those recovered from the fit of the data. The estimated errors for τ_{BS} < 5 ns (averages from independent experiments cannot be performed because the temperatures for each experiment are slightly different).

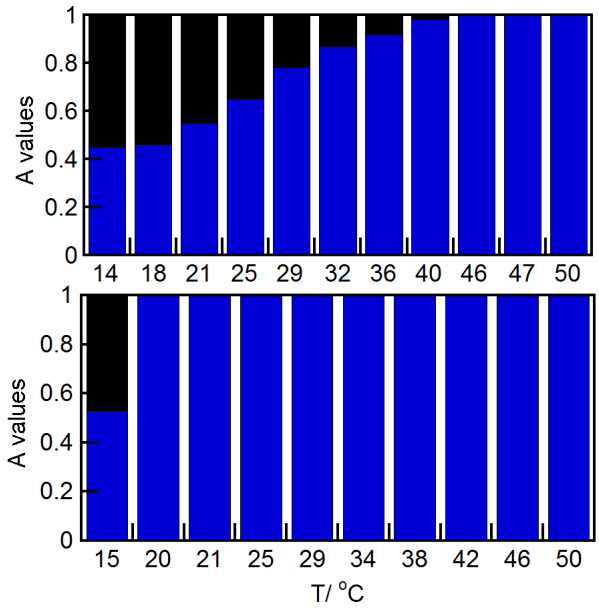

Figure 2.12. Dependence on temperature of the A_W (black) and A_{BS} (blue) values recovered from time-resolved fluorescence studies for the heating (top) and cooling cycles (bottom).

The hysteresis for the mobility of pyrene from water into the aggregates and the reverse was only observed when the sample passed the gel-sol transition temperature, i.e. the sol was formed during heating. If the sample was cooled before the phase change, then the amount of pyrene in water (A_w) was observed to increase gradually (Figure 2.13). This result showed that the formation of the sol is required for the hysteresis of the pyrene relocation between the heating and cooling cycles to occur.

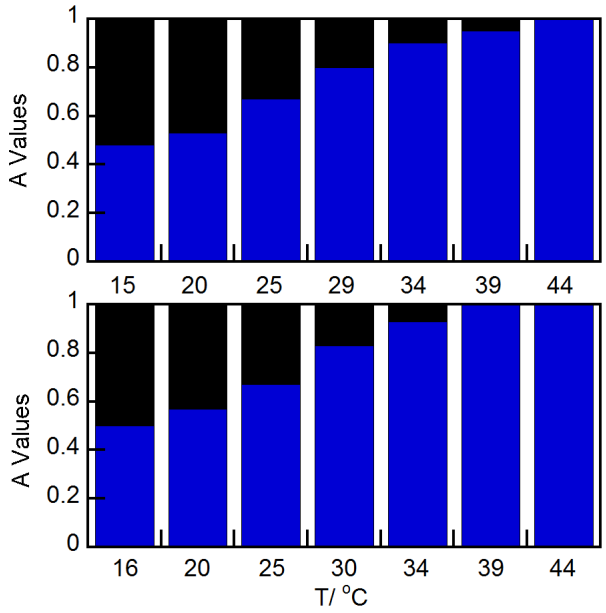

Figure 2.13. Dependence on temperature of the A_W (black) and A_{BS} (blue) values for the heating (top) and cooling (bottom) of the NaDC gel for a heating/cooling cycle where the sol was not formed when the sample was heated.

2.3.4 Steady-state and time-resolved experiments for pyrene in NaDC-CB[6] gels

Steady-state fluorescence measurements revealed that variation of the I/III ratio values with temperature for NaDC-CB[6] gels is similar to that observed for NaDC gels. However, it was observed that the sharp enhancement of the I/III ratio occurs at higher temperatures when CB[6] is present in the system (Figure 2.14).

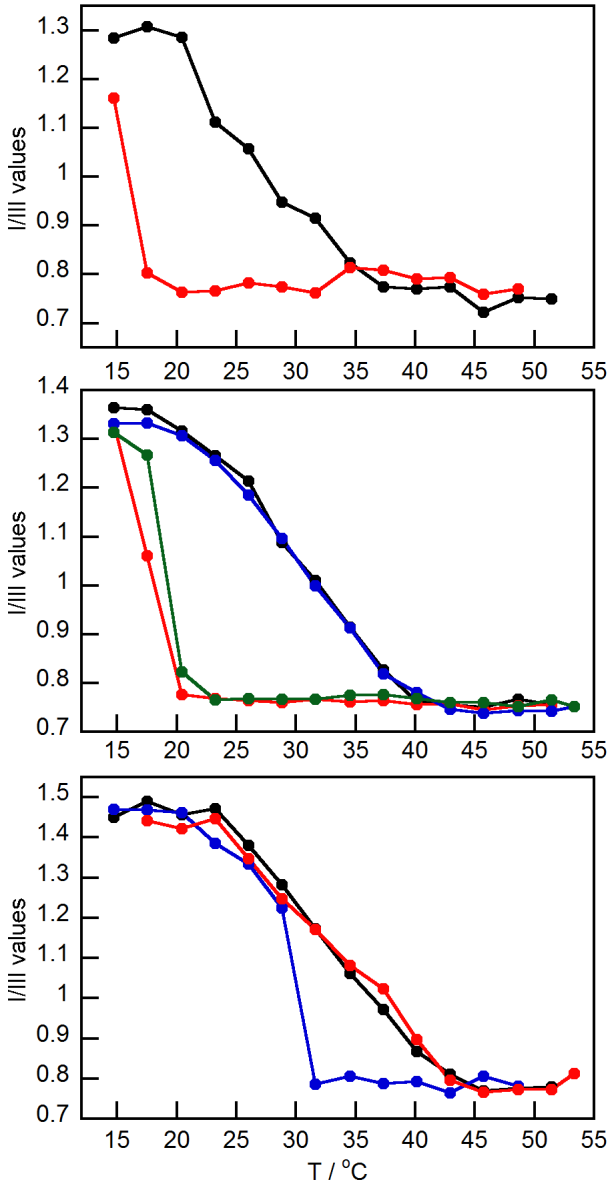

Figure 2.14. Dependence of the I/III ratio for the pyrene (5 μM) emission in NaDC-CB[6] gels ([NaDC] = 30 mM, top-[CB[6]]/[NaDC] = 0.05; middle-[CB[6]]/[NaDC] = 0.1; bottom-[CB[6]]/[NaDC] = 0.2) for heating (black and then blue) and cooling (red and then green) cycles. The lines are included to guide the eye.

The temperature at which the rise of the I/III ratio was observed is directly (but not linearly) dependent on the concentration of CB[6]. For the molar ratios of 0.05, 0.1 and 0.2 between CB[6] and NaDC the jump in I/III ratio values occurs at 17 °C, 20 °C and 31 °C respectively. It was important to ensure the change in the I/III ratio was not due to gelation during cooling. For this reason a gel sample was heated in a triangular cell inside the fluorimeter sample holder. The sol-to-gel transition (T_{sg}) was determined by inverting the cell at different temperatures during cooling. The T_{sg} for the gels with the molar ratio of 0.05 and 0.2 between CB[6] and NaDC were determined to be 40 and 42 °C, which are much higher than the temperatures at which the enhancement of I/III ratio happened. This result shows that the relocation of pyrene leading to the sharp increase in the I/III values is not related to the gelation of the gel.

Time-resolved fluorescence experiments were performed for the pyrene emission in the NaDC-CB[6] gels. The decays for the pyrene emission were initially fitted with a sum of the two exponentials where the assumption was made that pyrene was located in water and in the bile salt network. However, not all the decays could be fitted adequately to a sum of two exponentials. In addition, the trends in variation of pre-exponential factors did not match with the trends in the changes of I/III ratio values. This result suggested that a third emitting species was present, which I assigned to the complex of pyrene with CB[6] in the gel.

Pyrene was shown to have a weak interaction with CB[6] ($K = (3.1 \pm 0.9) \times 10^2$ M^{-1}), because pyrene is too large to fit inside the CB[6] cavity (Scheme 2.5).

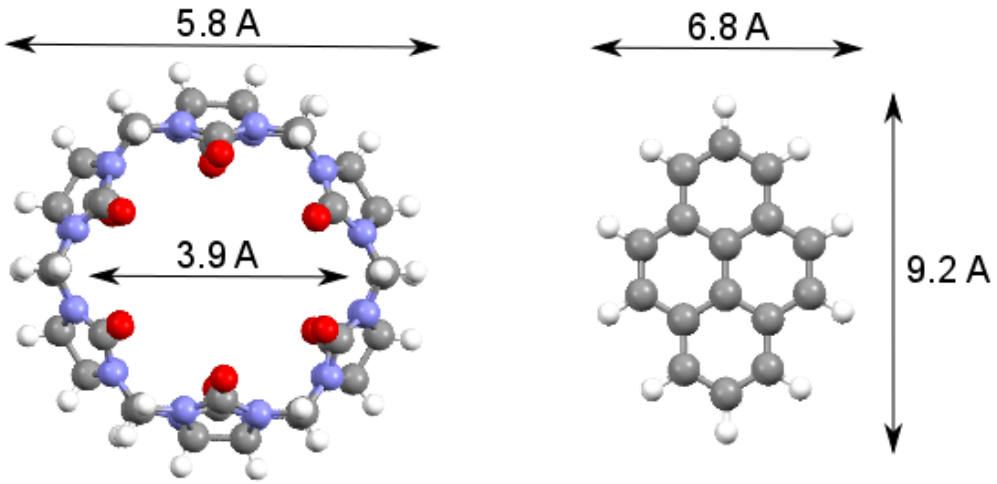

Scheme 2.5. Schematic representation of CB[6] and pyrene dimensions.

Despite the weak interaction, the concentration of CB[6] is sufficiently high in the gel for pyrene to interact with this macrocycle. In a 3 mM solution of CB[6] containing 0.5 μM pyrene in the absence of NaDC the pyrene emission decay was fitted with a sum of three exponentials. The shortest lifetime is related to an impurity emission from CB[6] (Figure 2.15, top).

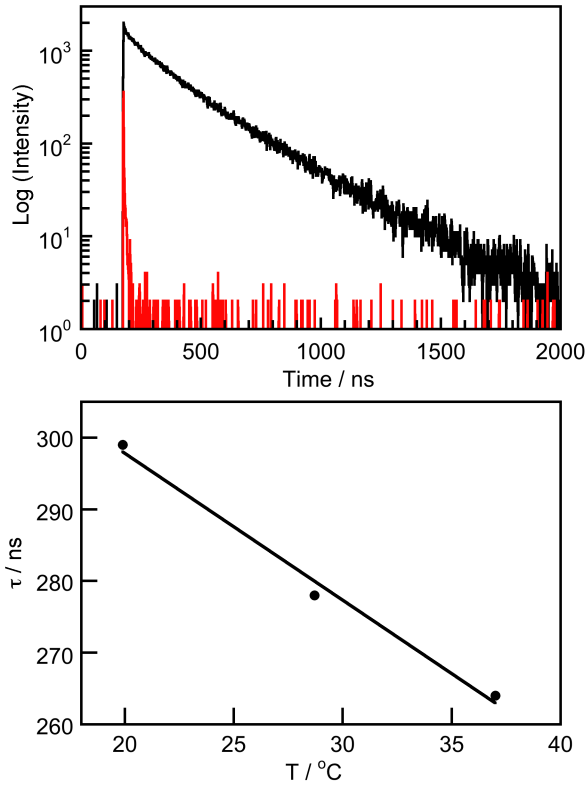

Figure 2.15. Top: Emission decay for pyrene (0.5 μM)/CB[6] (3 mM, black) and CB[6] (3 mM, red) in 50 mM phosphate buffer solutions where the decays were collected for the same amount of time. Bottom: Dependence of the singlet excited state lifetime of pyrene (0.5 μM) in the pyrene-CB[6] complex ([CB[6]] = 3 mM) in 50 mM phosphate buffer solution with temperature.

An intensity of 350 counts in the channel of maximum intensity was measured for a CB[6] sample when the emission was collected with the same instrumental settings and for the same amount of time as for the decay of the pyrene-CB[6] solution. The intensity of the short-lived species from the fit of the emission from the pyrene-CB[6] solution was 320 counts, supporting the assignment that the fast component is due to the impurity present in CB[6]. The second lifetime, which had a value around 130 ns, was fixed to this

value because pyrene has the lifetime of 130 ns when it is in water. The third lifetime, which had a value around 300 ns, was assigned to the emission of pyrene-CB[6]. The obtained values for the pre-exponential factors considering only the pyrene emission were 0.46 and 0.54 for pyrene in water and pyrene interacting with CB[6], respectively. These values are in good agreement with the estimated values considering the reported equilibrium constant of 4×10^2 M^{-1}, where in the presence of 3 mM CB[6] pyrene free in water is calculated to be 44 % of the total pyrene molecules, while 56% forms the complex with CB[6]. The lifetime of pyrene interacting with CB[6] was measured at different temperatures (Figure 2.15, bottom). The data were fitted to an empirical equation (τ = -2.05T + 339) and the pyrene lifetimes in the pyrene-CB[6] complex at specific temperatures were calculated using this equation.

The I/III ratio measured from the steady-state spectrum of the pyrene/CB[6] solution was 1.53 ± 0.07 (inset Figure 2.7, average from 3 independent experiments). The fractional intensities (F_i) for the steady-state spectra (Equation 2.4) were 0.31 ± 0.05 for pyrene in water (F_w) and 0.7 ± 0.1 for pyrene-CB[6] (F_{CB6}) (averages from 3 independent experiments).

$$F_i = \frac{A_i \tau_i}{\sum_1^i A_i \tau_i} \qquad \text{Equation 2.4}$$

The measured I/III ratio (I/III_{obs} = 1.53 ± 0.07) corresponds to the weighted average of the emission for pyrene in 50 mM aqueous sodium phosphate buffer (I/III_w =

1.73 ± 0.04) and complexes to CB[6] (I/III_{CB}, Equation 2.5), and the value for I/III_{CB} for pyrene-CB[6] was calculated to be 1.4 ± 0.3.

$$I/III_{obs} = F_w \times I/III_w + F_{CB6} \times I/III_{CB6} \qquad \text{Equation 2.5}$$

These results show that pyrene in the CB[6] complex experiences an environment that is still fairly polar because of the relatively high I/III ratio, but where pyrene is in a protected or relatively rigid environment leading to a longer lifetime than in water.

Fluorescence time-resolved experiments were used to understand the distribution of pyrene molecules between the three environments in the gels containing CB[6], which include the aqueous phase, interaction with CB[6] and bile salt aggregates. The pyrene decays were analyzed systematically so that the obtained pre-exponential factors were reliable at each temperature. For this reason the lifetime of pyrene in water and bound to CB[6] at each specific temperature were fixed to the values obtained from the empirical equation derived from the data in Figures 2.11 and 2.15. It was assumed that the lifetimes of excited pyrene in the bile salt network were close to those obtained in the experiments without CB[6]. These lifetimes (τ_{BS}) were calculated from the fit of the data in Figure 2.16 to an empirical equation ($\tau = -0.042T^2 + 0.026T + 373$) and a linear equation ($\tau = -4.14T + 475$) for heating and cooling processes, respectively. In some cases, fixing both of the lifetimes of pyrene bound to CB[6] and in the NaDC network led to the observation of high χ^2 values (> 1.3). In these cases, one of the lifetimes was kept floating and a good fit was obtained ($\chi^2 \leq 1.3$). Table 2.3 to Table 2.5 illustrate the obtained values for both fits.

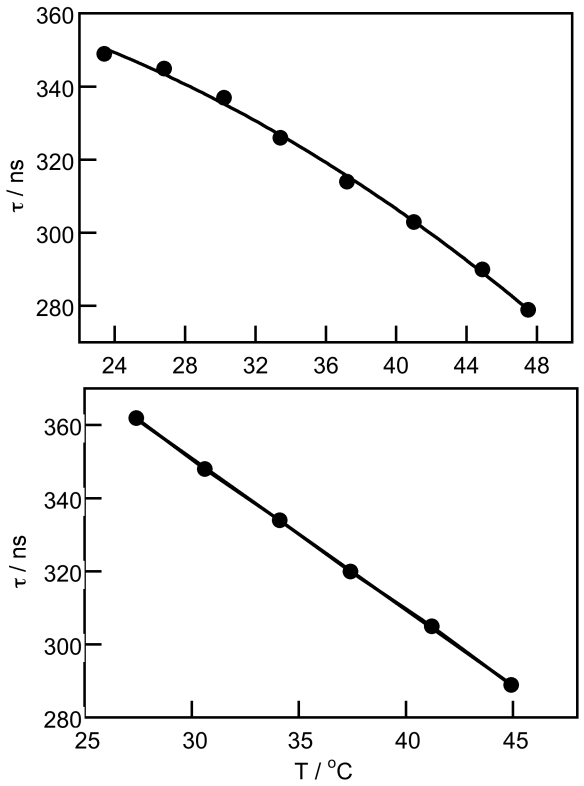

Figure 2.16. Dependence of the singlet excited state lifetime of pyrene (5 μM) in the NaDC gel with temperature for the heating cycle (top, fit to a quadratic equation) and cooling cycle (bottom, fit to a linear equation).

The A values obtained from the fits with the better χ^2 values were used for plots in Figure 2.17 to Figure 2.19. As mentioned above, the analysis of pyrene decays in NaDC gels with CB[6] were performed very systematically. First, the decay was fitted to a mono-exponential function using one of the three expected lifetimes (τ_w or τ_{CB} or τ_{BS}). The goodness of the fit was judged by inspection of the χ^2 value and the randomness of the residuals. If the fit was not adequate, the pyrene decay was fitted to the sum of the two exponentials where the lifetime of two of the pyrene species were fixed. The A

values for this fit were used if the obtained χ^2 value was satisfactory and the residuals were random. Otherwise, the decay was fitted to the sum of the three exponential where all the τ_w, τ_{CB} and τ_{BS} were fixed (Table 2.3-Table 2.5). In this case a term for the pyrene-CB[6] complex (A_{CB}, τ_{CB}) was added to the Equation 2.2.

Monitoring the variation of pre-exponential factors for each of the three possible species upon change in temperature revealed that pyrene was free in water or interacted with CB[6] at the beginning of the heating cycle when the temperatures were low. In fact, this was the case for all three molar ratios between CB[6] and NaDC that were studied (Figure 2.17-Figure 2.19). Gradual heating of the gel led to relocation of pyrene from water or the CB[6] complex to the bile salt aggregates. This relocation of pyrene to the bile salt aggregates is a gradual process and was complete before the gel-to-sol transition happened. The calculated lifetime for pyrene in the NaDC aggregate at 51 ºC was the same within the estimated error as the fit where the lifetime was floated. The decays could not be fitted to the sum of two exponentials, because the second lifetime was recovered with a negative A value, which is an artifact since no growth kinetics were observed. The small difference in the lifetimes could indicate that the bile salt aggregate in which pyrene resides is slightly different in the presence of CB[6].

Even after the conversion of the gel to the sol, all the pyrene molecules remained in the NaDC aggregates. Hysteresis was observed when the sample was cooled gradually. During cooling pyrene remained in the bile salt network and was released into water or was bound to CB[6] at higher temperatures in comparison to the temperature at which the

release occurred for the NaDC gel in the absence of CB[6]. Interestingly, the temperature at which the release of the guest happens is directly related to the concentration of CB[6] in the system. These results indicate that the presence of CB[6] as an additive plays a role in the partitioning of pyrene between different binding environments in the gel.

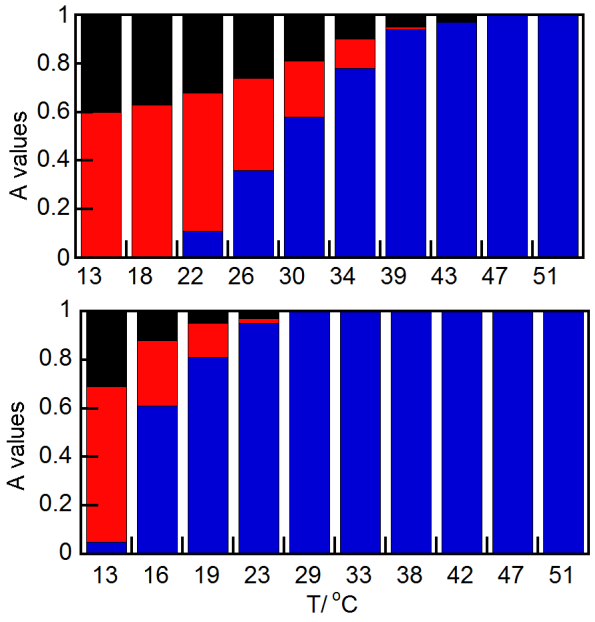

Figure 2.17. Dependence on temperature of the A_W (black), A_{CB} (red) and A_{BS} (blue) values for the heating (top) and cooling (bottom) of the NaDC-CB[6] gel ([CB[6]]/[NaDC] = 0.05).

Table 2.3. Lifetimes and pre-exponential factors for pyrene in water[a] (τ_w, A_w), interacting with CB[6][b] (τ_{CB}, A_{CB}) and in the bile salt network/aggregate[c] (τ_{BS}, A_{BS}) of a CB[6]-NaDC gel at a molar ratio of 0.05.[d]

T / °C	τ_w / ns	A_w	τ_{CB} / ns	A_{CB}	τ_{BS} / ns	A_{BS}	χ^2
13	141	0.40 ± 0.01	312	0.60 ± 0.01			1.200
18	134	0.37 ± 0.01	303	0.63 ± 0.01			1.022
22	128	0.32 ± 0.01	294	0.57 ± 0.03	354	0.11 ± 0.02	1.065
26	122	0.26 ± 0.01	285	0.38 ± 0.03	345	0.36 ± 0.02	0.949
30	117	0.19 ± 0.01	277	0.23 ± 0.03	335	0.58 ± 0.03	0.959
34	114	0.10 ± 0.01	268	0.12 ± 0.03	324	0.78 ± 0.03	1.033
39	110	0.05 ± 0.01	259	0.01 ± 0.03	310	0.94 ± 0.04	1.020
43	108	0.03 ± 0.01			296	0.97 ± 0.01	0.998
47					279	1	1.105
51					265	1	1.817
					(268)	1	(0.992)
47					282	1	1.185
42					301	1	1.140
38					320	1	0.981
33					339	1	1.189
29					358		1.016
23	125	0.03 ± 0.01	291	0.02 ± 0.02	378	0.95 ± 0.03	1.093
19	131	0.05 ± 0.01	300	0.14 ± 0.02	396	0.81 ± 0.03	0.899
16	136	0.12 ± 0.01	306	0.27 ± 0.02	407	0.61 ± 0.02	1.088
13	141	0.31 ± 0.01	311	0.64 ± 0.02	420	0.05 ± 0.01	1.076

[a], the lifetimes for pyrene in water were fixed to the values calculated from the data in Figure 2.11; [b], the pyrene lifetimes in the pyrene-CB[6] complex were fixed to the values calculated from the data in Figure 2.15; [c], the pyrene lifetimes in the NaDC network were fixed to the values calculated from the data in Figure 2.16; [d], the errors for the A values are those recovered from the fit of the data. Values in parenthesis correspond to parameters recovered when τ_{BS} was not fixed. The estimated error for the lifetime value that was not fixed is ± 5 ns.

Table 2.4. Lifetimes and pre-exponential factors for pyrene in water[a] (τ_w, A_w), interacting with CB[6][b] (τ_{CB}, A_{CB}) and in the bile salt network/aggregate[c] (τ_{BS}, A_{BS}) of a CB[6]-NaDC gel at a molar ratio of 0.1.[d]

T / °C	τ_w / ns	A_w	τ_{CB} / ns	A_{CB}	τ_{BS} / ns	A_{BS}	χ^2
19	130	0.37 ± 0.01	299	0.63 ± 0.01			1.529
		(0.29 ± 0.01)	(279)	(0.71 ± 0.01)			(1.084)
23	125	0.32 ± 0.01	291	0.68 ± 0.01			1.281
27	121	0.27 ± 0.01	284	0.65 ± 0.02	343	0.08 ± 0.01	1.104
30	117	0.22 ± 0.01	277	0.53 ± 0.02	335	0.25 ± 0.01	1.067
34	114	0.17 ± 0.01	270	0.37 ± 0.01	326	0.46 ± 0.01	0.988
37	111	0.10 ± 0.01	262	0.20 ± 0.02	315	0.70 ± 0.02	1.182
41	109	0.05 ± 0.01	256	0.10 ± 0.02	305	0.85 ± 0.02	1.011
45					288	1	1.373
					(290)	1	(1.244)
49					275	1	1.935
					(279)	1	(1.045)
51					265	1	1.141
49					273	1	3.581
					(285)	1	(1.098)
46					287	1	3.056
					(297)		(1.098)
41					305	1	1.876
					(312)	1	(0.952)
38					320	1	1.914
					(327)	1	(1.018)
34					334	1	1.244
31			275	0.18 ± 0.01	345	0.82 ± 0.01	1.208
27	120	0.25 ± 0.01	283	0.68 ± 0.01	362	0.07 ± 0.01	1.171
24	124	0.30 ± 0.01	289	0.70 ± 0.01			1.312
		(0.29 ± 0.01)	(281)	(0.71 ± 0.01)			(1.290)
21	129	0.33 ± 0.01	297	0.67 ± 0.01			1.553
		(0.28 ± 0.01)	(280)	(0.72 ± 0.01)			(1.269)

[a], the lifetimes for pyrene in water were fixed to the values calculated from the data in Figure 2.11; [b], the pyrene lifetimes in the pyrene-CB[6] complex were fixed to the values calculated from the data in Figure 2.15; [c], the pyrene lifetimes in the NaDC network were fixed to the values calculated from the data in Figure 2.16; [d], the errors for the A values are those recovered from the fit of the data. Values in parenthesis correspond to parameters recovered when τ_{BS} was not fixed. The estimated error for the lifetime value that was not fixed is ± 5 ns.

At high temperatures high χ^2 values were obtained when the lifetime for pyrene in the bile salt network was fixed. The lifetimes obtained when τ_{BS} was floated are close to the ones that were fixed and were calculated for the dependence in NaDC gels without CB[6]. Fits to the sum of two exponentials led to high χ^2 values and a negative A value for one of the lifetimes, which is an artifact since no growth kinetics were observed. These results indicate that the deviation observed is not due to the presence of a small amount of pyrene-CB[6]. In addition, if the deviations observed at high temperature were due to the presence of pyrene-CB[6], then larger deviations should have been observed at higher CB[6] concentrations (Table 2.5), which was not the case.

At the low temperatures when the best fits were obtained for pyrene in water and bound to CB[6], the fits were not adequate with the calculated τ_{CB} values (Table 2.4 and Table 2.5). The variations obtained for τ_{CB} when this parameter was floated could indicate that the lifetime for the pyrene-CB[6] complex in the gel is slightly different from the τ_{CB} lifetime for pyrene in the complex in aqueous solution. The lifetime recovered from the sum of two exponentials is much shorter than the lifetime for pyrene in the bile salt network (by ~ 60 ns for the heating cycle and ~ 90 ns for the cooling cycle) and the lifetime recovered when the second lifetime was floated is close to that of pyrene in the CB[6] complex, and cannot correspond to the emission from pyrene in the bile salt network.

Table 2.5. Lifetimes and pre-exponential factors for pyrene in water[a] (τ_w, A_w), interacting with CB[6][b] (τ_{CB}, A_{CB}) and in the bile salt network/aggregate[c] (τ_{BS}, A_{BS}) of a CB[6]-NaDC gel at a molar ratio of 0.2.[d]

T / °C	τ_w / ns	A_w	τ_{CB} / ns	A_{CB}	τ_{BS} / ns	A_{BS}	χ^2
20	130	0.38 ± 0.01	299	0.62 ± 0.01			2.163
		(0.23 ± 0.01)	(272)	(0.77 ± 0.01)			(1.007)
24	124	0.34 ± 0.01	289	0.66 ± 0.01			1.793
		(0.24 ± 0.01)	(269)	(0.76 ± 0.01)			(1.185)
29	119	0.29 ± 0.01	280	0.71 ± 0.01			1.087
33	115	0.23 ± 0.01	271	0.66 ± 0.02	328	0.12 ± 0.01	1.206
37	111	0.18 ± 0.01	262	0.41 ± 0.02	315	0.42 ± 0.01	1.026
42	109	0.09 ± 0.01	254	0.20 ± 0.02	301	0.71 ± 0.02	1.109
46	107	0.02 ± 0.01			285	0.98 ± 0.01	1.107
50					269	1	1.431
					(273)		(0.995)
46					284	1	1.144
42					302	1	1.114
38	111	0.01 ± 0.01			320	0.99 ± 0.01	1.139
33	115	0.14 ± 0.01	271	0.48 ± 0.03	338	0.38 ± 0.02	1.062
29	119	0.30 ± 0.01	280	0.70 ± 0.01			1.034
25	123	0.35 ± 0.01	288	0.65 ± 0.01			1.392
		(0.26 ± 0.01)	(269)	(0.74 ± 0.01)			(1.047)
20	130	0.38 ± 0.01	298	0.62 ± 0.01			1.728
		(0.23 ± 0.01)	(270)	(0.77 ± 0.01)			(0.948)

[a], the lifetimes for pyrene in water were fixed to the values calculated from the data in Figure 2.11; [b], the pyrene lifetimes in the pyrene-CB[6] complex were fixed to the values calculated from the data in Figure 2.15; [c], the pyrene lifetimes in the NaDC network were fixed to the values calculated from the data in Figure 2.16; [d], the errors for the A values are those recovered from the fit of the data. Values in parenthesis correspond to parameters recovered when τ_{BS} was not fixed. The estimated error for the lifetime value that was not fixed is ± 5 ns.

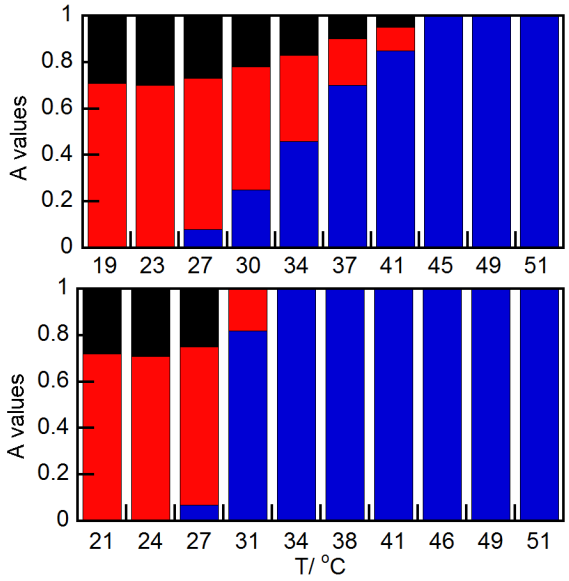

Figure 2.18. Dependence on temperature of the A_W (black), A_{CB} (red) and A_{BS} (blue) values for the heating (top) and cooling (bottom) of the NaDC-CB[6] gel ([CB[6]]/[NaDC] = 0.1).

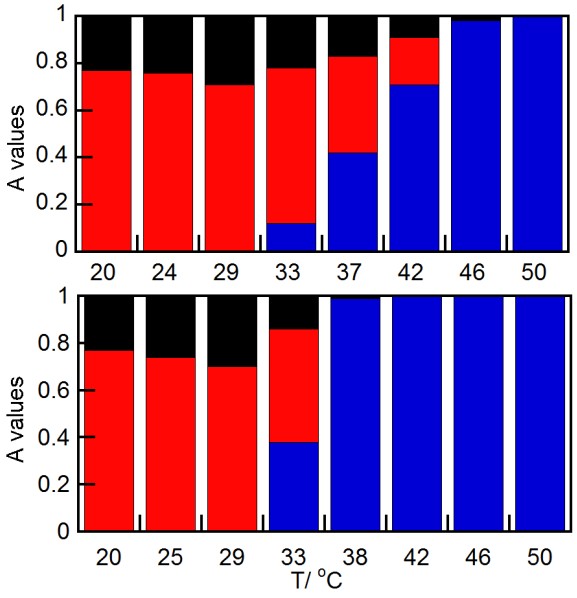

Figure 2.19. Dependence on temperature of the A_W (black), A_{CB} (red) and A_{BS} (blue) values for the heating (top) and cooling (bottom) of the NaDC-CB[6] gel ([CB[6]]/[NaDC] = 0.2).

The trends for the temperatures where changes to the I/III ratios were first observed during heating (T_+) and cooling (T_-) are similar to the trends observed for the appearance ($A_{BS} \neq 0$, T'_+) or disappearance ($A_{BS} = 0$, T'_-) of a pyrene species associated with the NaDC network (Table 2.6), indicating that the two experiments probed the relocation of pyrene between the various sites in the gel.

Table 2.6. Temperature for the onset of the changes for the I/III ratios during the heating (T_+) and cooling (T-) cycles and the temperature where A_{BS} first appears during heating ($A_{BS} \neq 0$, T'_+) or disappears during cooling ($A_{BS} = 0$, T'_-).

CB[6]/NaDC	**I/III change**		A_{BS} **change**	
	T_+ / °C	T_- / °C	T'_+ / °C	T'_- / °C
0	22	14	14	15
0.05	21	17	22	< 13
0.1	26	20	27	24
0.2	29	31	33	29

2.4 Discussion

Previous reports illustrate that although the variation of the concentration of NaDC, ionic strength and pH of the medium leads to changes in the mechanical properties of the NaDC gel, the mechanical strength of the gel is not significantly influenced by the variation of these parameters and the NaDC gel remained "weak".[29,56] If a material is a gel, it means that it has a yield stress and does not flow. The yield stress (σ) has two components (Equation 2.6).[83] G is the modulus and represents the rigidity or stiffness of the network, while γ_c is the critical strain, which is related to the strength of the bonds in

the network. For a gel to be strong both of these components should have high values.[83] The modulus G includes G', which is the storage modulus, and G", which is the loss modulus. In this work, the mechanical strength of the gel refers to the yield stress. The parameters which I was able to measure were G' and G". I do not have any direct evidence regarding the strength of the bonds in the gel system with or without CB[6]. Therefore, it is not possible to comment on the yield strain values. As a result, the term "mechanical strength" and stiffness are used alternatively in this chapter.

$$\sigma_c = G\,\gamma_c \qquad \text{Equation 2.6}$$

I observed that the addition of CB[6] to the NaDC gel leads to an increase in the storage and loss moduli and therefore a gel which is stiffer was obtained. Moreover, a higher gel-to-sol transition temperature (T_{gs}) was observed when CB[6] was added to the NaDC gel. Hydrogen bonds were suggested as the primary type of intermolecular interaction responsible for the formation of the NaDC gel.[29] Therefore, the conversion of the gel-to-sol at higher temperatures and larger G'/G" values in the presence of CB[6] could be related to the formation of hydrogen bonds between hydroxyl groups of NaDC and carbonyl groups at the portal of CB[6]. Nonetheless, the interactions formed between CB[6] and NaDC are not very strong since NaDC-CB[6] gels are still categorized as weak gels based on the magnitude of the G' and G" values.

Fluorescence of pyrene excimer was used to probe the gelation of NaDC, where the pyrene excimer intensity increased when gelation occurred.[22] An emission lifetime of 67

ns was recovered after 65 min of mixing two solutions of $NaOH/NaH_2PO_4$/NaDC and NaDC/pyrene. This lifetime was assigned to the formation of excimer due to the combination of two aggregates carrying a pyrene monomer. When the two aggregates form a larger aggregate, a pyrene in its ground state and a pyrene in its excited state are in close proximity, forming an excimer. In these experiments there was no spectroscopic signature that could be assigned to the presence of pyrene in water[22] and pyrene was exclusively incorporated in bile salt aggregates and the network. There are differences between this reported work and my work, and for this reason a direct comparison is not possible. First, the methods used for sample preparation are different. In Tato's et al. paper the mixing of the two solutions of NaDC was performed at 20.0 °C without preheating the solutions and a different concentration of phosphate buffer was used to adjust the pH. Moreover, the fluorescence emission and lifetime of pyrene was monitored between 0 and 105 min after mixing. In my sample preparation the solutions were prepared at high temperature and then cooled to RT. In addition, all of my experiments were performed more than 1 to 2 h after sample preparation. It is known that the history of a gel sample and the method of sample preparation are influential on the gel's properties.[89] Nonetheless, a small amount of excimer emission was observed in my preparation for the NaDC gel particularly at lower temperatures (Figure 2.9). Disappearance and reappearance of the excimer emission during the heating and cooling cycle showed that the formation of excimers is reversible and is not due to kinetically trapping two pyrene molecules during the uncontrolled cooling for sample preparation. This reversibility of the excimer emission is in line with relocation of pyrene from water

into aggregates with the reverse process occurring during cooling. This result could indicate that the excimer is formed in the water phase of the NaDC gel because at low temperatures the amount of pyrene in the water phase increases. At higher temperatures some of the pyrene molecules partition into the network decreasing the amount of pyrene in the water phase leading to the disappearance of the excimer emission. No excimer formation was observed for NaDC-CB[6] gels at all the three molar ratios investigated indicating that the presence of another binding site (CB[6]) decreases the possibility of pairing pyrene molecules in water that can lead to the formation of excimers. This result in the presence of CB[6] supports the hypothesis of the formation of excimer in the aqueous phase of the gel in the case of the NaDC gel.

Rheological measurements depicted the enhancement of stiffness of NaDC gel when CB[6] was used as an additive because the oscillatory stress sweep and time sweep experiments (Figures 2.3 and 2.4 respectively) showed that the G'/G" values are higher for the NaDC gel with CB[6]. Moreover, the disruption of the gel with CB[6] occurs at slightly higher stress values (Figure 2.3). The sharp decrease of moduli upon oscillatory stress is ca. 40 Pa for the NaDC-CB[6] gel versus 16 Pa for the NaDC gel. This stiffening is a macroscopic property of the system. In contrast, fluorescence of the guest pyrene was used to study the microscopic mobility of a small molecule within the gel. CB[6] was chosen over the other members of the cucurbit[n]uril family which have larger cavity sizes to ensure that the inclusion of pyene into the CB[6] cavity did not happen. Also, the fact that pyrene interacts with CB[6] weakly, makes this macrocyclic compound suitable to study the partitioning of the guest between different possible binding sites in the gel. If

the interaction of pyrene with the host was too strong the mobility of pyrene between different binding sites would not occur. Data obtained from steady-state and time-resolved fluorescence measurements were analyzed systematically and provided information on changes in the distribution of the guest between different environments upon variation of temperature. To the best of my knowledge there are not many, if any, reports in the literature similar to my work that characterized the mobility of a guest molecule in a supramolecular gel at the microscopic level. The characterization of the mobility is in particular important, since many of the techniques which are currently used to study gels, such as rheological measurements and imaging methods, are not able to provide information on the dynamics of individual molecules in the gel. In this respect my work showed that there is no direct correlation between macroscopic properties of the gel measured with rheology experiments or using the inversion test and the mobility of the guest at the microscopic level studied using fluorescence techniques.

Relocation of pyrene from water to the bile salt network and the reverse process during heating and cooling of the NaDC gel is a reversible phenomenon (Figure 2.9). However, the release of the guest into the water from the network during cooling is not a gradual process as is observed during heating. The release of pyrene into water during cooling only occurs at low temperatures (around 15 °C). The dependence of the hydrophobic interactions and hydrogen bonds with the increase in temperature can provide an explanation for trends observed when the gel sample is heated and cooled. The NaDC gel network is primarily held together by hydrogen bonds. Since hydrogen bonds are disfavored at high temperatures, the network becomes weaker as the temperature is

raised. On the other hand, thermodynamic studies showed that NaDC aggregation in solution is favored at high temperatures because the hydrophobic effect is favored at higher temperatures.[24] The gradual heating of the NaDC gel sample leads to the break-up of hydrogen bonds in the system with a concurrent increase in the hydrophobic effect leading to the formation of the aggregates that are ultimately soluble in water. As a result, pyrene as a hydrophobic molecule relocates to the most favored binding site as the temperature is raised, which is the hydrophobic primary aggregate of bile salts. The complete relocation of pyrene into hydrophobic sites occurs at temperatures where the material is a gel, suggesting that these sites become available when a number of hydrogen bonds are broken but the network is still sufficiently strong to entrap the water.

During cooling of the sample the hydrogen bonds reform. The hysteresis observed for pyrene release could be related to the number of hydrogen bonds that are required to change the structure of the aggregates containing pyrene in order to release the guest to the water phase. Formation of hydrogen bonds on the outer surface of the aggregates leads to the distortion (or partial distortion) of the aggregates in the network which leads to the release of the pyrene molecules into the water.. A sufficient number of hydrogen bonds are needed to form for this “outer” force to become strong enough to be able to influence the aggregate structures. This only happens at very low temperatures where we see that the relocation of pyrene occurs.

Addition of CB[6] facilitates the release of the guest into the water phase of the gel during cooling because this release occurs at increasingly higher temperatures with the

increase in the CB[6] content (Figures 2.14, 2.17 and 2.19). Based on the rheological experiments which indicated that the addition of CB[6] to the NaDC gel led to a stronger gel, I can assume that there is an interaction between CB[6] and the NaDC network. The fact that the temperature at which the release of the guest happens is directly related to the concentration of CB[6] also supports that the interaction of CB[6] with the NaDC network plays a role in the relocation of the guest.

Hydrogen bonds formed between hydroxyl groups of NaDC and the carbonyls of CB[6] or/and electrostatic interactions between the carboxylate moiety of deoxycholate and Na^+ ions bound to the portal of CB[6] are possible interactions involved in the formation of the network for the NaDC-CB[6] gel. For the gel with CB[6], the presence of 12 carbonyl groups on the portals of CB[6] provides another source for hydrogen bond formation in addition to the other hydrogen bonds that can be formed in the NaDC gel in the absence of CB[6]. The higher the concentration of CB[6], the higher the possibility of hydrogen bond formation. Therefore, the change in the aggregates that leads to the release of pyrene into the water can happen at higher temperatures when CB[6] is added to the gel. In addition, the presence of CB[6] in the system provides another binding site for pyrene and pyrene-CB[6] can be formed as soon as pyrene is released from the aggregate.

There are different events which need to be accounted for in order to have a comprehensive understanding of the thermodynamics for the mobility of the guest within the NaDC gel with or without CB[6]. Aggregation of NaDC monomers, assembly of

aggregates to form the network, interactions between NaDC and CB[6], interactions of pyrene with either CB[6] or NaDC, and the effect of ions present in the system (Na^+ and phosphate) are the various processes to be considered to explain the relocation of pyrene from one binding site to another from the thermodynamic point of view. Although, a quantitative analysis is not possible because the values for the relevant parameters of the individual processes are not known, qualitatively an explanation can be provided.

Understanding the aggregation of bile salts through thermodynamic studies has been the point of interest for many research groups.[14,24,25,90] Since bile salts are amphiphilic molecules, sometimes the aggregation of bile salts in aqueous solution is called micellization in the literature and "demicellization" is the term used for the dissociation of aggregates. Although the reported values for thermodynamic parameters, such as critical micellar concentration and number of monomers involved in aggregate formation, are not the same for all these reports, there are trends that are useful to understand the aggregation of NaDC in aqueous medium. The enthalpy of micellization or demicellization (ΔH_{demic}) of NaDC aggregates in the presence of 0.1-0.15 M NaCl is dependent on temperature.[14,24] In addition, ΔH_{demic} was shown to be almost independent of the ionic strength.[24] It was also shown that the aggregation of NaDC is entropy driven below 350 K (77 °C).[24] The experiments in all these references are performed in solution and not in the gel phase, and I am assuming that the trends observed for the enthalpy and entropy changes for aggregate formation are the same in solution and in the gel.

Blume et al. were able to measure the $\Delta H°_{demic}$ using isothermal titration calorimetry experiments.[24] They showed that the $\Delta H°_{demic}$ changes from -3.8 kJ mol^{-1} at 10 °C to 11.0 kJ mol^{-1} at 55 °C. They were able to measure the critical micellar concentration (cmc) of the system and therefore the $\Delta G°_{demic}$ using the Equation 2.7. The $\Delta G°_{demic}$ were determined to be 22.3 kJ mol^{-1} at 10 °C and 26.0 kJ mol^{-1} at 55 °C.

$\Delta G°_{demic} = - RT\ln cmc$ Equation 2.7

By knowing the $\Delta G°_{demic}$ values for $T\Delta S°_{demic}$ were calculated to be -26.1 $kJmol^{-1}$ at 10 °C to -15 $kJmol^{-1}$ at 55 °C. The increase of $\Delta H°_{demic}$ and $T\Delta S°_{demic}$ shows that the demicellization is more disfavored upon increase in the temperature. As a consequence, the aggregation of NaDC monomers is both enthalpy and entropy favored when the temperature is raised.

To be able to make a connection between the thermodynamic parameters and the forces involved in aggregation the changes in heat capacity (ΔC_p) should be taken into account. The ΔC_p of the system is positive when hydrophobic molecules are transferred from a nonpolar environment to water.[24] The absolute value of ΔC_p is shown to be linearly dependent to the hydrophobic surface area of the monomers that is exposed to water when the aggregates dissociate. Blume et al. determined the $\Delta C_{p_{demic}}$ to be 340 J mol^{-1} K^{-1} for NaDC in 0.1 M NaCl solution at 25 °C.[24] They showed that the $\Delta C_{p_{demic}}$ decreases when temperature increases. The decrease of the $\Delta C_{p_{demic}}$ value indicates that less of the overall hydrophobic surface area is exposed to water when the temperature is

raised. This is in agreement with the formation of a larger number of aggregates in the system at higher temperatures.

Although pyrene has been widely used as the probe to study the aggregation of bile salts, there is no report on the thermodynamics of the binding of pyrene to sodium deoxycholate aggregates. Therefore, the thermodynamic data which we can rely on to describe the relocation of pyrene in NaDC gel is based on the thermodynamic of aggregation/deaggregation of bile salts. By heating the gel, molecular motions in the system increase leading to higher degrees of freedom and thus the entropy of the system increases. With the assumption that the aggregates of NaDC in the gel are the same as in solution, I can infer that the increase in entropy of the system leads to further association of NaDC monomers and formation of a larger number of aggregates. At the gel-to-sol transition temperature the molecular motions are such that the network of the gel collapses. At this temperature the most suitable binding site for pyrene is the bile salt aggregates that are stable in solution.

The association constant of pyrene and CB[6] in a 55% w/v solution of formic acid was shown to be $(3.1 \pm 0.9) \times 10^2$ M^{-1} at 15 °C and $(4.8 \pm 0.7) \times 10^2$ M^{-1} at 42 °C.[74] The authors determined that the complexation of pyrene and CB[6] is entropy driven by calculating the ΔH and ΔS values using the van't Hoff plot. Veglia et al.'s paper[74] is the only report which discusses the thermodynamics of the pyrene-CB[6] complex. However, the difference in experimental conditions and accuracy of the method used prevents me from using these data to infer the complexation of pyrene with CB[6] in the NaDC-CB[6]

gel system. Besides, the thermodynamics of NaDC and CB[6] interactions has not been explored. Therefore, it is difficult to explain the relocation of pyrene from a thermodynamic perspective when CB[6] is used as the additive.

Overall and based on the thermodynamic data for the aggregation of bile salt, I can conclude that the formation of a larger number of primary aggregates of bile salt, at higher temperatures as the most favored binding site for a hydrophobic guest leads to the relocation of pyrene into the network of the NaDC gel. It is expected that the same phenomena happen even if CB[6] is added to the gel. For this reason the relocation of pyrene from water and bound to CB[6] into the bile salt network is observed at the raised temperatures for the NaDC gel with CB[6]. The role of CB[6] on the relocation of the guest becomes significant when the sample is cooled by providing hydrogen bonds to enforce changes in aggregates structures and eventually release of the pyrene out of the network at higher temperatures in comparison to the gel without CB[6].

2.5 Conclusion

The results presented in this chapter illustrate the mobility of a small guest molecule in a complex hydrogel system which contains an additive and ions. The guest molecule shows different affinities for different binding environments in the gel at different temperatures. Presence of CB[6] in the NaDC gel as an additive not only increases the mechanical strength of the gel, but also has an influence on mobility of the guest at the microscopic level.

3 Investigation of the dynamics of NaDC aggregates for a NaDC gel formed on different surfaces

Some of the results presented in this chapter were conducted by researchers in the group of Gonzalo Cosa at McGill University and the group of Alexandre Brolo at the University of Victoria. Robert Godin performed the FCS experiments at McGill University and Regivaldo Gomes performed the silanization of glass coverslips.

3.1 Introduction

Properties of materials can be different at the interface from the bulk of solutions or solids because different chemical reactions and physical interactions can happen at the interface of the material. Understanding the effect of surfaces is essential in many fields, such as design of heterogeneous catalysts or prevention of corrosion. Understanding the effect of surfaces on gel formation and properties is important for the purpose of using the gels in potential applications in advanced technologies such as tissue engineering. For example, biological tissues are not only strong materials (elastic modulus of 10^4-10^7 Pa) but also show low surface sliding friction between cartilages and strong adhesion between hard bones and tendons.[36] Therefore, understanding the gel-surface interactions

is important to be able to design materials which display the surface sliding friction properties similar or close to those in biological tissues.

The effect of the properties of surfaces on polymer gels has been studied in more cases in comparison to supramolecular gels because the polymer gels are relatively strong. In the case of polymer gels it is possible to prepare the gel sample in the molds with different surface properties, remove the gel sample and then do the characterization using different techniques. In the case of supramolecular gels, the sample cannot always be moved and in situ measurements are required. The only work which describes the effect of surface properties on a supramolecular gel was published recently by Zelzer et al.[41] They used a cytidine derivative (C14-cytidine, Scheme 3.1) as the gelator and showed that the presence of different functional groups on the surface affects the fiber structure and mechanical properties of the C14-cytidine gel film.

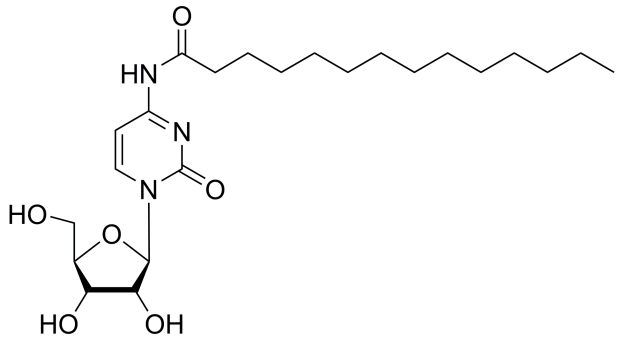

Scheme 3.1. Chemical structure of C14-cytidine.

Fluorescence correlation spectroscopy (FCS) is a powerful technique for the analysis of dynamics of fluorescent molecules or fluorescently labeled macromolecules

and surpermolecules in systems such as colloids, polymers, gels and biological systems.[61,91,92] This technique is based on monitoring fluorescence intensity fluctuations over time. The fluctuation of the fluorescence intensity is normally caused by the translational diffusion of the fluorophore or the fluorescently tagged species into and out of a small observation volume defined as the spot where the laser beam is focused and the confocal aperture collects the emitted light (Scheme 3.2). The correlation function G(τ) is informative about the average number of fluorescent species in the observation volume, N, and the diffusion time, τ_D.

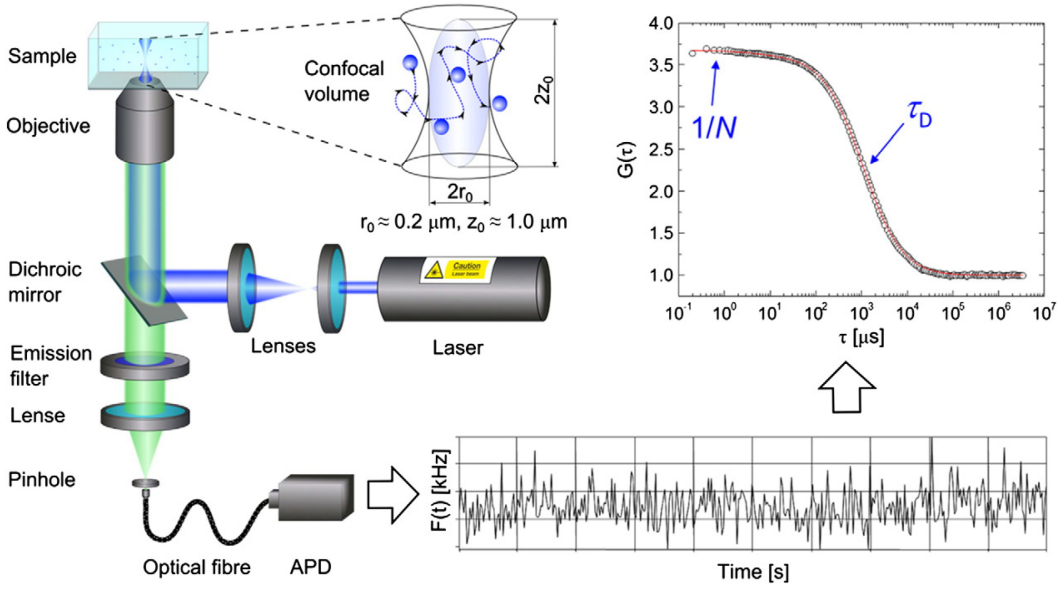

Scheme 3.2. Schematic representation of FCS setup and its principle of operation. Reprinted with permission from reference 92. Copyright © 2016, Elsevier.

The objective for the experiments performed in this chapter was to understand the effect of surfaces with different hydrophilicity on NaDC gel formation and the effect on the gel's network structure. For this purpose glass coverslips and glass cylinders modified with different functional groups were used as the vessel for NaDC gel preparation. FCS experiments were performed to obtain information regarding the properties of the gel close to the glass-gel interface (ca. 10-80 μm above the surface). Steady-state and time-resolved fluorescence experiments were performed with the aim to characterize the bulk properties of the gel when the gel was formed on surfaces bearing different functional groups.

3.2 Experimental section

3.2.1 Materials

FisherfinestTM premium cover glasses (Fisher Scientific) were used as the substrate for the surface modification. Diethylphosphatoethyltriethoxysilane (diethylphosphato), 3-iodopropyltrimethoxysilane (iodo) and n-decyltriethoxysilane (n-decyl) (Scheme 3.3) were purchased from Oakwood chemicals and were used without further purification.

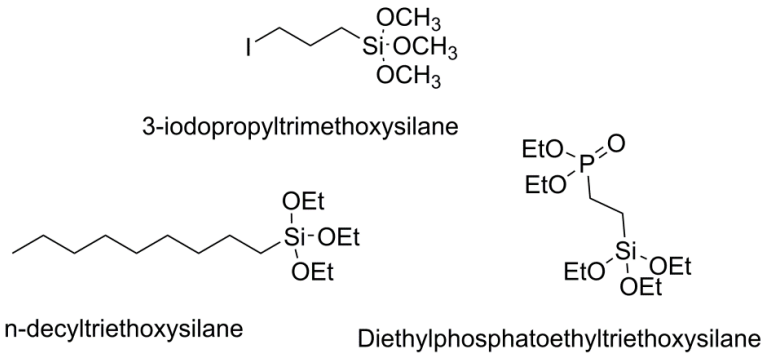

Scheme 3.3. Chemical structures of 3-iodopropyltrimethoxysilane, n-decyltriethoxysilane and diethylphosphatoethyltriethoxysilane.

NaDC (Fluka, > 98%, used for fluorescence measurements), NaDC (Acros extra pure, purchased from Fisher AC21859-0250, used for FCS measurements), methanol (Fisher Scientific, spectral grade, > 99.9%) and phosphate buffer (Sigma-Aldrich, P8165, dissolved in 129.2 mL of deionized water, pH 6.6 at 25 °C), 1,1'-dioctadecyl-3,3,3',3'-tetramethylindodicarbocyanine perchlorate (DiD) (Invitrogen Canada) were used as received. Sulfo-Cy5-maleimide was purchased from Lumiprobe (Scheme 3.4). Pyrene (Fluka, 99%) was recrystallized from ethanol. The purity of pyrene was confirmed by fluorescence lifetime measurements in water, where a single-exponential decay with the lifetime of 130 ns was obtained.[75,76] Deionized water (Barnstead NANOpure deionizing systems ≥ 17.8 MΩ cm) was used for the gel sample preparation for fluorescence, single photon counting as well as contact angle measurements. ProPlate 8 well, 7 mm × 16 mm, silicon gaskets (Grace Bio Labs) were used for the control gels that do not contain pyrene used for fluorescence steady-state and time-resolved measurements. Epoxy glue

(Hardman®, McMaster-Carr) and silicon glue (Premium waterproof silicon, General electric company) were used in the assembly of the coverslips and glass cylinders. Sterile polypropylene tubes (50 mL Corning® centrifuge tubes) and a Coplin staining jar (Wheaton® 900520 Coplin Staining Jar with Screw Cap, 55mL Capacity) were used as the container for the silanization of glass cylinders and coverslips respectively.

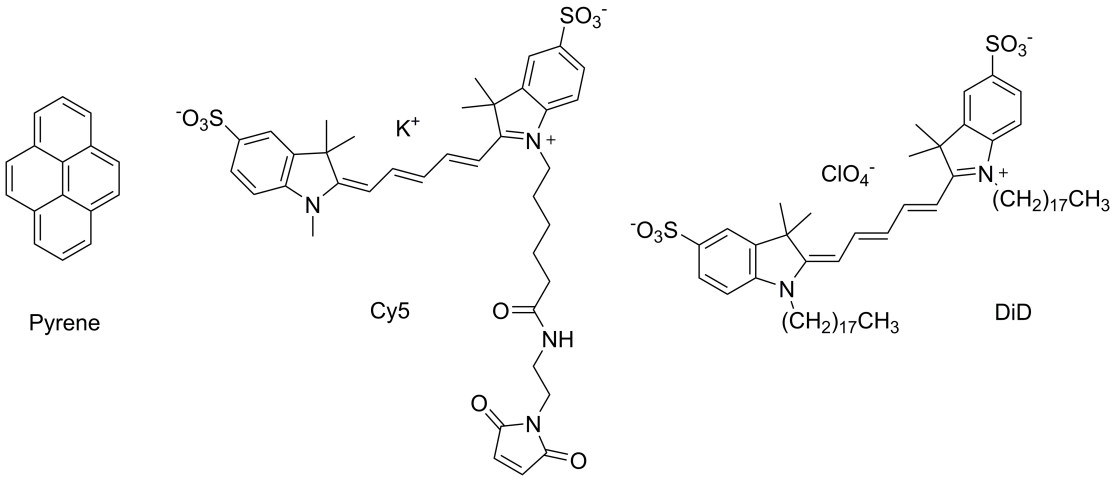

Scheme 3.4. Chemical structures of the pyrene, Cy5 and DiD.

3.2.2 Silanization of glass substrates

A modified protocol based on a previous report[93] was employed to modify the surface of the glass coverslips. Coverslips and cylinders were immersed in piranha solution for 1 h and were washed thoroughly with ultrapure water (Barnstead Nanopure System- 18.2 MΩ cm). All the substrates were dried in an oven before the silanization. A solution of each silane in toluene with concentration of 25% (v/v) was prepared. Coverslips were arranged in a Coplin staining jar and the silane solution was poured into

the jar in a way that the slides were entirely immersed in the solution. The jar's cap was tightened to ensure that hydration of the solution does not occur during the silanization. Silanization of the glass cylinders was performed using sterile polypropylene tubes. The glass cylinder was immersed into the silane solution in a tube closed with a screw cap. The cap was sealed well to prevent the diffusion of water into the tube. Samples were left undisturbed on the bench top at RT for ca. 18 h. The reaction of the silane molecules with the surface occurs during this time. Each of the coverslips and each of the cylinders were transferred into to an individual 50 mL polypropylene tube containing ca. 50 mL of anhydrous ethanol. The ethanol was replaced every 12 h for 10 times to ensure complete removal of the silane molecules which are physically absorbed on the surface. The washing steps were crucial because the reproducibility of the data obtained between different batches of modified glass surfaces is affected if the physically absorbed silanes are not removed entirely. After washing with ethanol the substrates were transferred into clean glass vials and were kept in an oven at 110 °C for ca. 3 h in order to promote cross-linking of siloxane bonds.[94] After the thermal treatment of samples, they were stored at RT.

3.2.3 Sample preparation for FCS, steady-state and time-resolved fluorescence experiments

NaDC gel samples were prepared by dissolving the NaDC in an adequate amount of water to obtain the concentration of 13.8 mg/mL. This solution was heated at 60 °C for

15 min. A required volume of the desired probe molecule was injected into the solution while hot. The concentration of the stock solution of DiD (probe for the FCS experiments) and pyrene (probe for the fluorescence experiments) was 2 μM in ethanol and 5 mM in methanol, respectively. A required volume of phosphate buffer at a pH of 6.6 was added to the solution. The sample was then heated for another 15 min at 60 °C. Around 1 mL of the hot solution was transferred to a sample chamber and left undisturbed to cool down to RT. The sample chambers were prepared by affixing a glass cylinder on top of a glass slide bearing the same functional group. Epoxy glue was used for the assembly for the FCS experiments while the coverslip and the cylinder were assembled using silicon glue for the fluorescence experiments. The epoxy was cured in an oven (110°C) for ca. 30 min. The glass chambers were taken out of the oven and the NaDC solution at 60 °C was transferred to the warm chambers. The chamber was covered with a plastic stopper and the gel formed when the sample was cooled. In the case of fluorescence experiments, the top part of the chamber was covered with a second coverslip bearing the same functional group after transferring the hot solution into the chamber. The top slide was glued to the cylinder after the gel formation. Moreover, gaskets were used instead of glass cylinders to prepare the control gels for fluorescence experiments. Control experiments using glass cylinders led to the observation of the same spectra as for control samples where gaskets were used. The final concentrations of NaDC and phosphate buffer were 30 and 100 mM respectively. Final concentrations of DiD and pyrene were 10 nM and 5 or 2 μM respectively. There was a minimum 2 h time gap between sample preparation and the measurements. In the case of the gel prepared

between coverslips bearing diethylphosphato, the fluorescence intensity of the impurity in the control gel was very high which made it impossible to do the baseline correction on the emission spectrum of pyrene.

3.2.4 Equipment setup

The measurements of the contact angle for water with the glass surfaces were performed with a home-built setup. White light illumination was achieved with a PTI lamp housing (model A1010) using a 75 W Xe-arc lamp. The glass slide with a 3 μL water drop was placed at ca. 2.5 inches from the lamp while a lens with 3 inch focal length was placed after the sample at a distance of 8 inches from the lamp. The camera (ThorLABS, DCC1545M) was placed at ca. 6.5 inches after the lens at the focal plane for imaging the drop. Pictures were taken using the ThorCam software. The obtained images were analyzed with ImageJ software where the contact angle was measured. When required the light intensity from the lamp was attenuated by using a neutral density filter (31% transmission) placed between the light source and the sample.

FCS acquisitions were performed on an Olympus IX-71 inverted microscope fitted with an optical-axis piezo-Z positioner (P-721 PIFOC®, Physik Instrumente, Germany) and a nanopositioner (P-733, Physik Instrumente) controlled by a digital piezo controller (E-710, Physik Instrumente). The laser excitation was provided by a supercontinuum laser (WhiteLase SC-400-4, Fianium, Beverly, MA) coupled to a single mode, polarization maintaining fiber optic and launched into the microscope. A center excitation wavelength of 633 nm was spectrally separated from the broadband emission

by a computer-controlled acousto-optical tunable filter (AOTF, Fianium). A Z488-543-633rdc dichroic mirror (Chroma, Rockingham, VT) projected the pulsed laser excitation (40 MHz repetition rate, 11 μW out of the objective) towards the water-immersion objective (UPLSAPO 60XW, N.A. = 1.20, Olympus). An excitation beam diameter of ca. 3 mm was used to underfill the back aperture of the objective in order to provide a better approximate Gaussian observation volume.[95] The laser excitation (70 kW/cm^2) was typically focused 80 μm above the glass-water interface and fluorescence emission was collected through the objective. The emission passed through a 50 μm diameter pinhole positioned at the image plane and was relayed to the detectors. A Hanbury Brown and Twiss (HBT) intensity correlation setup was used to calculate the correlation traces where the emission output (cleaned by a 685/80m emission filter, Chroma) was split by a 50/50 non-polarising cube beam splitter (05BC17MB.1, Newport Corporation, Irvine, CA), focused onto two avalanche photodiode detectors (SPCM-AQR-14, Perkin Elmer) in pseudo-cross-correlation format.[96] This setup was used to observe μs dynamics that are obscured by the detector after pulsing in a single detector setup. Acquisitions were performed using PicoHarp 300 electronics and autocorrelation functions calculated from SymPhoTime software (PicoQuant, Germany). A typical FCS trace was calculated from a 5 minute-long time point acquisition. The fitting was performed using the open source FCS fitting software PyCorrFit (v. 0.8.4). The concentration of dye was 10 nM in all cases.

Fluorescence emission spectra were collected using a PTI QM-2 fluorimeter. Emission spectra were recorded between 350-550 nm at the excitation wavelength of 331

nm. The step size of 0.5 nm was used to ensure accuracy in the determination of the I/III ratios for the pryene emission. The slits for both monochromators were set to 1 nm bandwidths.

Fluorescence decays were recorded using an Edinburgh Instruments OB920 single photon counter (SPC). A 330 nm light emitting diode (LED) was used as the source of light. The excitation and the emission wavelength were 335 and 390 nm respectively and the emission monochromator had a bandwidth of 16 nm. The number of counts in the channel with maximum intensity was 10000. The emission decays for pyrene were fitted using Equation 3.1 with the F900 software package from Edinburgh Instruments. In this equation *I* is the fluorescence intensity, A_i and τ_i are the pre-exponential factor and the lifetime of the emissive species "i". The A_i value is related to the amount of species i in the environment. The sum of the A_i values is equal to 1 by definition. The goodness of the fits was determined by the analysis of the χ^2 values (0.9-1.3) and the randomness of the residuals. The sample holder had a front face arrangement between the excitation and emission optics for steady-state and time-resolved measurements.

$$I(t) = I_0 \sum_{1}^{i} A_i \, e^{-t/\tau_i} \qquad \text{Equation 3.1}$$

3.2.5 Method of analysis for FCS experiments

In FCS experiments, the observation volume is defined by the overlap between the laser excitation beam and the collection efficiency function of the confocal microscope.

Under the experimental conditions where only few fluorescent molecules are present in the observation volume, the fluctuations in fluorescence intensity are large enough to obtain a satisfactory correlation trace. The correlation function of the fluorescence fluctuations is constructed by measuring the fluorescence intensity over time (Equation 3.2)

$$G(\tau) = \frac{\langle \delta F(0) \delta F(\tau) \rangle}{\langle F \rangle^2} \qquad \text{Equation 3.2}$$

In Equation 3.2, τ is the delay time between fluorescence intensity data. F and $\langle F \rangle$ represent the fluorescence intensity and the mean fluorescence intensity respectively. The term δF shows the difference between F and $\langle F \rangle$. With the assumption that the observation volume has a 3D Gaussian profile, the correlation function of species diffusing in 3 dimensions can be described as the following equation:

$$G(\tau) = G(0)\left(1 + \frac{\tau}{\tau_D}\right)^{-1}\left(1 + \frac{\tau}{\kappa^2 \tau_D}\right)^{-1/2} \qquad \text{Equation 3.3}$$

where the structure parameter (κ) is defined as the ratio of the long axis (ω_z) to the short axis (ω_{xy}) of the observation volume. The parameter τ_D, which is the translational diffusion time of the fluorophore, is inversely related to the diffusion constant of the molecule (D) through the following equation:

$$\tau_D = \frac{\omega_{xy}^2}{4D}$$ Equation 3.4

The correlation function value at $\tau = 0$ has an inverse relationship with the average number of molecules in the observation volume (Equation 3.5). Therefore, the lower the concentration of freely diffusing fluorescent molecules, the larger the initial amplitude of the correlation function.

$$G(0) = \frac{1}{N}$$ Equation 3.5

There are other processes that influence the correlation traces. For example, formation of excited triplet states or photoisomerization of molecules are processes that need to be accounted for in the analysis of the correlation traces. For each process a term is added to Equation 3.3. For instance, $G^{triplet}(\tau)$ is the term accounting for the triplet state dynamics which is defined in Equation 3.6. In this equation the parameters T and τ_T are the triplet fraction and triplet lifetime.

$$G^{triplet}(\tau) = \left[1 + \frac{T}{1-T} exp(-\tau/\tau_T)\right]$$ Equation 3.6

Cyanine dyes have been shown to undergo photoisomerization upon photoexcitation.[97] To account for this photophysical pathway, an additional term is added to the correlation model.

$$G^{photoisomerization}(\tau) = \left[1 + \frac{f}{1-f} exp(-\tau/\tau_{ISO})\right] \quad \text{Equation 3.7}$$

For example, Equation 3.3 could be rewritten as Equation 3.8 when photoisomerization, a triplet state and a diffusional processes are involved in the correlation trace.

$$G(\tau) = G(0)\left[1 + \frac{T}{1-T} exp(-\tau/\tau_T)\right]\left[1 + \frac{f}{1-f} exp(-\tau/\tau_{ISO})\right]\left(1 + \frac{\tau}{\tau_D}\right)^{-1}\left(1 + \frac{\tau}{\kappa^2\tau_D}\right)^{-1/2} \quad \text{Equation 3.8}$$

3.3 Results

3.3.1 Contact angle measurements

The surfaces of glass coverslips were modified with diethylphosphatoethyltriethoxysilane (diethylphosphato), 3-iodopropyltrimethoxysilane (iodo) or n-decyltriethoxysilane (n-decyl). The contact angle between a drop of water and the modified glass surface was measured to ensure the surface was bearing the corresponding functional group. To ensure that the surface was modified homogeneously, random spots were chosen on each coverslip. Also, the reproducibility of the modification from one batch of slides to another was checked by measuring the contact angles. The average contact angle values are 33 ± 6°, 50 ± 4°, 63 ± 7° and 17 ± 1° for

diethylphosphato, iodo, n-decyl and unmodified coverslips respectively (Figure 3.1). These contact angles are the average of 2 different sets of slides. Three drops were randomly placed on different parts of each slide. Therefore, the reported values are the average of 6 experimental values. It has been shown that the measured contact angle value is dependent on many different parameters, such as the size of the drop used for the measurements[98] and the morphology of the substrate surface.[99] Therefore, a direct comparison between my results and values in the literature is not possible.

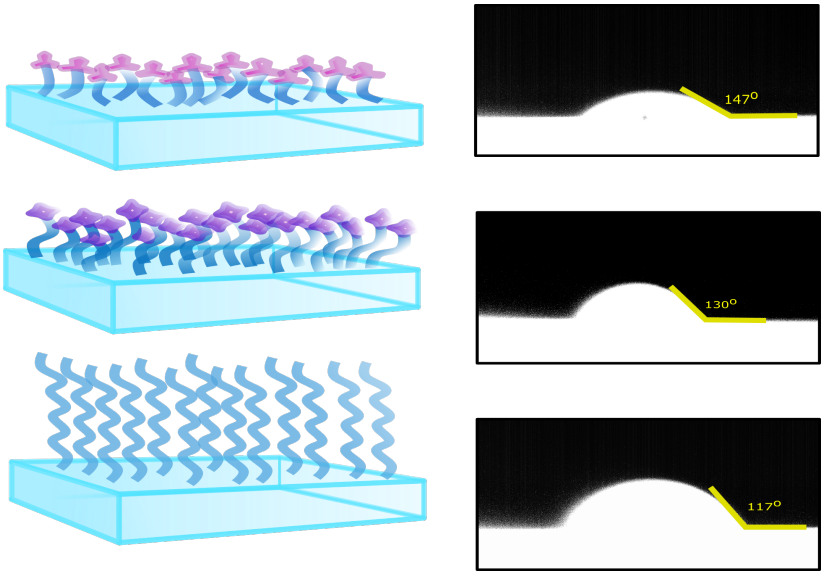

Figure 3.1. Schematic representation and contact angles measured for a 3 µL drop of water on the glass surfaces modified with diethylphosphate (top), iodo (middle) and n-decyl (bottom) functional groups. The angles shown in the pictures are the supplementary of the contact angle.

3.3.2 FCS measurements

FCS experiments are used to measure the dynamics of photophysical processes that occur in the µs to s time range. For example, formation of a triplet excited state

which leads to a non-emissive excited state can be followed in a FCS experiment because the fluorescence intensity changes when intersystem crossing occurs. Diffusional processes lead to changes in fluorescence intensity when the excited state exits the observation volume. Diffusional processes occur in the ms to s time scale and are detected in FCS experiments. Analysis of the fluorescence intensity fluctuation in the small observation volume provides information on all processes that lead to changes in the fluorescence intensity. The concentration of fluorophore is kept low (ca. nM) to ensure that only a few fluorescent molecules are simultaneously present in the observation volume to ensure sufficient amplitude for the FCS experiment.

Cy5 (10 nM) in 100 mM phosphate buffer was used to calibrate the observation volume based on the Cy5 diffusion coefficient of 2.5×10^{-10} m^2s^{-1} (Figure 3.2).[97] The width of the observation volume (ω_{xy}) was determined to be ca. 295 nm. To ensure the system is well focused the width of the observation volume should be as close as possible to ca. 250 nm.[91] The same experiment yielded the structure parameter of the instrument (κ) of ca. 5.4. Satisfactory fitting of the trace was obtained when a triplet term and a diffusional term were included in Equation 3.8. The values of the recovered parameters are $T = 0.44$, $\tau_T = 2.4$ μs, $\tau_D = 0.089$ ms. It is reported that the triplet state lifetime is around 1 μs for a similar Cy5 dye.[97] Therefore, the obtained value of 2.4 μs was attributed to the formation of the triplet excited state of Cy5 by intersystem crossing. In this experiment no photoisomerization of the Cy5 was observed. Therefore, $f = 0$ in Equation 3.8. The black and red lines in Figure 3.2 illustrate the correlation traces for DiD in NaDC aggregates in the gel sample and Cy5 in the buffer solution, respectively.

The satisfactory fit for the FCS trace of the gel sample with DiD was obtained with two excited state dynamics terms defined as T and τ_T for the triplet state and as f and τ_{ISO} for the photoisomerization process, and one diffusional term using Equation 3.8. The values of the fitted parameters are $T = 0.18 \pm 0.01$, $\tau_T = 2.6 \pm 0.3$ μs, $f = 0.20 \pm 0.01$, $\tau_{ISO} = 16.6 \pm 1.8$ μs, $\tau_D = 0.33 \pm 0.03$ ms. These values are obtained from the average of all the experiments including those which were performed on different surfaces since there was no difference between them (4 individual experiments).

DiD forms aggregates in phosphate buffer solution. In a control experiment, the diffusion time of DiD aggregates in the buffer was measured to be 9.2 ms (Figure 3.3). In this experiment $f = 0$ and $T = 0$, since there is no triplet excited state formation or photoisomerization.

None of the two dye diffusion time values in solution (0.089 ms or 9.2 ms) were recovered for the traces of DiD in the gel sample suggesting that DiD is neither freely diffusing nor is incorporated in its aggregated form in the NaDC gel. Therefore, it can be concluded that DiD is completely incorporated into NaDC aggregates as a monomer.

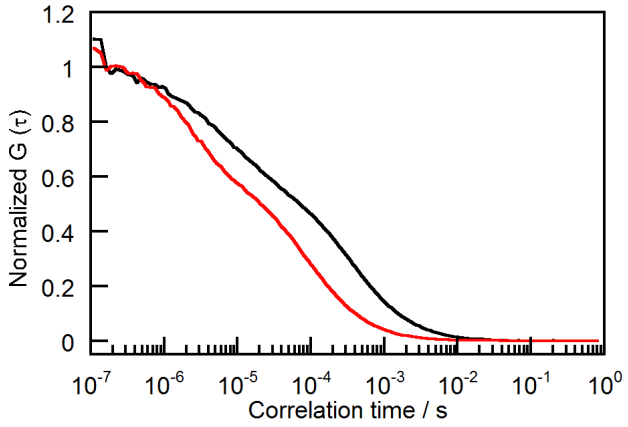

Figure 3.2. Correlation function obtained for 10 nM DiD in a NaDC gel (black line) and freely diffusing Cy5 (red line), both in 100 mM phosphate buffer.

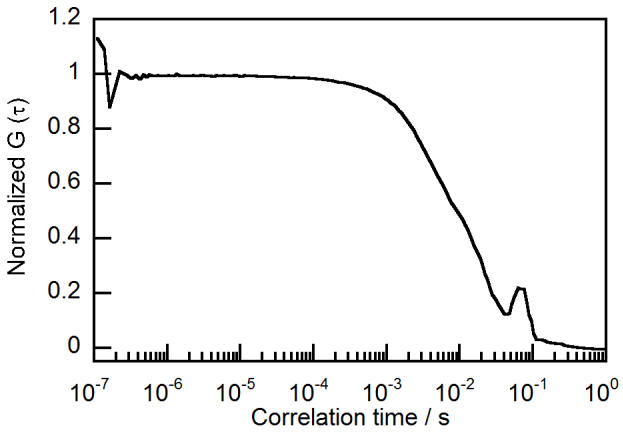

Figure 3.3. Correlation function obtained for 10 nM DiD in 100 mM phosphate buffer.

The normalized correlation traces obtained for DiD bound to NaDC aggregates in solution (in the presence of 10 mM phosphate buffer, pH = 6.6) and DiD bound to NaDC in the gel (100 mM phosphate buffer, pH = 6.6) are very similar (Figure 3.4). No gelatinization happened even after 12 h for the solution of NaDC with 10 mM phosphate

buffer. Therefore, a minimum concentration of phosphate is required for gel formation and phosphate ions and Na^+ and K^+ cations have a role in facilitating the assembly of the aggregates into the gel's network.

The fluorescence intensity observed in these experiments is from the NaDC aggregates tagged with DiD. There are three different possibilities for the diffusion of the tagged aggregates in the gel system. First, the diffusion of aggregates within the network. Second, the exchange between the aggregates in the network with the aggregates floating in the aqueous phase entrapped in the gel. Third, the diffusion of aggregates that are floating in the aqueous phase. It was expected that a different τ_D value would be obtained for the diffusion of aggregates within the network or for the exchange of the aggregates between the network and water phase than the τ_D value measured for the NaDC aggregates in solution when no gel is formed. The correlation traces for the tagged NaDC aggregates in solution and in the gel are the same, indicating that the observed process is not correlated to the dynamics of network self-assembly. In fact, the observed traces are related to the mobility of the aggregates in the water phase of the gel. With the assumption that the exchange of aggregates between the network and aqueous phase is slower than the FCS time resolution and if the distance between the two neighboring compartment of the network was smaller than the observation volume a different τ_D would have been obtained. This result suggests that the network structures are not located within the observation volume of the FCS experiments and only the entrapped water is probed. Besides, the fact that the FCS traces are the same indicates that the aggregates in the water phase of the gel are the same as in NaDC solutions. The

observation of the same aggregates in the entrapped water phase of the gel and in solution suggests that the aggregates in the network are also similar to the aggregates in the solution if one assumes that the aggregates in the network and the entrapped water are in a dynamic exchange.

The comparison of the non-normalized FCS traces shows a higher G(0) value for the gel sample (Figure 3.4,inset). This result indicates that a smaller number of tagged NaDC aggregates are present in the observation volume of the gel (Equation 3.5). It is expected that a significant amount of NaDC aggregates are involved in the network formation in a gel sample and as a result fewer aggregates appear in the observation volume which contains the aggregates in the trapped water phase. The amplitude of G(0) for gel and solution is 0.152 and 0.095 respectively. These values suggest that ca. 40% of aggregates in the NaDC gel are diffusing freely and the remaining 60% are incorporated into the network.

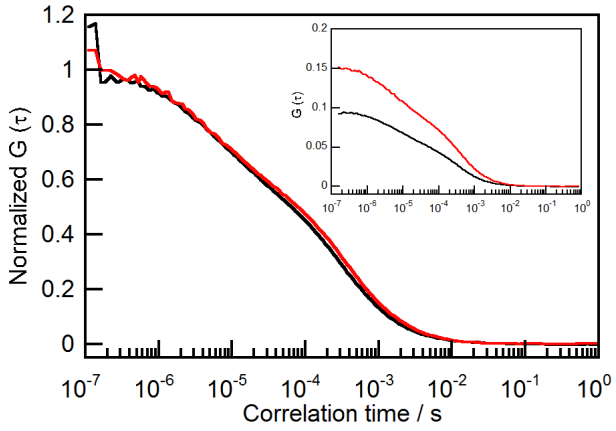

Figure 3.4. Normalized and non-normalized (inset) correlation functions obtained for DiD in a sample of NaDC aggregates in buffer solution (black) and NaDC as a gel (red).

The effect of hydrophilicity of the surfaces on which the NaDC gel was formed on the diffusion of the NaDC aggregates containing DiD was investigated with FCS experiments. Figure 3.5 illustrates the normalized traces obtained for DiD in the NaDC gel samples prepared in glass chambers functionalized with different silanes. There is no significant difference between these traces indicating that the hydrophilicity of the surface is not influential on the type of NaDC aggregates in the aqueous phase of the gel. However, the initial values of the correlation function are different for gels formed on different surfaces which suggests different amount of NaDC aggregates tagged with DiD are present in the aqueous phase of the gel when the gel is prepared inside the glass chambers with different functional groups.

A control experiment was performed for an observation volume located at 10 μm above the surface where the gels formed on different surfaces led to the same FCS traces (Figure 3.6). Therefore, it can be concluded that between the distances of 10 to 80 μm the properties of the surface do not affect the mobility of the NaDC aggregates in the aqueous phase of the gel suggesting that if there is any change in the network it does not affect the mobility of the aggregates in the aqueous phase.

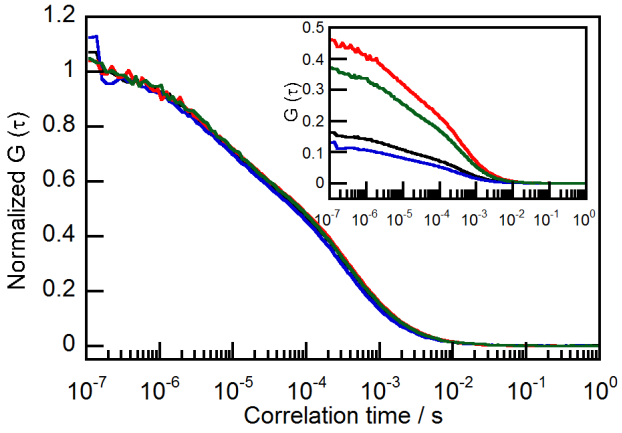

Figure 3.5. Normalized and non-normalized (inset) correlation functions for DiD/NaDC gel prepared on surfaces modified with different functional groups. Black, blue, red and green lines represent unmodified glass and glasses modified with diethylphosphate, iodo and n-decyl functional groups, respectively.

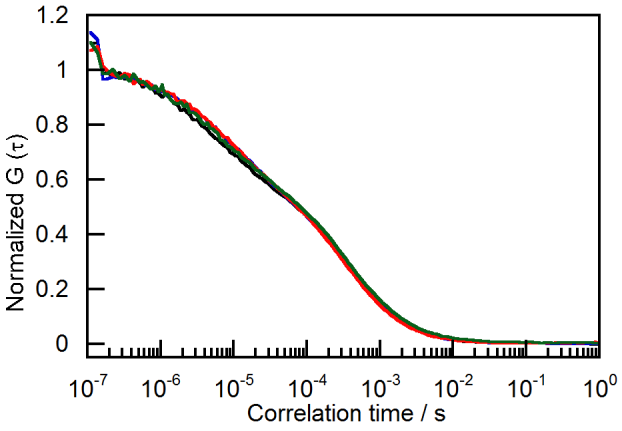

Figure 3.6. Normalized correlation functions obtained for DiD in NaDC gels. Acquisitions were performed 10 µm above the glass-gel interface in different surface-modified sample chambers. Black, blue, red and green lines represent unmodified glass and glasses modified with diethylphosphate, iodo and n-decyl functional groups, respectively.

The diffusion coefficient for the NaDC aggregates in the gel was calculated from Equation 3.4 by using the average diffusional time (τ_D) for the NaDC aggregates from the FCS measurements with all samples (0.33 ± 0.03 ms) leading to an average $D_{\text{NaDC agg.}}$ value of (0.65 ± 0.06) × 10^{-10} m^2s^{-1}.

Steady-state and time-resolved fluorescence measurements were performed with the aim of probing the properties of the bulk of the gel when the gel was prepared on coverslips that have different hydrophilicities. For this purpose pyrene was chosen as the fluorophore. Photophysical properties of pyrene are highly dependent on the polarity of the environment surrounding this molecule.[86] For instance, the emission intensity at 371 nm (band I) changes with the polarity of the solvent while the intensity at 382 nm (band III) does not. The I/III ratio of pyrene is around 1.7 and 0.6 in water and cyclohexane respectively.[86] For a NaDC gel sample prepared by uncontrolled cooling from 60 °C to RT, the I/III ratio was measured to be 1.17 ± 0.06 (average of 3 independent experiments). This value is different from the one reported in chapter 2, because a different phosphate buffer solution was used for the sample preparation in this chapter. When the NaDC gel samples were prepared in the glass chamber bearing diethylphosphato, iodo and n-decyl groups, the measured values for the I/III ratios were 1.1 ± 0.2 , 1.12 ± 0.01 and 1.06 ± 0.08 respectively (Figure 3.7). The errors correspond to average deviations from two independent experiments. The error for the NaDC gel prepared on the coverslips bearing diethylphosphato is fairly large due to interference of the impurity emission in the control gel sample. No significant difference was observed

between the I/III ratio values obtained with respect to the functional group used for the modification of the surface.

Time-resolved fluorescence is used for the characterization of systems that contain a fluorescent probe located in different environments, such as binding sites in supramolecular hosts.[88] The probe when bound to different binding sites can have different excited-state lifetimes. A monoexponential fluorescence decay would be observed when the fluorophore is placed in one environment. The decay can be fitted to a sum of exponentials when the fluorophore is bound to different binding sites and the fluorophore has different lifetimes (Equation 3.1). The emission from excited pyrene in water has a monoexponential decay with a lifetime around 130 ns.[75,76] The lifetime of pyrene in 30 mM NaDC in the presence of 0.2 M NaCl was measured as 386 ± 6 ns.

The time-resolved fluorescence decays were recorded for the samples that were prepared between coverslips functionalized with different groups (inset in Figure 3.7). The obtained lifetimes are summarized in Table 3.1. The control experiments showed that the lifetimes with 5 and 50 ns are from the impurities in the bile salt and from the impurities resulting from the modification of the glasses with silanes respectively (Figure 3.8). These lifetimes were fixed during the analysis. The lifetime of pyrene in water was also fixed to 130 ns. Results showed that the lifetime of pyrene in the bile salt network is almost the same for the gels prepared between coverslips bearing different functional groups. This result shows that the environment to which pyrene is bound in the gel

network and for the aggregates in the aqueous phase is the same for all the gels formed on surfaces with different hydrophilicities.

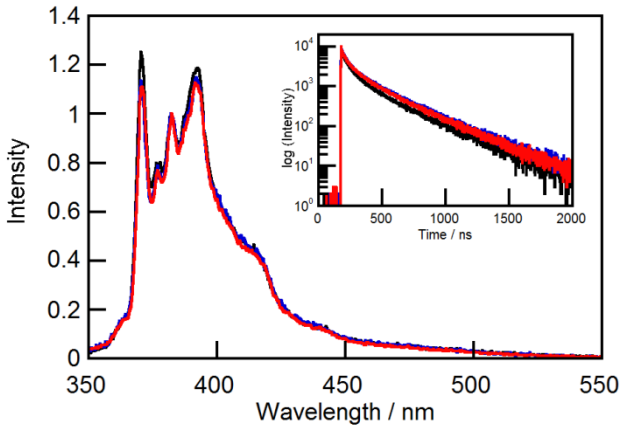

Figure 3.7. Fluorescence emission and decay (inset) of pyrene in NaDC gel prepared between the coverslips bearing diethylphosphato (black), iodo (blue) and n-decyl (red) functional groups. The excitation wavelength for the steady-state and time resolved experiments were 331 and 335 nm respectively. The steady-state spectra were normalized at peak III (~ 383 nm).

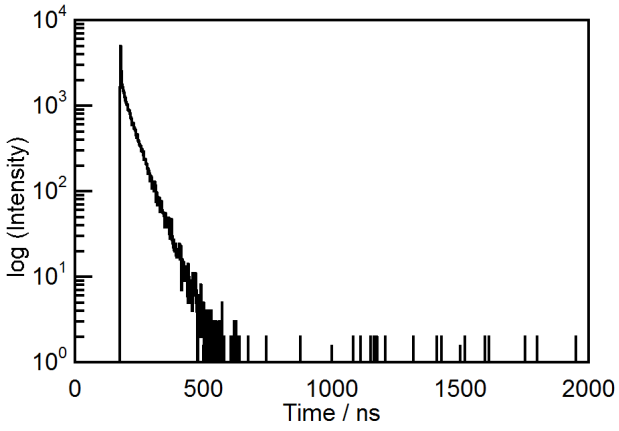

Figure 3.8. An example of the decay for the control gel samples without pyrene. The lifetime around 5 and 50 ns were recovered by fitting these decays.

Table 3.1. Pyrene lifetimes and their corresponding pre-exponential factors in NaDC gel samples prepared between coverslips functionalized with different groups.

Functional group	**τ_1 /ns**	**A_1**	**τ_2 / ns**	**A_2**	**τ_3 / ns**	**A_3**	**τ_4 [c] / ns**	**A_4**
Diethylphosphato	5 [b]	0.22 [a]	50 [b]	0.49 [a]	130 [b]	0.13 [a]	300 ± 3	0.16 [a]
Iodo	5 [b]	0.21 [a]	50 [b]	0.44 [a]	130 [b]	0.13 [a]	310 ± 2	0.22 [a]
n-decyl	5 [b]	0.22 [a]	50 [b]	0.40 [a]	130 [b]	0.17 [a]	306 ± 2	0.21 [a]
Control[d]	5 [b]	0.17 ± 0.02			130 [b]	0.45 ± 0.01	314 ± 2	0.38 ± 0.01
Control[e]	4.5 ± 0.7	0.40 ± 6	47 ± 0	0.60 ± 6				

[a], The error for all the A values is less than ± 0.01 and was recovered from the fit of the data. [b], The lifetimes at 5 (impurity in bile salts), 50 (impurity in silanes), 130 ns (pyrene in water) were fixed. [c], The error for lifetime of pyrene in bile salt aggregates was recovered from the fit of the data. [d], This experiment was performed with a NaDC gel in a 10 × 10 mm absorption cell with 2 μM pyrene. [e], Average of the two experiments for a NaDC gel without pyrene. The gels were prepared between coverslips bearing iodo or n-decyl functional groups (Figure 3.8). The lifetimes of 5 and 50 ns which were fixed in other experiments, were obtained from this control experiment.

3.4 Discussion

Comparison of the black and red lines in Figure 3.2 shows that there are two differences between these two correlation traces. First, the trace for DiD in the gel is more complex which suggests that there is more than one excited state deactivation process occurring in addition to the diffusional term. Second, a slower process is present for the DiD in the gel sample. The values of the fitted parameters for the FCS trace for DiD in the gel are $T = 0.18 \pm 0.01$, $\tau_T = 2.6 \pm 0.3$ μs, $f = 0.20 \pm 0.01$, $\tau_{ISO} = 17 \pm 2$ μs, $\tau_D = 0.33 \pm 0.03$ ms. The characteristic diffusion time of 0.33 ms for DiD in the gel sample is much slower than the 0.089 ms diffusion time that was obtained for Cy5 freely diffusing in solution. The 0.33 ms diffusion time in the gel is different from the τ_D value

of 9.2 ms recovered for DiD in buffer where aggregates are formed. DiD in the gel sample is neither free DiD nor DiD aggregated in the water phase. The diffusion time for DiD in the gel and in aggregates in solution was the same. Therefore, this observed diffusing process for DiD in the gel is related to the diffusion of DiD in NaDC aggregates present in the aqueous phase of the gel. This basically means that there are NaDC aggregates that are tagged by the fluorescent dye. The almost identical traces of the gelled and non-gelled samples show that the diffusion of dye is not hindered. The NaDC gel network is constructed by assembly of NaDC aggregates and there is likely an equilibrium between the NaDC in the network and in the aggregates soluble in the aqueous phase of the gel. No dynamics was observed for this exchange, which is likely due to be different from the diffusion of the individual aggregates in the entrapped water phase. Therefore the dynamics is either too slow to be followed or its contribution is too small to be detected.

The values for the excited state dynamics of DiD in the gel support the assignment that DiD is incorporated in the NaDC aggregates. The parameters τ_T, τ_{ISO}, T and f are assigned to the intersystem crossing to the triplet state of DiD and to the photoisomerization of all-trans form of the DiD molecule to the mono-cis form. The rate of isomerization of the different dye, Cy5, was shown to depend on the viscosity of the solution.[97] Widengren and Schwille showed that k_{ISO} (isomerization rate constant) for Cy5 decrease from 25×10^6 s^{-1} in water to the 8×10^6 s^{-1} in a 40% sucrose water solution. The viscosity increased from 1.0 cP in water to 6.2 cP in water containing 40% sucrose, with corresponding τ_{ISO} values of 0.04 and 0.125 μs for Cy5 in water and in the

water/sucrose solutions respectively. It is expected that the isomerization of DiD will be a slower process due to the presence of longer alkyl chains in its structure compared to Cy5. The lengthening of τ_{ISO} to ca. 17 μs in the NaDC gel suggests that incorporation of DiD into the NaDC aggregate limits the conformational freedom of the molecule and decreases the rate of photoisomerization.

Different functional groups with different hydrophilicity were attached to the glass surface. The obtained correlation time for DiD in the gels prepared on glass chambers with different functional groups was the same (Figure 3.5) even if the acquisitions were performed at 10 μm which was closer to the surface compared to the regular measurements (Figure 3.6). Therefore, one can conclude that the properties of the surface do not lead to structural changes in the gel beyond 10 μm that affect the mobility of the NaDC tagged DiD complexes in the entrapped water phase.

The inset of Figure 3.5 illustrates the non-normalized traces for the gels prepared on different surfaces. The initial amplitude of the correlation function (G(0)) is different for different functional groups. This difference may be related to the different affinity of DiD for surfaces with different hydrophilicity. The amount of DiD which is absorbed on the surface changes for each sample. Therefore, the amount of DiD available for tagging the NaDC aggregates in the aqueous phase changes leading to the different N values in Equation 3.5 and thus the G(0) values. Another possibility is that the presence of different functional groups on the surfaces leads to some structural change in the network in a way that the affinity of the DiD molecules for aggregates in the network is altered from one

surface to another. In this case the amount of DiD available for tagging the aggregates in the aqueous phase would change for the gels prepared on different surfaces. Although, it is not possible to directly observe the structural changes in the network with the FCS, the variation of amount of labeled NaDC aggregates in the aqueous phase could be an indication of the structural changes in the network. It seems unlikely that the variation of G(0) for different surfaces is related to the concentration of NaDC aggregates in the water phase of the gel since the concentration of NaDC is very high even if it is taken into account that the 40% of overall concentration is in the aqueous phase for the unmodified glass chamber.

Results of steady-state and time-resolved florescence experiments revealed that pyrene senses the same environment when it is in the gel prepared on the coverslips bearing different functional groups. The overall distribution of pyrene between water and bile salt aggregates (A_3 and A_4 values) is the same for the gels prepared on all the three surfaces in these experiments. The lifetime of pyrene in the aggregates (τ_4) is also the same. This result indicates that the gel bulk structure is not influenced by hydrophilicity of the surface.

3.5 Conclusion

Fluorescence correlation spectroscopy revealed that the type of aggregates in NaDC gel and NaDC solution are the same. Presence of functional groups with different hydrophilicity does not have an influence on the type of NaDC aggregates formed in the

gel. Moreover, steady-state and time-resolved fluorescence studies showed that the hydrophilicity of the surface does not affect the bulk structure of the NaDC gel.

4 Investigation of the effect of inorganic salts on the properties of the NaDC gel

4.1 Introduction

Understanding the effect of salts on supramolecular gels is important due to the potential application of these gels. For example, gels targeted for biomedical applications need to be resistant to ions present in the biological system or need to be responsive to specific ions. There are many examples in the literature where hydrogels are shown to be sensitive to ions as external stimuli.[6,50,51] On the other hand there are many examples where gel formation is triggered or gel properties are tuned by the addition of salts.[47-49,53,100] Although these research efforts have provided some insights regarding the effect of ions on gels, there is still a lack of general rules to describe the effect of ions on the properties of gels.

More than 100 years ago Franz Hofmeister introduced a conceptual framework on how different cations and anions affect the solubility of proteins in water.[101] He classified some of the ions as “kosmotropes” which decrease the solubility of proteins (salting-out) and some other ions as “chaotropes” which increase the solubility of proteins (salting-in). Kosmotropes are normally hard ions with high charge density. These ions are highly

hydrated and are known to be water structure-making, where the water molecules have a more organized structure compared to in bulk water. Chaotropes are soft ions with low charge density and known to be water structure-breaking. Since the time when the Hofmeister series was introduced, researchers tried to rationalize the solubility of not only proteins but also many other molecules using the Hofmeister series[102] including molecules involved in supramolecular systems.[103] There are also a few examples where researchers tried to logically design and describe the effect of ions on supramolecular gels using the Hofmeister series.[104,105] For example, Ogden et al. investigated the hydrogelation of a proline-functionalized calix[4]arene in presence of different salts. They showed that the anions at the borderlines of the Hofmeister series can trigger the gelation. However, strong chaotropic anions lead to the formation of the gel followed by crystallization, whereas strong kosmotropes prevent the gelation of the solution.[104] As another example, Ulijn et al. showed that the anions of the Hofmeister's series have different effects on the morphology and mechanical properties of the hydrogels based on 9-fluorenylmethoxycarbonyldipeptide.[106] Miravet et al. also investigated the effect of the Hofmeister series on the gelation and the gel properties of a pseudo-peptide hydrogelator. They showed that the kosmotropic anions can increase the strength of the gel while the chaotropics decrease the strength.[105] All these reports were mainly focused on the anion ranking of the Hofmeister series, since it seems that the effect of anions is more pronounced in different systems.[101,105] However, it is reasonable to expect that the cations play a significant role in self-assembly and properties of the gels in which the building blocks of the gel are negatively charged species such as deoxycholate. Miravet et al.

investigated the effect of few cations on their pseudo-peptide hydrogel system and they noticed that the guandinium cation increases the solubility of the gelator significantly. Based on this observation they designed a hydrogel system which unlike most of the supramolecular gels forms by heating the solution and remains a moderately strong gel after cooling down.[105]

One shortcoming regarding the studies of the effect of salts on gels is the precipitation of the salts in ambient conditions. For example, the precipitation of salts during the fixing of samples for microscope studies can prevent researchers from obtaining the desired information regarding the structural properties of the gels.

The objective of this chapter was to understand how different ions affect the properties of the NaDC gel. Gels based on bile salts, such as NaDC have the potential to be used as drug delivery systems.[30,31] Blood and body fluids contain different ions which are present at different concentrations.[107] Therefore, it is important to have information on how the properties of the NaDC gel change in the presence of ions. It is particularly important to rationalize the effect of cations on the NaDC gel because the gelator is negatively charged. Another goal for this chapter was to investigate the behavior of a small guest molecule in the gel in the presence of salts. We were interested in understanding the effect of salts at the molecular level by studying the behavior of a small guest molecule in the gel since there is substantial lack of understanding of the effect of salts on the gels at the molecular level. Such an understanding of gel properties at a molecular level could be helpful in the rational design of gels.

4.2 Experimental

4.2.1 Materials

NaDC (Fluka, > 98%), $Na_2H_PO_4$ (Anachemia, anhydrous, > 99%), $NaH_2PO_4•H_2O$ (Anachemia, > 99%), methanol (Fisher, spectral grade, > 99.9%) were used as received. Pyrene (Fluka, 99%) was recrystallized from ethanol twice and its purity was established by the observation of a mono-exponential fluorescence decay in aerated water (127 ns).[75,76] NaCl (Sigma-Aldrich, > 99.5%), $NaNO_3$ (Caledon, 99.0%), $MgCl_2$ (Aldrich, Anhydrous, 98%), $CaCl_2$ (Anachemia, Anhydrous, Lot 210809), KCl (Sigma > 99.0%) NH_4Cl (Signa-Aldrich, 99.99%) were used as received. Deionized water (Barnstead NANOpure deionizing systems ≥ 17.8 MΩ cm) was used for the preparation of all solutions.

4.2.2 Sample preparation

A stock solution of each salt was prepared by dissolving the required mass of the salt in deionized water. The concentrations of the stock solutions for divalent cation salts like $CaCl_2$ and $MgCl_2$ were between 10 and 20 mM. Both $CaCl_2$ and $MgCl_2$ are hygroscopic salts, therefore, a mass of these salts was weighed quickly and directly into the glassware. The concentration of the stock solution for monovalent salts was 1 M. The titration of the $CaCl_2$ with EDTA showed that there is ca. 10% error in the concentrations of the solutions. The solutions for each sample were not titrated since the objective of experiments was to compare the effect of salt concentration on the gel and this is a relative comparison.

The phosphate buffer solution at pH of 6.5 was prepared by dissolving the required mass of Na_2HPO_4 (anhydrous) and NaH_2PO_4 (monohydrate) in deionized water. The final concentration of each of Na_2HPO_4 (anhydrous) and NaH_2PO_4 (monohydrate) was 0.5 M.

NaDC gels were prepared by dissolving solid NaDC into water. A required volume of the stock solution of the salt was then added to the aqueous solution of NaDC. The volumes of water and salt solutions were chosen in a way that the sum of the volumes was 1800 μL. The obtained solutions were heated at 60 °C for 15 min. In the next step, 200 μL of phosphate buffer was added to the solutions which were heated for another 15 min at 60 °C. The hot solutions were transferred into a 10 × 10 mm absorption cell. Cylindrical glass vials with an inner diameter of ca. 1.5 cm were used for the inversion test experiments. Gels were formed by cooling the samples to RT. For some of the salts at higher concentrations the solution at 60 °C was not transparent and the obtained gels were opaque. However, the sample converted to transparent gels over time. The experiments reported in this chapter were all performed with transparent gels.

The final concentration of NaDC was 30 mM. All gels have a baseline concentration of Na^+ cations of 180 mM since in addition to the contribution from NaDC the concentration of each Na_2HPO_4 (anhydrous) and NaH_2PO_4 (monohydrate) were 50 mM in the gel. Concentrations of salt stated below are in addition to the baseline Na^+ concentration of 180 mM.

4.2.3 Equipment setup

Fluorescence emission and excitation spectra were collected using a PTI QM-2 fluorimeter. Emission spectra were recorded between 350-550 nm at the excitation wavelength of 331 nm. The minimum step size of 0.5 nm was used to ensure accuracy in the determination of the I/III ratios for the pryene emission. The slits for both monochromators were set to a 1 nm bandwidth.

Fluorescence decays were recorded using an Edinburgh Instruments OB920 single photon counter (SPC). A 330 nm light emitting diode (LED) was used as the source of light. The excitation and the emission wavelength were 335 nm and 390 nm respectively and the emission monochromator had a bandwidth of 16 nm. The number of counts in the channel with maximum intensity was 10,000. The decays of pyrene were fitted to Equation 4.1 using the F900 software package from Edinburgh Instruments. In this equation A_i is the normalized pre-exponential factor for each emissive species with the lifetime τ_i. The goodness of the fits was determined by inspection of the χ^2 vales (0.9-1.3) and the randomness of the residuals. All the decays were fitted with a sum of three exponentials. The lifetimes with values at 10 ns and 130 ns correspond to the emission of impurities from the bile salt and the emission of pyrene in water and these values were fixed during the analysis. The third lifetime corresponds to the emission from pyrene bound to the bile salt aggregates in the network. The contribution of the 10 ns lifetime in the decay was not considered for the calculation of A values presented in the results section, in order to be able to compare the fraction of pyrene molecules in water and in the gel network for samples containing different salts with different concentrations. The

sample holder had a front-face arrangement between the excitation and emission optics for steady-state and time-resolved measurements. All the measurements were performed at RT.

$$I(t) = I_0 \sum_{1}^{i} A_i \, e^{-t/\tau_i} \qquad \text{Equation 4.1}$$

4.3 Results

4.3.1 Vial inversion test

The gel-to-sol transition temperature was determined by inversion of samples in a water bath and the results are shown in Table 4.1. The concentration used for all the salts except $CaCl_2$ were the maximum concentration that could be added to the NaDC gel without any precipitation occurring. In the case of $CaCl_2$, the concentration chosen for the inversion test was half of the maximum concentration used for fluorescence experiments. During the preparation of $CaCl_2$, it was observed that the 1 mM $CaCl_2$ solution was turbid when the solution was hot and at ca. 60 °C. However, the obtained gel at 1 mM $CaCl_2$ was transparent. Therefore, the 0.5 mM $CaCl_2$ gel sample was chosen for the inversion test to ensure that the precipitation of the salt would not occur during heating. Precipitation of the salt can affect the T_{gs} determination in an inversion test experiment.

In general, there is an increase in the gel-to-sol transition temperature for the salts studied, including for those salts where their concentrations are lower than the baseline Na^+ concentration of 180 mM. Moreover, comparison between NaCl, KCl, NH_4Cl and

$NaNO_3$ shows that although addition of salt leads to a significant increase in the gel-to-sol transition temperature, the type of salt does not have a significant influence on T_{gs}.

Table 4.1. Determination of the gel-to-sol transition temperature of the NaDC gel in the presence of different salts. T_1 and T_{gs} represent the change at the interface and when the gel fell due to gravity, respectively.

Salt	Concentration / mM	Baseline [Na+] / mM	T_1 / °C [a]	T_{gs} / °C [a]
Without salt	-	180	40.5 ± 0.7	43 ± 1
$CaCl_2$	0.5	180	46 ± 1	48 ± 1
$MgCl_2$	2	180	40 ± 1	49 ± 1
NaCl	400	180	53 ± 1	58 ± 2
KCl	400	180	53 ± 3	57 ± 1
NH_4Cl	400	180	57 ± 2	60 ± 1
$NaNO_3$	400	180	53 ± 1	57 ± 2

[a], The errors correspond to two independent experiments.

4.3.2 Steady-state and time-resolve fluorescence of pyrene in the NaDC gel in the presence of added salts

4.3.2.1 $CaCl_2$

Figure 4.1 illustrates the emission spectra of pyrene in the NaDC gel at different concentrations of $CaCl_2$. The spectra were measured on the same day as the sample preparation (Figure 4.1, left panel) and 5 days after sample preparation (Figure 4.1, right panel). The emission spectra of pyrene did not change upon the variation of $CaCl_2$

concentration when the experiments were performed on the same day as sample preparation as well as five days after sample preparation. However, the spectra were changed over time. The I/III ratio of pyrene was slightly increased from 1.02 ± 0.02 to 1.09 ± 0.02 over the period of 5 days (average of the I/III ratio values for different concentrations of $CaCl_2$). In addition to the monomer emission, a low intensity emission from pryene excimers is observed for both sets of experiments. The excimer emission arises from the close proximity of an excited pyrene with a ground state pyrene molecule leading to the excited dimer, i.e. the excimer. Similar to the monomer emission the intensity of the excimer emission was not dependent to the concentration of $CaCl_2$ for experiments performed on the same day. The excimer emission remained almost the same when the spectra were recorded after five days. The relative amount of excimer can be expressed as the intensity ratio for the excimer at 470 nm to the monomer intensity at the peak close to 382 nm. This ratio was around 0.07-0.09 for all the spectra.

Lifetime measurements showed that the partitioning of pyrene between the water phase, which corresponds to the species with 130 ns lifetime, and the bile salt network, which corresponds to the longer lived species, did not change with the increase in $CaCl_2$ concentration. The lifetime of pyrene in the network of the NaDC gel without salts was measured to be 350 ± 10 ns (3 individual experiments).

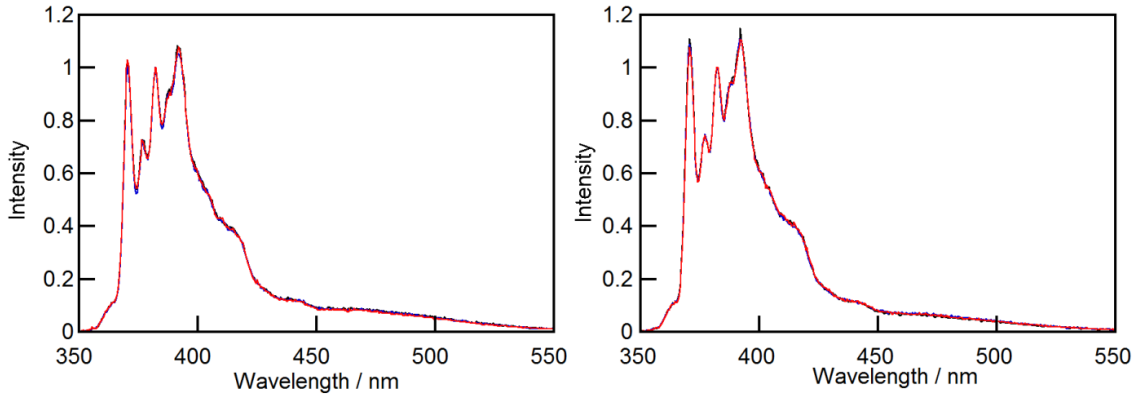

Figure 4.1. Emission spectra of 2 µM pyrene in NaDC gels containing 1 mM (black), 0.5 mM (blue) and 0.1 mM (red) $CaCl_2$. Spectra were measured on the same day as sample preparation (left) and 5 days after sample preparation (right). The excitation wavelength was 331 nm.

Table 4.2. Pyrene lifetimes and their corresponding A values in NaDC gel at different concentrations of $CaCl_2$. Sample preparation and measurements were performed on the same day.

[$CaCl_2$] / mM	**Baseline [Na^+] / mM**	**τ_1 / ns**	**A_1**	**τ_2 / ns**	**A_2**	**I/III**
1	180	130 [a]	0.48 ± 0.01 [b]	350 ± 2 [b]	0.52 ± 0.01 [b]	1.03 [d]
0.5	180	130 [a]	0.46 ± 0.01 [b]	345 ± 2 [b]	0.54 ± 0.01 [b]	1.00 [d]
0.1	180	130 [a]	0.45 ± 0.01 [b]	346 ± 2 [b]	0.55 ± 0.01 [b]	1.03 [d]
0	180	130 [a]	0.40 ± 0.09 [c]	350 ± 10 [c]	0.60 ± 0.09 [c]	0.94

[a], The lifetime of pyrene in water (~ 130 ns) was fixed. [b], The errors were recovered from the fit of the data. [c], The average of three independent experiments. [d], The estimated errors for the I/III ratio values are ca. 0.05.

Experiments were performed where the concentration of phosphate buffer was doubled or halved and formation of the NaDC gel at different concentrations of $CaCl_2$ was monitored (Table 4.3 and Table 4.4). These experiments were performed to

determine if it is possible to increase the concentration of $CaCl_2$ to more than 1 mM in the gel.

On the other side, the experiments with the halved phosphate buffer concentration were performed with the hypothesis that the decrease of buffer concentration leads to the overall decrease of cations and anions in the gel resulting in the decrease of ionic strength of the medium. Therefore, the capacity of the gel for incorporating another salt, $CaCl_2$, would increase.

The results of these experiments suggest that the amount of calcium chloride which could be added to the gel without precipitation is dependent on the concentration of phosphate buffer. For example, if the concentration of phosphate buffer was 0.025 M it was impossible to prepare a gel with 1 mM $CaCl_2$. However, it was possible to prepare the gel with 1 mM $CaCl_2$ when the concentration of phosphate buffer was 0.1 M and the ionic strength of the medium was increased.

The emission spectra of pyrene showed that the I/III ratio value is higher when the concentration of phosphate buffer is higher (comparison of Table 4.3 and Table 4.4). The observed I/III ratio value for pyrene is a weighted average of the I/III ratio of pyrene located in different environments within the gel. For example, the I/III ratio of pyrene in NaDC gel at the baseline Na^+ ion concentration and without any salt being added was 0.94. This value is in between the measured I/III ratio of pyrene in 50 mM phosphate buffer (1.73 ± 0.04) and in a 30 mM NaDC solution in the presence of 0.2 M NaCl (0.69 ± 0.01). The variation of the I/III ratio for the gels at constant $CaCl_2$ concentration (i.e.

0.5 mM $CaCl_2$) and at different buffer concentrations is either related to the different partitioning of the pyrene between the water phase and the NaDC aggregates in the gel or there are different binding sites for pyrene in the gel's network when the buffer concentration is changed.

Table 4.3. Pyrene lifetimes and their corresponding A values in the NaDC gel at different concentrations of $CaCl_2$. Concentration of phosphate buffer was 0.1 M, which is twice the concentration used regularly.

[$CaCl_2$] / mM	**Baseline [Na^+] / mM**	**τ_1 / ns**	**A_1**	**τ_2 /ns**	**A_2**	**I/III**
5[a]	330	-	-	-	-	-
1	330	130[b]	0.55 ± 0.01[c]	309 ± 2[c]	0.45 ± 0.01[c]	1.29[d]
0.5	330	130[b]	0.56 ± 0.01[c]	307 ± 2[c]	0.44 ± 0.01[c]	1.32[d]
0.1	330	130[b]	0.53 ± 0.01[c]	298 ± 2[c]	0.47 ± 0.01[c]	1.28[e]
0	180	130[b]	0.40 ± 0.09[d]	350 ± 10[d]	0.60 ± 0.09[d]	0.94

[a], At 5 mM $CaCl_2$ a turbid gel was formed. Therefore it was impossible to measure the pyrene lifetime and I/III ratio. [b], The lifetime of pyrene in water (~ 130 ns) was fixed. [c], The errors were recovered from the fit of the data. [d], The average of three independent experiments. [e], The estimated errors for the I/III ratio values are ca. 0.05.

Table 4.4. Pyrene lifetimes and their corresponding A values in the NaDC gel at different concentration of $CaCl_2$. Final concentration of phosphate buffer was 0.025 M, which is half of the concentration used regularly.

[$CaCl_2$] / mM	**Baseline [Na^+] / mM**	**τ_1 / ns**	**A_1**	**τ_2 / ns**	**A_2**	**I/III**
1[a]	105	-	-	-	-	-
0.5	105	130 [b]	0.14 ± 0.01 [c]	370 ± 1 [c]	0.86 ± 0.01 [c]	0.73 [e]
0	105	130 [b]	0.40 ± 0.09 [d]	350 ± 10 [d]	0.60 ± 0.09 [d]	0.94

[a], At 1 mM $CaCl_2$ a turbid gel was formed. Therefore it was impossible to measure the pyrene lifetime and I/III ratio. [b], The lifetime of pyrene in water (~ 130 ns) was fixed. [c], The errors were recovered from the fit of the data. [d], The average of three independent experiments. [e], The estimated errors for the I/III ratio values are ca. 0.05.

The results of the time-resolved fluorescence experiments at 0.5 mM $CaCl_2$ showed that the lifetime of pyrene in NaDC aggregates (τ_2) is shorter when the concentration of buffer is higher. Moreover, the amount of pyrene in the aggregates (A_2) is less at higher buffer concentrations. These results suggest that the properties of bile salt primary aggregate to which pyrene is bound is dependent on the concentration of buffer. Besides, partitioning of pyrene between the water phase and aggregates is also affected by the concentration of buffer.

In another experiment, NaCl was added to the gel with halved phosphate buffer concentration to examine if the change in capacity of the gel for accepting Ca^{2+} is related to the concentration of phosphate ions or Na^+ ions coming from phosphate buffer (Table 4.5). The concentration of NaCl was chosen at 75 mM so that the total concentration of Na^+ ions was 180 mM which corresponds to the regular baseline Na^+ ion concentration in

the gels. A transparent gel with 0.5 mM $CaCl_2$ could be prepared when the concentration of phosphate buffer was 0.025 M and no NaCl was added (the baseline [Na^+] of 105 mM, Table 4.4). However, it was impossible to prepare a gel with 0.5 mM $CaCl_2$ when the concentration of phosphate buffer was 0.025 M and 75 mM NaCl was added (the baseline [Na^+] of 180 mM, Table 4.5). The result of this experiment clarified that the amount of $CaCl_2$ that could be incorporated into the gel is less when another salt such as NaCl is added. This experiment clarified that the species which are responsible for the amount $CaCl_2$ that could be added to the gel are anions in phosphate buffer.

Table 4.5. Pyrene lifetimes and their corresponding A values in the NaDC gel at different concentrations of $CaCl_2$. Final concentration of phosphate buffer was 0.025 M, which is half of the concentration used regularly. NaCl with the final concentration of 75 mM was added to keep the concentration of Na^+ the same as the regular gels.

[$CaCl_2$] / mM	**Baseline [Na^+] / mM**	**τ_1 / ns**	**A_1**	**τ_2 / ns**	**A_2**	**I/III**
1[a]	180	-	-	-	-	-
0.5[a]	180	-	-	-	-	-
0.1	180	130 [b]	0.39 ± 0.01 [c]	360 ± 1 [c]	0.61 ± 0.01 [c]	0.90 [e]
0	180	130 [b]	0.40 ± 0.09 [d]	350 ± 10[d]	0.60 ± 0.09 [d]	0.94

[a], At 1 and 0.5 mM $CaCl_2$ a turbid gel was formed. Therefore, it was impossible to measure the pyrene lifetime and I/III ratio. [b], The lifetime of pyrene in water (~ 130 ns) was fixed. [c], The errors were recovered from the fit of the data. [d], The average of three independent experiments. [e], The estimated errors for the I/III ratio values are ca. 0.05.

The results of experiments with $CaCl_2$ illustrate that addition of the divalent cation as well as variation of the ionic strength of the medium affect the photophysical properties of pyrene in the NaDC gel. However, these results were not sufficiently informative to be able to explain the effect of the salt on the gel. Therefore, $MgCl_2$ with a different divalent cation (Mg^{2+}) and the same anion (Cl^-) as $CaCl_2$ was studied.

4.3.2.2 $MgCl_2$

Emission spectra of pyrene in NaDC gels with different concentrations of $MgCl_2$ were recorded for the same gels with different time gaps after sample preparation (Figure 4.2). No significant difference in the I/III ratios was observed at different concentrations of $MgCl_2$. However, the I/III ratio values slightly increased overtime. The experiment was repeated twice and the same results were obtained. Tables 4.6, 4.7 and 4.8 illustrate the results of lifetime measurements for different concentrations of the $MgCl_2$ which were measured with different time gaps after sample preparation. The variation of lifetimes and A values is not significant when the concentration of $MgCl_2$ is varied. However, a slight shortening of the lifetime of pyrene in the bile salt network (τ_2) and slight decrease of the A_2 values were observed when the fluorescence decays were recorded several days after sample preparation. These results indicate that the presence of $MgCl_2$ leads to changes in the gel structure in a way that relocation of pyrene from the network into the water occurs over time.

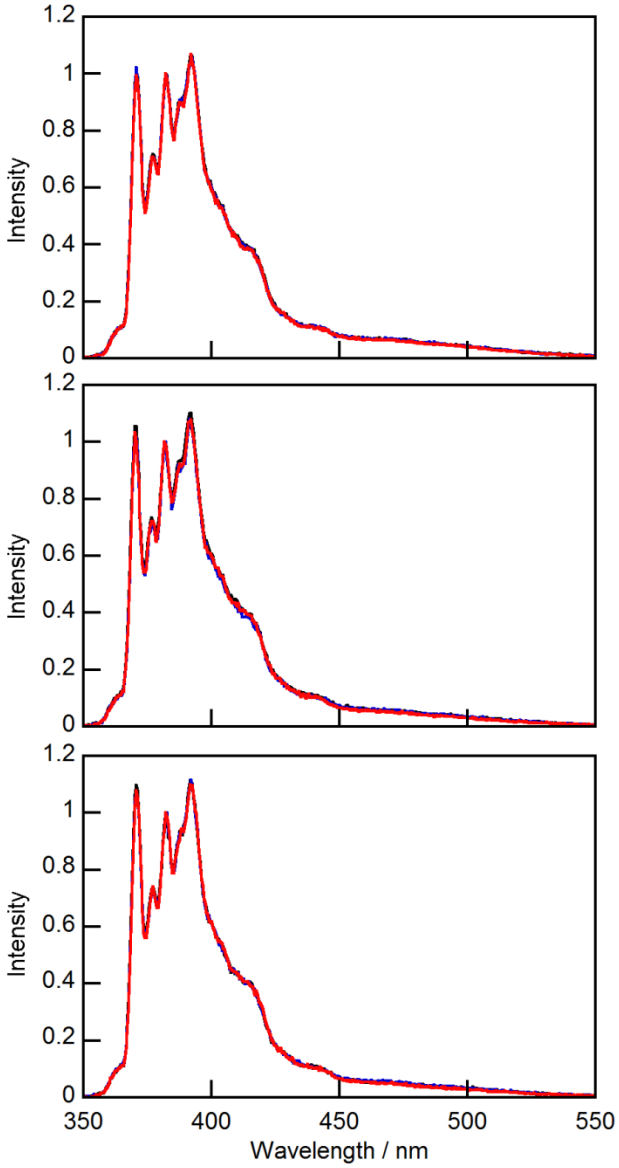

Figure 4.2. Emission spectra of 2 μM pyrene in NaDC gels containing 2 mM (black), 1 mM (blue) and 0.5 mM (red) $MgCl_2$. Spectra were measured on the same day as sample preparation (top) and 3 days (middle) and 8 days (bottom) after sample preparation.

Table 4.6. Pyrene lifetimes and their corresponding A values in the NaDC gel at different concentrations of $MgCl_2$. Concentration of pyrene was 2 μM and data were recorded the same day that the samples were prepared.

[$MgCl_2$] / mM	**Baseline [Na^+] / mM**	**τ_1 / ns**	**A_1**	**τ_2 / ns**	**A_2**	**I/III**
2[a]	180	130 [b]	0.46 ± 0.01 [c]	344 ± 2 [c]	0.54 ± 0.01 [c]	1.02 ± 0.01 [c]
1	180	130 [b]	0.46 ± 0.01 [c]	345 ± 3 [c]	0.54 ± 0.01 [c]	1.01 ± 0.01 [c]
0.5	180	130 [b]	0.47 ± 0.02 [c]	346 ± 1 [c]	0.53 ± 0.02 [c]	0.99 ± 0.01 [c]
0	180	130 [b]	0.40 ± 0.09 [d]	350 ± 10 [d]	0.60 ± 0.09 [d]	0.94

[a], At 2 mM $MgCl_2$ the gel was not entirely transparent and some fibrillar particles were visible with naked eye. [b], The lifetime of pyrene in water (~ 130 ns) was fixed. [c], The errors are the average of two independent experiments. [d], The average of three independent experiments.

Table 4.7. Pyrene lifetimes and their corresponding A values in the NaDC gel at different concentrations of $MgCl_2$. Concentration of pyrene was 2 μM and data were recorded 3 days after sample preparation.

[$MgCl_2$] / mM	**Baseline [Na^+] / mM**	**τ_1 / ns**	**A_1**	**τ_2 / ns**	**A_2**	**I/III**
2	180	130 [a]	0.50 ± 0.01 [b]	338 ± 2 [b]	0.50 ± 0.01 [b]	1.06 ± 0.01 [b]
1	180	130 [a]	0.49 ± 0.01 [b]	337 ± 5 [b]	0.51 ± 0.01 [b]	1.03 ± 0.01 [b]
0.5	180	130 [a]	0.49 ± 0.01 [b]	339 ± 1 [b]	0.51 ± 0.01 [b]	1.01 ± 0.04 [b]
0	180	130 [a]	0.40 ± 0.09 [c]	350 ± 10 [c]	0.60 ± 0.09 [c]	0.94

[a], The lifetime of pyrene in water (~ 130 ns) was fixed. [b], The errors are the average of two independent experiments. [c], The average of three independent experiments.

Table 4.8. Pyrene lifetimes and their corresponding A values in the NaDC gel at different concentrations of $MgCl_2$. Concentration of pyrene was 2 μM and data were recorded 8 days after sample preparation.

[$MgCl_2$] / mM	**Baseline [Na^+] / mM**	**τ_1 / ns**	**A_1**	**τ_2 / ns**	**A_2**	**I/III**
2	180	130 [a]	0.53 ± 0.01 [b]	333 ± 1 [b]	0.48 ± 0.01 [b]	1.12 ± 0.03 [b]
1	180	130 [a]	0.51 ± 0.01 [b]	334 ± 3 [b]	0.49 ± 0.01 [b]	1.09 ± 0.01 [b]
0.5	180	130 [a]	0.50 ± 0.01 [b]	335 ± 2 [b]	0.50 ± 0.01 [b]	1.08 ± 0.01 [b]
0	180	130 [a]	0.40 ± 0.09 [c]	350 ± 14 [c]	0.60 ± 0.09 [c]	0.94

[a], The lifetime of pyrene in water (~ 130 ns) was fixed. [b], The errors are the average of two independent experiments. [c], The average of three independent experiments.

A slight emission from excimer was also observed for all three concentrations of $MgCl_2$ studied. The intensity of excimer emission did not change when the spectra were recorded days after sample preparation. The excimer/monomer ratio was measured to be ca. 0.06-0.07 for the three concentrations of $MgCl_2$ when the measurements were performed on different days.

One shortcoming regarding the experiments with $CaCl_2$ and $MgCl_2$ was the precipitation that was observed at concentrations higher than 1-2 mM. The baseline concentration of the Na^+ ions in the NaDC gels was 180 mM which was much higher than the concentrations of the divalent salts. However, the results clearly showed that the presence of salts can induce changes to the NaDC gel. In particular, it was interesting that the effect of salt on the gel happens as the samples age. It seemed reasonable for the next step to be the choice of salts which have cations that are less kosmotropic than Ca^{2+} and Mg^{2+} to enable studying the effect of salts at high concentrations. Preliminary

experiments on monovalent salts such as NaCl, KCl and $NaNO_3$ showed that it is possible to add much higher concentrations of these salts (ca. 400 mM) to the NaDC gel without any precipitation. Among monovalent salts NaCl was chosen because its counter ion was the same as for $CaCl_2$ and $MgCl_2$. $NaNO_3$ was also tested to investigate the effect of a salt with a different anion.

4.3.2.3 NaCl

Three different concentrations of NaCl were added to the NaDC gel and the variation of photophysical properties of pyrene with the concentration and also over time was studied. Figure 4.3 illustrates the emission spectra of pyrene in NaDC gels at different concentrations of NaCl when the spectra were recorded on the same day as sample preparation (left) and 5 days after sample preparation (right). There is an increase in I/III ratio values when the concentration of NaCl is increased for the spectra that were recorded on the same day as sample preparation. Although the I/III ratio values which are presented in Table 4.9 seem to be the same considering the errors (average of two independent experiments), the decrease of the I/III ratio upon the decrease of the NaCl concentration was clearly observed for each individual experiment. Moreover, a slight excimer emission was observed when the spectra were recorded on the same day as sample preparation (Figure 4.3, left). The excimer/monomer intensity ratio was ca 0.06 ± 0.01, 0.09 ± 0.01 and 0.08 ± 0.01 for 400, 200 and 100 mM NaCl when the measurements were performed within couple of hours after sample preparation. This ratio

changed to 0.04 ± 0.01, 0.03 ± 0.01 and 0.05± 0.01 for 400, 200 and 100 mM NaCl when the spectra were recorded after 5 days.

Pyrene emission spectra were recorded for the same samples after 5 days (Figure 4.3, right). In this case, the measured I/III ratios were almost the same (ca. 1.33 ± 0.03) for all the three concentrations of NaCl (Table 4.10). The I/III ratio value around 1.3 is much higher than the I/III ratio value measured for the gel without NaCl (I/III ca. 0.9). These results indicate that the environment which pyrene senses in the gel after 5 days is independent from the concentration of NaCl. However, presence of NaCl leads to the structural change in the gel system in a way that the overall pyrene surrounding environment is more polar in comparison to the gel without NaCl.

Time-resolved fluorescence experiments were performed to understand the effect of NaCl on the gel. Neither the lifetimes nor the A values showed any dependence to the concentration of NaCl when the decays were recorded on the same day as sample preparation as well as after 5 days. The average lifetime of pyrene in NaDC aggregates in the network, τ_2, for the three concentrations of NaCl is 295 ± 7 ns and 300 ± 5 ns when the experiments were performed on the same day as sample preparation and after 5 days respectively. The measured lifetime for pyrene in aggregates is shorter in NaDC gels with NaCl in comparison to the gel without NaCl (τ_2 ca. 350 ns). For both freshly prepared and 5-day old gels the population of pyrene in water and the network is around 55% and 45% respectively. This result suggests that unlike the gels with $MgCl_2$ the relocation of the guest does not happen over time when NaCl is added.

The key result to interpret the effect of NaCl on the NaDC gel is the disappearance of excimer emission over time. This result suggests that the NaDC gel with NaCl is not at its most stabilized state when the measurements are performed a couple of hours after sample preparation. With time, structural changes happen in the gel in a way that prevents the two adjacent pyrene molecules from coming close to each other. Therefore, excimer formation does not happen and the excimer emission disappears when the spectra are recorded after 5 days.

Disappearance of excimer emission over time indicates that the NaDC gel does not reach to the equilibrium at shorter time periods when NaCl is added to the gel. This can be called the "kinetically" formed gel. The equilibration within the gel happens over time and therefore a "thermodynamically" stable gel forms.

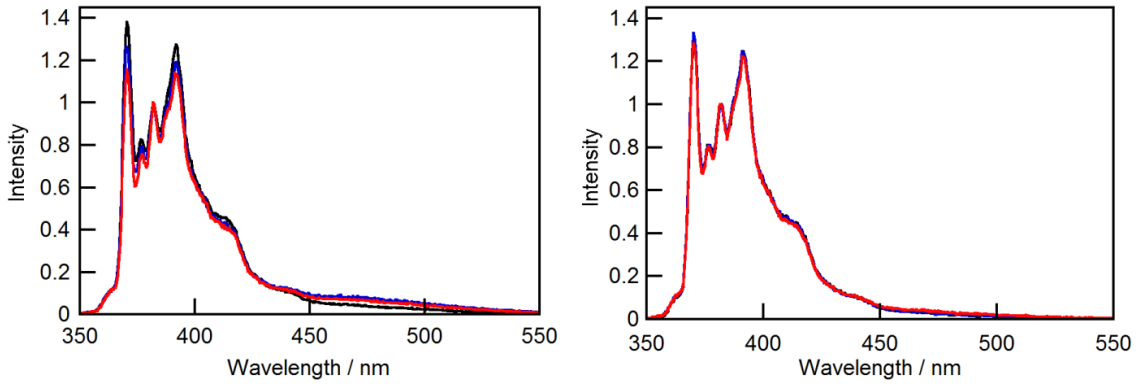

Figure 4.3. Emission spectra of pyrene in NaDC gel containing 400 (black), 200 (blue) and 100 (red) mM NaCl. Concentration of pyrene was 2 µM and spectra were recorded on the same day as sample preparation (left) and five days after sample preparation (right).

Table 4.9. Pyrene lifetimes and their corresponding A values in the NaDC gel at different concentrations of Na^+ ion. Concentration of pyrene was 2 μM and data were recorded the same day that samples were prepared.

[NaCl] / mM	Total [Na^+] / mM	τ_1 / ns	A_1	τ_2 / ns	A_2	I/III
400	580	130 [a]	0.56 ± 0.05 [b]	287 ± 1 [b]	0.44 ± 0.05 [b]	1.41 ± 0.04 [b]
200	380	130 [a]	0.57 ± 0.01 [b]	301 ± 1 [b]	0.43 ± 0.01 [b]	1.28 ± 0.02 [b]
100	280	130 [a]	0.53 ± 0.01 [b]	296 ± 14 [b]	0.47 ± 0.01 [b]	1.22 ± 0.08 [b]
0	180	130 [a]	0.40 ± 0.09 [c]	350 ± 10 [c]	0.60 ± 0.09 [c]	0.94

[a], The lifetime of pyrene in water (~ 130 ns) was fixed. [b], The errors are the average of two independent experiments. [c], The average of three independent experiments.

Table 4.10. Pyrene lifetimes and their corresponding A values in the NaDC gel at different concentrations of Na^+ ion. Concentration of pyrene was 2 μM and data were recorded five days after the sample's preparation.

[NaCl] / mM	Total [Na^+] / mM	τ_1 / ns	A_1	τ_2 / ns	A_2	I/III
400	580	130 [a]	0.58 ± 0.03 [b]	296 ± 4 [b]	0.42 ± 0.03 [b]	1.35 ± 0.07 [b]
200	380	130 [a]	0.59 ± 0.02 [b]	298 ± 4 [b]	0.41 ± 0.02 [b]	1.35 ± 0.02 [b]
100	280	130 [a]	0.58 ± 0.01 [b]	306 ± 2 [b]	0.42 ± 0.01 [b]	1.29 ± 0.01 [b]
0	180	130 [a]	0.40 ± 0.09 [c]	350 ± 10 [c]	0.60 ± 0.09 [c]	0.94

[a], The lifetime of pyrene in water (~ 130 ns) was fixed. [b], The errors are the average of two independent experiments. [c], The average of three independent experiments.

4.3.2.4 $NaNO_3$

The pyrene fluorescence can be quenched by NO_3^- ions.[108] Three sets of data were collected for NaDC gel containing 400, 200, and 100 mM $NaNO_3$ at different time intervals between sample preparation and fluorescence measurements. These

concentrations were chosen to be able to compare the data with those determined for the addition of NaCl. Measurements were performed 1-2 h, 1 day and 6 days after sample preparation. The same gel samples were used for the measurements performed within 1-2 h and the ones on the 6^{th} day. Different sets of gels with the same concentrations of $NaNO_3$ were prepared for the measurements after 1 day. In another experiment, the measurements were performed on the same gel samples after 1-2 h, 1 day and 6 days and the same results were obtained for the two sets of experiments.

Figure 4.4 illustrates the emission spectra of pyrene in NaDC gels with $NaNO_3$ recorded at 1-2 h (top), 1 day (middle) and 6 days (bottom) after sample preparation. Fluorescence emission spectra illustrate that the I/III ratio value increases upon increase of the concentration of $NaNO_3$ when the spectra are recorded within a couple of hours. However, no significant change in I/III ratio values was observed over time. Pyrene excimer emission was observed when spectra were recorded within 1-2 h of sample preparation. The excimer emission intensity was decreased when the spectra were recorded after 1 day and disappeared after 6 days. The excimer/monomer intensity ratios were 0.13 ± 0.03, 0.11± 0.01 and 0.12 ± 0.01 for the gels with 400, 200 and 100 mM $NaNO_3$ when the measurements were performed on the same day as sample preparation. These ratios were reduced to ca. 0.04 ± 0.01, 0.05 ± 0.01 and 0.06 ± 0.01 for the gels containing 400, 200 and 100 mM $NaNO_3$ after 6 days. The disappearance of excimer emission over time can be explained with the same logic as the one used to describe the effect of NaCl on the NaDC gel. When the measurements are performed within couple of

hours the gel is in a kinetically favored state. The structural changes happen and the gel reaches its equilibrated state over time.

Results of time-resolved fluorescence experiments are shown in Tables 4.11, 4.12 and 4.13. Knowing that nitrate is a quencher, fluorescence decays of pyrene were analyzed without fixing the lifetime for the emission of pyrene in water. The shortening of τ_1, lifetime of pyrene in the aqueous phase, is observed when the concentration of $NaNO_3$ is increased. This is because NO_3^- quenches the fluorescence of excited pyrene molecules located in the water phase of the gel. In addition, the τ_2 values were shortened upon increasing the concentration of $NaNO_3$ when the measurement was performed 1-2 h after sample preparation (Table 4.11). This result indicates that the gel network is not completely stabilized within 1-2 h after sample preparation. Thus, NO_3^- ions can access the pyrene in bile salt aggregates which leads to the quenching of fluorescence of pyrene. The quenching rate constant (k_q) was calculated according to Equation 4.2 where the τ_0 and τ are the lifetimes in the absence and presence of the quencher respectively and the [Q] is the concentration of the fluorescence quencher. The k_q is approximately calculated to be 1×10^6 $s^{-1}M^{-1}$.

$$\frac{\tau_0}{\tau} = 1 + k_q \tau_0 [Q] \qquad \text{Equation 4.2}$$

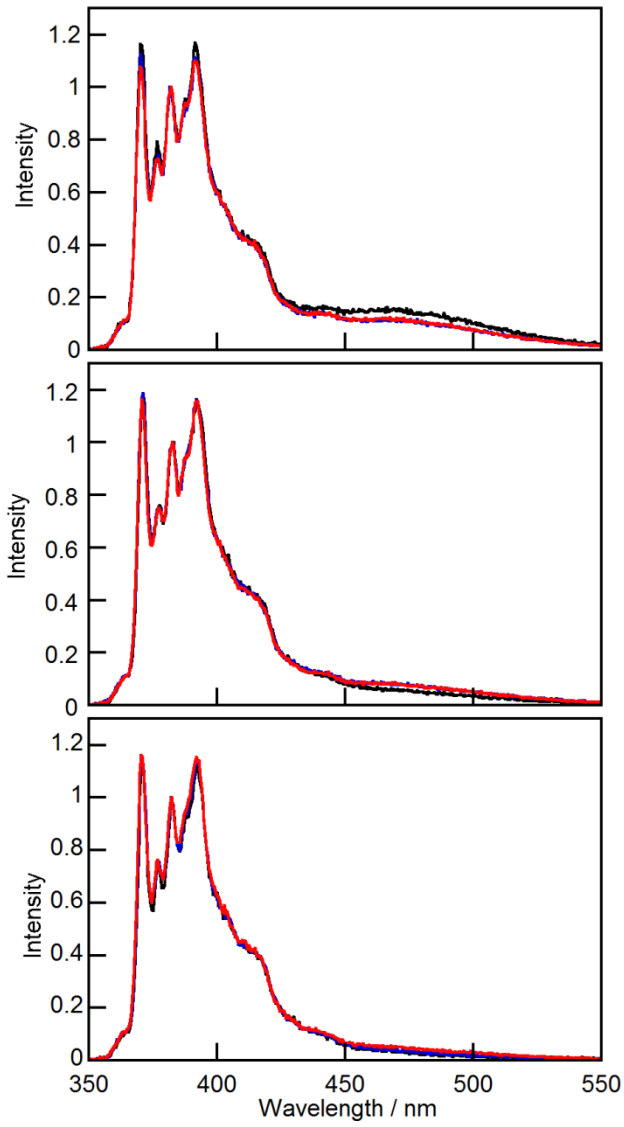

Figure 4.4. Fluorescence emission of 2 μM pyrene in the NaDC gels at different concentrations of $NaNO_3$. Measurements were performed 1-2 h (top), 1 day (middle) and 6 days (bottom) after sample preparation. Black, blue and red lines correspond to the 400, 200 and 100 mM $NaNO_3$ respectively.

There is no significant difference in the distribution of pyrene molecules between water and the network at different concentrations of $NaNO_3$. Similar to the experiments performed for the gel with NaCl, around 60% of pyrene is in water when $NaNO_3$ is added to NaDC gel system. This value remains almost the same even after 6 days. This result indicates that the structural changes which happen over time, do not lead to the relocation of pyrene from one binding environment to another.

Table 4.11. Pyrene lifetimes and their corresponding A values in the NaDC gel at different concentrations of $NaNO_3$. Measurements were performed 1-2 h after sample preparation. Pyrene concentration is 2 μM.

[$NaNO_3$] / mM	**Total [Na^+] / mM**	**τ_1 / ns**	**A_1**	**τ_2 / ns**	**A_2**	**I/III**
400	580	59 ± 3 [b]	0.67 ± 0.01 [b]	318 ± 4 [b]	0.33 ± 0.01 [b]	1.17 ±0.01 [b]
200	380	73 ± 1 [b]	0.66 ± 0.01 [b]	324 ± 1 [b]	0.34 ± 0.01 [b]	1.15 ± 0.03 [b]
100	280	95 ± 2 [b]	0.61 ± 0.02 [b]	340 ± 1 [b]	0.39 ± 0.01 [b]	1.07 ± 0.02 [b]
0	180	130 [a]	0.40 ± 0.09 [c]	350 ± 10 [c]	0.60 ± 0.09 [c]	0.94

[a], The lifetime of pyrene in water (~ 130 ns) was fixed. [b], The errors are the average of two independent experiments. [c], The average of three independent experiments.

Table 4.12. Pyrene lifetimes and their corresponding A values in the NaDC gel at different concentrations of $NaNO_3$. Measurements were performed 1 day after sample preparation. Pyrene concentration is 2 μM.

$[NaNO_3]$ / mM	Total $[Na^+]$ / mM	τ_1 / ns	A_1	τ_2 / ns	A_2	I/III
400	580	60 ± 2 [b]	0.59 ± 0.02 [b]	305 ± 4 [b]	0.41 ± 0.02 [b]	1.20 ± 0.02 [b]
200	380	73 ± 2 [b]	0.65 ± 0.01 [b]	313 ± 2 [b]	0.35 ± 0.01 [b]	1.17 ± 0.03 [b]
100	280	94 ±1 [b]	0.61 ± 0.01 [b]	327 ± 5 [b]	0.39 ± 0.01 [b]	1.12 ± 0.06 [b]
0	180	130 [a]	0.40 ± 0.09 [c]	350 ± 10 [c]	0.60 ± 0.09 [c]	0.94

[a], The lifetime of pyrene in water (~ 130 ns) was fixed. [b], The errors are the average of two independent experiments. [c], The average of three independent experiments.

Table 4.13. Pyrene lifetimes and their corresponding A values in the NaDC gel at different concentrations of $NaNO_3$. Measurements were performed 6 days after sample preparation. Pyrene concentration is 2 μM.

$[NaNO_3]$ / mM	Total [Na+] / mM	τ_1 / ns	A_1	τ_2 / ns	A_2	I/III
400	580	61 ± 1 [b]	0.62 ± 0.02 [b]	308 ± 9 [b]	0.38 ± 0.02 [b]	1.14 ± 0.04 [b]
200	380	72 ± 1 [b]	0.62 ± 0.03 [b]	307 ± 2 [b]	0.38 ± 0.03 [b]	1.15 ± 0.01 [b]
100	280	94 ± 1 [b]	0.61 ± 0.01 [b]	321 ± 2 [b]	0.39 ± 0.01 [b]	1.13 ± 0.04 [b]
0	180	130 [a]	0.40 ± 0.09 [c]	350 ± 14 [c]	0.60 ± 0.09 [c]	0.94

[a], The lifetime of pyrene in water (~ 130 ns) was fixed. [b], The errors are the average of two independent experiments. [c], The average of three independent experiments.

4.4 Discussion

All the gels studied (except those with doubled or halved buffer concentrations) contain a baseline Na^+ concentration of 180 mM. Among the cations that were tested to understand the effect of salts on NaDC gels, Ca^{2+} was the one which could be used only

at very low concentrations. Addition of 2 mM $CaCl_2$ leads to the immediate precipitation of the solution. Therefore, the maximum concentration used in fluorescence experiments was 1 mM. The maximum amount of cation that was incorporated into the gel without causing precipitation is in agreement with Hofmeister series with slight variations. According to the Hofmeister series the ability of the cations for salting-out is as follow[109]:

$$Mg^{2+} > Ca^{2+} > Na^{+} > K^{+} \sim NH_4^{+}$$

Therefore, it was expected that the solubility of NaDC in water decreases when the divalent cations, such as Mg^{2+} or Ca^{2+}, were added to system. In fact the obtained results were in line with predictions based on the Hofmeister series. Nonetheless, a slight deviation from Hofmeister series was observed. The order of cations for forming precipitate in the NaDC gel system is as follow:

$$Ca^{2+} > Mg^{2+} > NH_4^{+} \sim Na^{+} \sim K^{+}$$

Cations such as Na^{+}, K^{+} and NH_4^{+} are on the borderline between kosmotropes and chaotropes in the Hofmeister series. Therefore, it is not surprising to observe the same behavior when these monovalent salts are added to the NaDC solutions. Both Mg^{2+} and Ca^{2+} are kosmotropic cations. It is expected that Mg^{2+} should have shown more kosmotropic properties due to its higher charge density of Mg^{2+} than Ca^{2+}. However, it was reported that because of the higher charge density the ion-water interaction is partially covalent. For example, Mg^{2+} in aqueous solutions forms a complex of $Mg[H_2O]_6^{2+}$ with the net charge of 1.18.[109] The presence of the hydration shell around Mg^{2+} ions leads to a decrease of the kosmotrpic properties for Mg^{2+}. It was shown that

the interaction of Mg^{2+} ions with biological components in cells occurs via both inner and outer sphere complexes whereas Ca^{2+} ions mostly form inner sphere complexes.[109] Moreover, the calcium phosphate salt is hardly water soluble. However, the magnesium phosphate salt is moderately soluble.[109] Therefore, it is expected that the amount of Mg^{2+} which could be incorporated into the NaDC gel is higher than the amount of Ca^{2+}.

Results of the T_{gs} measurements depict that addition of salts leads to the increase of the gel-to-sol transition temperature. The salts with divalent cations show the same effect on the T_{gs} that was ca. 48 °C for the addition of 0.5-2 mM of $CaCl_2$ or $MgCl_2$. Besides, monovalent salts also showed a similar enhancement of T_{gs} regardless of the type of salt. Although the concentrations of Mg^{2+} or Ca^{2+} were much lower than the concentrations of Na^+, they were able to change some of the gel properties such as T_{gs}. This result indicates that addition of salts leads to more thermally stable NaDC gels.

Experiments at which the concentration of phosphate buffer were varied depicted that the amount of phosphate buffer can play a role in terms of capacity of the gel for incorporating Ca^{2+} ions, where at higher concentration of the buffer higher concentration of $CaCl_2$ could be added to the NaDC gel. These results may seem in contradiction with the fact that the calcium phosphate salt is hardly soluble. Nonetheless, this observation is related to not only one possible interaction but for the many interactions which happen in a complex system such as the NaDC gel. The anions in the gel are PO_4^{3-}, HPO_4^{2-}, $H_2PO_4^-$ and deoxycholate ($R\text{-}COO^-$). The solubility of the $Ca_3(PO_4)_2$, $CaHPO_4$ and $Ca(H_2PO_4)_2$ are ca. 1.4×10^{-7}, 1.5×10^{-3} and 88×10^{-3} M respectively.[110] Addition of phosphate

buffer leads to the presence of three different anions of which two form salts with the water solubility in the mM concentration range. Moreover, Hofmann et al. reported that at low concentrations of deoxycholic acid precipitates are formed with Ca^{2+} (between 1 to 2 mM of the deoxycholic acid forms precipitate in a 2.5 mM Ca^{2+} solution).[111] The requirement for the formation of a transparent gel is that all cation-anion interactions be such that the precipitation of salts does not occur. The decrease of the concentration of phosphate buffer leads to lower concentrations of negatively charged species such as $H_2PO_4^-$, HPO_4^{2-} and PO_4^{3-} in the system. Therefore, it is less probable that the salts with relatively higher solubility ($CaHPO_4$ and $Ca(H_2PO_4)_2$) formed. On the other hand, the concentration of deoxycholate (R-COO^-) is constant and $Ca(OOC\text{-}R)_2$ complex can form easily. Therefore, the precipitation happens at lower concentrations of Ca^{2+} when the buffer concentration is less.

Results of the fluorescence experiments on the gels with $CaCl_2$ showed that the I/III ratio of pyrene changes over time. The photophysical properties of pyrene were not dependent on the concentration of $CaCl_2$, but they were affected by the concentration of phosphate buffer. These results indicate that the variation of baseline Na^+ and anion concentrations can lead to a change in the gel's network. When the concentration of phosphate buffer is higher the percentage of pyrene molecules in water is also higher. Presence of higher amounts of pyrene in water leads to the observation of a larger I/III ratio value. Besides, a shorter lifetime for pyrene in the network was observed. These results indicate that the aggregates involved in the formation of the network are different when the ionic strength of the medium is changed. It seems that at higher ionic strength

the structure of aggregates in the network allow the mobility of pyrene to the water phase to happen which leads to the larger A_1 value. This essentially means that the aggregates of the network are not formed very "tightly". The access of oxygen molecules to the pyrene inside the aggregates would also be easier for the same reason. Therefore, the fluorescence quenching occurs and a shorter lifetime is observed for the pyrene molecules in the aggregates.

The results of fluorescence experiments with another divalent cation, Mg^{2+}, revealed that the relocation of pyrene from the network to the water phase happens over time. Similar to Ca^{2+}, the photophysical characteristics of pyrene did not show any dependence on the concentration of $MgCl_2$. However, the increase in I/III ratio value, the shortening of τ_2 and the increase of the A_1 value of pyrene occurred over time which suggests that a change in structure of the gel happened. Based on the photophysical properties of pyrene, it is hard to picture the structural changes induced by divalent cations. It seems that the high affinity of the divalent cations for the deoxycholate anions prevents the formation of aggregates where the NaDC monomers are tightly bound. Therefore, the gradual release of pyrene out of the network occurs over time.

The results of steady-state and time-resolved fluorescence measurements of pyrene in the NaDC gel containing NaCl indicate that a kinetically favored gel forms within couple of hours after sample preparation. In this case, ca. 55% of pyrene molecules are in water and 45% of them are in the bile salt aggregates.

The gel network is constructed when the self-assembly of the NaDC aggregates in solution takes place. The assembly of the aggregates for the construction of the network occurs continuously until the point at which the number of aggregates which are associating into the network are equal to the number of aggregates which are dissociating from the network into the water phase. In other words, an equilibrium forms between the aggregates in the network and aggregates floating in the water phase. The presence of high concentrations of NaCl prevents the equilibration of the aggregates floating in the water phase and the aggregates involved in the network at shorter time periods. However, the equilibrium between aggregates in the network and those floating in the water phase occurs over time. In fact, the presence of NaCl facilitates the extension of the network. After 5 days the A values show that still around 55% of pyrenes are in the water and 45% are in the aggregates. The constant value for the amount of pyrene in any of the two environments depicts that the extension of the network does not lead to the relocation of pyrene from water into the network or the reverse. However, the network extension leads to the separation of pyrene molecules which were close to each other to form excimer in the kinetically formed gel. This gel with the extended network can be considered as the thermodynamically stable gel. Scheme 4.1 illustrates the formation of excimer in the kinetically formed gel (left) followed by formation of thermodynamically stable gel (right). The fact that quite a large portion of pyrene molecules are in water (A_2 value) explains the high I/III ratio value in comparison to the gel without NaCl. There is no direct evidence that the excimer formation happens in the water phase of the gel or in the network. However, since the amount of pyrene molecules in water is high and water is

the least favored environment for pyrene as a hydrophobic molecule, it seems reasonable that the excimer formation happens in the aqueous phase of the gel. Tato et al. used the pyrene excimer formation as a sign of gelation of NaDC.[22] They showed that the association of the aggregates bearing a pyrene monomer during the gel formation leads to the pyrene excimer formation. The method of sample preparation is different between Tato's work and my experiments. Moreover, in Tato's paper the pyrene excimer formation was monitored between 0 and 105 min after sample preparation. It is shown that the methods of sample preparation and the history of the gel sample can affect the gel properties.[89] Therefore, the results of experiments presented in this chapter are not in contradiction with Tato's work.

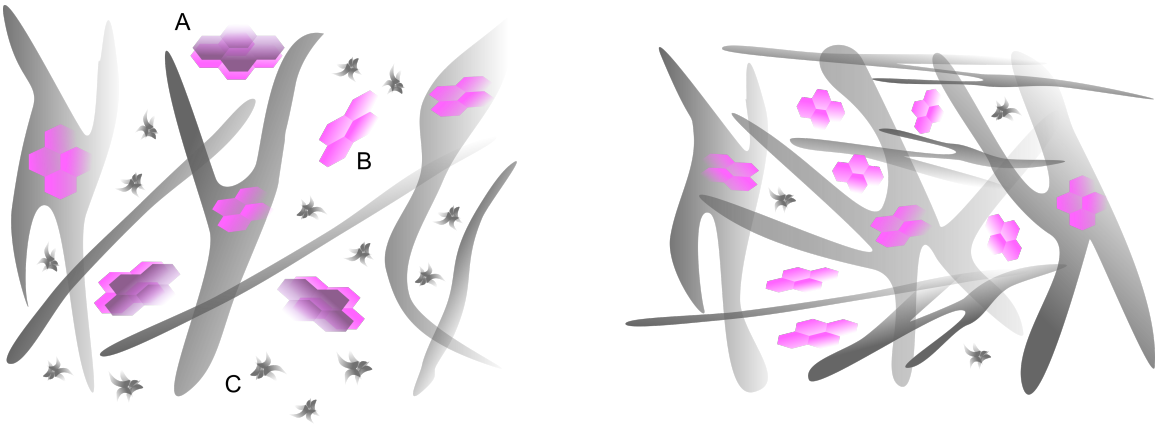

Scheme 4.1. Cartoon representation for the kinetically formed NaDC gel (left) and thermodynamically stable gel (right) in the presence of NaCl. Network extension and branching prevents the excimer formation in the thermodynamically stable gel. A, B and C represent pyrene excimer, pyrene monomer and NaDC aggregates in the aqueous phase of the gel (not to scale), respectively. The salting-out effect of NaCl leads to the extension of the gel network over time.

Results of the experiments with $NaNO_3$ are in line with the results of the experiments with NaCl. Disappearance of excimer emission occurs over time, which proves that the gel structure changes from a kinetically formed gel to the thermodynamically stable gel.

In the experiments with $NaNO_3$, the observed trends for the variation of the I/III ratio values is similar to the ones observed for the gels with NaCl. The measured I/III ratio values for the gels with $NaNO_3$ are slightly lower in comparison to the gels with NaCl when the experiments were performed within a couple of hours after sample preparation. This result is expected, because the NO_3^- ions quench the fluorescence of the pyrene molecules in the water phase. The observed I/III value is sum of the I/III ratio values of all the species present in the system which are pyrene in water and pyrene in the network. The I/III ratio of pyrene in water is larger than the I/III ratio of pyrene in the network. The access of the quencher to the pyrene molecules in water is easier than to those in the network because aggregates around pyrene can protect it from the access of the quencher. Therefore, the quenching of pyrene in water occurs with higher efficiency and as a result the contribution of I/III ratio of pyrene in water into the observed I/III ratio value decreases.

The shortening of τ_2 values upon increase of the concentration of $NaNO_3$ was observed in the kinetically formed gel. This result suggests that dynamic (or collisional) quenching of pyrene excited state in the network occurs when NO_3^- is added to the gel. In a dynamic quenching process the quencher has to diffuse to the molecule during the

lifetime of the excited state.[112] For a diffusion-controlled quenching process the k_q is close to the 1×10^{10} $s^{-1}M^{-1}$.[112] The smaller value for the k_q is normally related to the shielding of fluorophore or a low quenching efficiency. The k_q is approximately calculated to be 1×10^6 $s^{-1}M^{-1}$. The k_q value for other hydrophobic guest molecules such as naphthalene and acenaphtene in 40 mM NaDC solution are reported to be 3.4×10^7 $s^{-1}M^{-1}$ and 4.3×10^6 $s^{-1}M^{-1}$ respectively.[113] The k_q value which is measured for pyrene in NaDC gel is approximately in the same range as those which are measured in NaDC solution. This result indicates that the shielding around pyrene in the gel network is similar to the shielding of fluorophores in NaDC solution, suggesting that the aggregates involved in the network are structurally similar to those in solution of NaDC. This result is in agreement with the results of FCS experiments (chapter 3) where the correlation traces of DiD in the gel and in solution were the same indicating the similarity of the aggregates in the network and in the NaDC solution.

The results of the fluorescence correlation spectroscopy experiments presented in chapter 3 showed that there are quite a significant percentage of NaDC aggregates floating in the water phase of the gel. One hypothesis could be that the presence of the salts in the water phase plays a “salting-out” role. As a result a higher percentage of aggregates would be absorbed into the network. It would be expected that the stability (thermal or mechanical) of the gels increases if a larger percent of aggregates are involved in the network. The increase of the T_{gs} proves that the gels are thermally more stable when the salts are added. Moreover, the extension of the network over time is

another phenomenon which shows that the “salting-out” of the aggregates occurs when the salts are added to the gel.

4.5 Conclusion

Investigation of the effect of different salts on the NaDC gel as a supramolecular gel system showed that the addition of salts can change properties such as the gel’s thermal stability and structure of the network. Cations with different charge densities can induce different changes in the gels network. Moreover, the interaction of salts with different species in the gel can lead to changes in the dynamics of the gel by disturbing the equilibrium between aggregates in the aqueous phase and the aggregates in the network. Overall, the results of the experiments presented in this chapter show that in a supramolecular gel system which is formed based on multiple non-covalent interactions, the presence of salts is influential from many different aspects. Therefore, to be able to design the gels for required purposes it is necessary to have a deep understanding of the effect of salts on the structural properties and dynamics of the gels. Moreover, this work demonstrates that the effect of cationic species on a supramolecular gel system should not be ignored even though it is believed that the anions of the Hofmeister series are more influential in structural changes in many systems. In particular, the results of this chapter show that the effect cations needs to be taken into account for a system where negatively charged species are the building blocks of the network of a supramolecular gel.

5 Conclusion

Although supramolecular gels have been a point of interest for many research groups, not all aspects of the supramolecular gels are well-understood. The properties of the sodium deoxycholate hydrogel as a supramolecular gel system were investigated in presence of cucurbit[6]uril, on the surfaces with different hydrophilicity and in the presence of inorganic salts with the aim of shedding lights on some aspects of supramolecular hydrogels.

Addition of CB[6] to the NaDC gel provides another binding site for pyrene in addition to the primary aggregates of the bile salts. Temperature annealing experiments showed that the temperature at which the release of pyrene from the network happens, can be tuned by addition of CB[6]. Besides, the results of studies on the NaDC gel with CB[6] revealed that there is no direct correlation between the macroscopic properties of the gel and the dynamic properties which occur at the molecular level. To the best of my knowledge, this is the first time that partitioning of a guest molecule between different binding environment in a gel is reported. My observation on the relocation of the guest by temperature variation provides the insight into the gel system at molecular level suggesting that the location of the guest can be tuned and may have a direct effect on the overall release of the guest from a functional gel. This information will be helpful for researchers who will develop to use gels as a carrier for the guest molecules, i.e. drugs.

Fluorescence correlation spectroscopy experiments illustrated that the diffusion of NaDC aggregates in the water phase of the gel is the same as the diffusion of the

aggregates in the NaDC solution. With the assumption that there is equilibrium between the aggregates involved in the network and aggregates in the aqueous phase of the gel, one can conclude that the aggregates involved in the gel network formation are the same as those that are present in NaDC solution. Moreover, the FCS results indicated that a significant amount of material is not incorporated into the network of the gel. The minimum gelator concentration for gel formation is a parameter that is normally reported, but there is no literature report which addresses how much of the gelator is used to build the network and how much of the gelator diffuses freely in the aqueous/organic phase of the gel. Based on our result, it is important that the "efficient" concentration of the gelator in the network be taken into account for the rational design of gel systems. Moreover, the results presented in chapter 3 clearly suggest that the understanding of the effect of surface on the gel requires creative design of the experiments and inventive use of techniques in order to understand the effect of surface on the gel properties.

The results of experiments presented in chapter 4 revealed that addition of monovalent inorganic salts leads to a kinetically formed gel at shorter time periods. The extension of the NaDC network happens over time, perhaps by "salting-out" of the aggregates floating in the aqueous phase of the gel which leads to the formation of a thermodynamically stable gel. Addition of inorganic salts with divalent cations leads to dramatic changes in solubility of the species in the gel which is expected considering the ranking of the cations in Hofmeister series. These results indicated that the effect of cations on the gels should not be ignored in particular on the gels where the network is formed by assembly of negatively charged species such as deoxycholate aggregates.

Overall, the results of projects presented in this thesis indicate that the characterization of the gels at microscopic level is required since the macroscopic properties of the gel are not necessarily representative of the processes happening inside the gel. Molecular gels are dynamic systems. If we want to control the gel properties and design the gels for specific purposes, we need to understand the dynamic processes occurring in the gel systems at the molecular level. This includes but is not limited to self-assembly of the gelator, interactions and forces involved between the gelator-solvent-additives-ions and the surface.

The next important step for exploring the NaDC gel system is to understand how the assembly of the aggregates occurs when the network forms. Also, it would be interesting to understand the dynamics of the exchange of the aggregates between the network and the aqueous phase when the gel has reached its thermodynamically stable state. These experiments can then be followed with the studies of the mobility of guests when bound to the aggregates and not as individual species. These new directions build on the work I described in this thesis and will lead to the long-term goal of being able to rationally design the function of gels.

6 References

(1) Buerkle, L. E.; Rowan, S. J. *Chemical Society Reviews* **2012**, *41*, 6089.

(2) Weiss, R. G. *Journal of the American Chemical Society* **2014**, *136*, 7519.

(3) Steed, J. W. *Chemical Communications* **2011**, *47*, 1379.

(4) Yan, N.; Xu, Z.; Diehn, K. K.; Raghavan, S. R.; Fang, Y.; Weiss, R. G. *Journal of the American Chemical Society* **2013**, *135*, 8989.

(5) Pal, A.; Basit, H.; Sen, S.; Aswal, V. K.; Bhattacharya, S. *Journal of Materials Chemistry* **2009**, *19*, 4325.

(6) Foster, J. A.; PiepenbrockMarc-Oliver, M.; Lloyd, G. O.; Clarke, N.; HowardJudith, A. K.; Steed, J. W. *Nature Chemistry* **2010**, *2*, 1037.

(7) Ayabe, M.; Kishida, T.; Fujita, N.; Sada, K.; Shinkai, S. *Organic & Biomolecular Chemistry* **2003**, *1*, 2744.

(8) Miravet, J. F.; Escuder, B. In *Functional Molecular Gels*; The Royal Society of Chemistry: 2014, p 117.

(9) Chen, X.; Huang, Z.; Chen, S.-Y.; Li, K.; Yu, X.-Q.; Pu, L. *Journal of the American Chemical Society* **2010**, *132*, 7297.

(10) Shumburo, A.; Biewer, M. C. *Chemistry of Materials* **2002**, *14*, 3745.

(11) Gu, W.; Lu, L.; B. Chapman, G.; G. Weiss, R. *Chemical Communications* **1997**, 543.

(12) Carey, M. C.; Small, D. M. *Archives of Internal Medicine* **1972**, *130*, 506.

(13) Malik, N. A. *Applied Biochemistry and Biotechnology* **2016**, 1.

(14) Maestre, A.; Guardado, P.; Moyá, M. L. *Journal of Chemical & Engineering Data* **2014**, *59*, 433.

(15) Small, D. M. In *Molecular Association in Biological and Related Systems*; AMERICAN CHEMICAL SOCIETY: 1968; Vol. 84, p 31.

(16) Small, D. M.; Penkett, S. A.; Chapman, D. *Biochimica et Biophysica Acta (BBA) - Lipids and Lipid Metabolism* **1969**, *176*, 178.

(17) O'Connor, C. J.; Ch'ng, B. T.; Wallace, R. G. *Journal of Colloid and Interface Science* **1983**, *95*, 410.

(18) Djavanbakht, A.; Kale, K. M.; Zana, R. *Journal of Colloid and Interface Science* **1977**, *59*, 139.

(19) Mazer, N. A.; Carey, M. C.; Kwasnick, R. F.; Benedek, G. B. *Biochemistry* **1979**, *18*, 3064.

(20) Paul, R.; Mathew, M. K.; Narayanan, R.; Balaram, P. *Chemistry and Physics of Lipids* **1979**, *25*, 345.

(21) Amundson, L. L.; Li, R.; Bohne, C. *Langmuir* **2008**, *24*, 8491.

(22) Jover, A.; Meijide, F.; Rodríguez Núñez, E.; Vázquez Tato, J.; Mosquera, M.; Rodríguez Prieto, F. *Langmuir* **1996**, *12*, 1789.

(23) Mukherjee, B.; Dar, A. A.; Bhat, P. A.; Moulik, S. P.; Das, A. R. *RSC Advances* **2016**, *6*, 1769.

(24) Garidel, P.; Hildebrand, A.; Neubert, R.; Blume, A. *Langmuir* **2000**, *16*, 5267.

(25) Kumar, K.; Patial, B. S.; Chauhan, S. *Journal of Chemical Thermodynamics* **2015**, *82*, 25.

(26) Sobotka, H.; Czeczowiczka, N. *Journal of Colloid Science* **1958**, *13*, 188.

(27) Blow, D. M.; Rich, A. *Journal of the American Chemical Society* **1960**, *82*, 3566.

(28) Tanaka, F. In *Molecular Gels: Materials with Self-Assembled Fibrillar Networks*; Weiss, R. G., Terech, P., Eds.; Springer Netherlands: Dordrecht, 2006, p 17.

(29) Jover, A.; Meijide, F.; Rodríguez Núñez, E. *Langmuir* **2002**, *18*, 987.

(30) Valenta, C.; Nowack, E.; Bernkop-Schnürch, A. *International Journal of Pharmaceutics* **1999**, *185*, 103.

(31) McNeel, K. E.; Das, S.; Siraj, N.; Negulescu, I. I.; Warner, I. M. *Journal of Physical Chemistry B* **2015**, *119*, 8651.

(32) Nonappa; Maitra, U. *Organic & Biomolecular Chemistry* **2008**, *6*, 657.

(33) Chakrabarty, A.; Maitra, U.; Das, A. D. *Journal of Materials Chemistry* **2012**, *22*, 18268.

(34) Sangeetha, N. M.; Maitra, U. *Chemical Society Reviews* **2005**, *34*, 821.

(35) Somorjai, G. A.; Li, Y. *Proceedings of the National Academy of Sciences* **2011**, *108*, 917.

(36) Gong, J. P.; Osada, Y. In *High Solid Dispersions*; Cloitre, M., Ed.; Springer Berlin Heidelberg: Berlin, Heidelberg, 2010, p 203.

(37) Oogaki, S.; Kagata, G.; Kurokawa, T.; Kuroda, S.; Osada, Y.; Gong, J. P. *Soft Matter* **2009**, *5*, 1879.

(38) Huang, G.; Yu, Q.; Cai, M.; Zhou, F.; Liu, W. *Advanced Materials Interfaces* **2016**, *3*, n/a.

(39) Kurokawa, T.; Gong, J. P.; Osada, Y. *Macromolecules* **2002**, *35*, 8161.

(40) Sudre, G.; Hourdet, D.; Cousin, F.; Creton, C.; Tran, Y. *Langmuir* **2012**, *28*, 12282.

(41) Angelerou, M. G. F.; Sabri, A.; Creasey, R.; Angelerou, P.; Marlow, M.; Zelzer, M. *Chemical Communications* **2016**, *52*, 4298.

(42) Yamanaka, M.; Sada, K.; Miyata, M.; Hanabusa, K.; Nakano, K. *Chemical Communications* **2006**, 2248.

(43) Ikeda, S.; Hayashi, S.; Imae, T. *Journal of Physical Chemistry* **1981**, *85*, 106.

(44) Zana, R.; Guveli, D. *Journal of Physical Chemistry* **1985**, *89*, 1687.

(45) D'Archivio, A. A.; Galantini, L.; Gavuzzo, E.; Giglio, E.; Mazza, F. *Langmuir* **1997**, *13*, 3090.

(46) Thota, B. N. S.; Savyasachi, A. J.; Lukashev, N.; Beletskaya, I.; Maitra, U. *European Journal of Organic Chemistry* **2014**, *2014*, 1406.

(47) Roy, S.; Javid, N.; Sefcik, J.; Halling, P. J.; Ulijn, R. V. *Langmuir* **2012**, *28*, 16664.

(48) Li, J.; Fan, K.; Niu, L.; Li, Y.; Song, J. *Journal of Physical Chemistry B* **2013**, *117*, 5989.

(49) Hwang, D.; Lee, E.; Jung, J. H.; Lee, S. S.; Park, K.-M. *Crystal Growth & Design* **2013**, *13*, 4177.

(50) Segarra-Maset, M. D.; Nebot, V. J.; Miravet, J. F.; Escuder, B. *Chemical Society Reviews* **2013**, *42*, 7086.

(51) Lin, Q.; Sun, B.; Yang, Q.-P.; Fu, Y.-P.; Zhu, X.; Zhang, Y.-M.; Wei, T.-B. *Chemical Communications* **2014**, *50*, 10669.

(52) Xiong, M.; Wang, C.; Zhang, G.; Zhang, D. In *Functional Molecular Gels*; The Royal Society of Chemistry: 2014, p 67.

(53) Gareth, O. L.; Jonathan, W. S. *Nature Chemistry* **2009**, *1*, 437.

(54) Steed, J. W. *Chemical Society Reviews* **2010**, *39*, 3686.

(55) Piepenbrock, M.-O. M.; Lloyd, G. O.; Clarke, N.; Steed, J. W. *Chemical Communications* **2008**, 2644.

(56) Sun, X.; Du, Z.; Li, E.; Xin, X.; Tang, N.; Wang, L.; Yuan, J. *Colloids and Surfaces A: Physicochemical and Engineering Aspects* **2014**, *457*, 345.

(57) Sun, X.; Xin, X.; Tang, N.; Guo, L.; Wang, L.; Xu, G. *Journal of Physical Chemistry B* **2014**, *118*, 824.

(58) Raeburn, J.; Chen, L.; Awhida, S.; Deller, R. C.; Vatish, M.; Gibson, M. I.; Adams, D. J. *Soft Matter* **2015**, *11*, 3706.

(59) Lin, Y.; Li, L.; Li, G. *Carbohydrate Polymers* **2013**, *92*, 429.

(60) Lane, T.; Holloway, J. L.; Milani, A. H.; Saunders, J. M.; Freemont, A. J.; Saunders, B. R. *Soft Matter* **2013**, *9*, 7934.

(61) Woll, D. *RSC Advances* **2014**, *4*, 2447.

(62) Masson, E.; Ling, X.; Joseph, R.; Kyeremeh-Mensah, L.; Lu, X. *RSC Advances* **2012**, *2*, 1213.

(63) Dsouza, R. N.; Pischel, U.; Nau, W. M. *Chemical Reviews* **2011**, *111*, 7941.

(64) Cao, L.; Šekutor, M.; Zavalij, P. Y.; Mlinarić-Majerski, K.; Glaser, R.; Isaacs, L. *Angewandte Chemie International Edition* **2014**, *53*, 988.

(65) Hwang, I.; Jeon, W. S.; Kim, H.-J.; Kim, D.; Kim, H.; Selvapalam, N.; Fujita, N.; Shinkai, S.; Kim, K. *Angewandte Chemie International Edition* **2007**, *46*, 210.

(66) Yang, H.; Tan, Y.; Wang, Y. *Soft Matter* **2009**, *5*, 3511.

(67) Park, K. M.; Yang, J.-A.; Jung, H.; Yeom, J.; Park, J. S.; Park, K.-H.; Hoffman, A. S.; Hahn, S. K.; Kim, K. *ACS Nano* **2012**, *6*, 2960.

(68) Rowland, M. J.; Atgie, M.; Hoogland, D.; Scherman, O. A. *Biomacromolecules* **2015**, *16*, 2436.

(69) Appel, E. A.; Loh, X. J.; Jones, S. T.; Dreiss, C. A.; Scherman, O. A. *Biomaterials* **2012**, *33*, 4646.

(70) Yang, H.; Chen, H.; Tan, Y. *RSC Advances* **2013**, *3*, 3031.

(71) Oun, R.; Plumb, J. A.; Wheate, N. J. *Journal of Inorganic Biochemistry* **2014**, *134*, 100.

(72) Sollich, P. In *Molecular Gels: Materials with Self-Assembled Fibrillar Networks*; Weiss, R. G., Terech, P., Eds.; Springer Netherlands: Dordrecht, 2006, p 161.

(73) Raeburn, J.; Zamith Cardoso, A.; Adams, D. J. *Chemical Society Reviews* **2013**, *42*, 5143.

(74) Sueldo Occello, V. N.; de Rossi, R. H.; Veglia, A. V. *Journal of Luminescence* **2015**, *158*, 435.

(75) Xu, W.; Demas, J. N.; DeGraff, B. A.; Whaley, M. *Journal of Physical Chemistry* **1993**, *97*, 6546.

(76) Yang, H.; Bohne, C. *Journal of Physical Chemistry* **1996**, *100*, 14533.

(77) Zhang, H. T.; Li, R.; Yang, Z.; Yin, C.-X.; Gray, M. R.; Bohne, C. *Photochemical & Photobiological Sciences* **2014**, *13*, 917.

(78) Day, A.; Arnold, A. P.; Blanch, R. J.; Snushall, B. *Journal of Organic Chemistry* **2001**, *66*, 8094.

(79) Kim, J.; Jung, I.-S.; Kim, S.-Y.; Lee, E.; Kang, J.-K.; Sakamoto, S.; Yamaguchi, K.; Kim, K. *Journal of the American Chemical Society* **2000**, *122*, 540.

(80) Rekharsky, M. V.; Ko, Y. H.; Selvapalam, N.; Kim, K.; Inoue, Y. *Supramolecular Chemistry* **2007**, *19*, 39.

(81) Feng, Y.; Xue, S.-F.; Fan, Z.-F.; Zhang, Y.-Q.; Zhu, Q.-J.; Tao, Z. *Journal of Inclusion Phenomena and Macrocyclic Chemistry;* **2009**, *64*, 121.

(82) Christensen, J. J.; Izatt, R. M.; Wrathall, D. P.; Hansen, L. D. *Journal of the Chemical Society A: Inorganic, Physical, Theoretical* **1969**, 1212.

(83) Raghavan, S. R.; Cipriano, B. H. In *Molecular Gels: Materials with Self-Assembled Fibrillar Networks*; Weiss, R. G., Terech, P., Eds.; Springer Netherlands: Dordrecht, 2006, p 241.

(84) Almdal, K.; Dyre, J.; Hvidt, S.; Kramer, O. *Polymer Gels and Networks* **1993**, *1*, 5.

(85) Ross-Murphy, S. B. *Journal of Texture Studies* **1995**, *26*, 391.

(86) Kalyanasundaram, K.; Thomas, J. K. *Journal of the American Chemical Society* **1977**, *99*, 2039.

(87) Fuentealba, D.; Thurber, K.; Bovero, E.; Pace, T. C. S.; Bohne, C. *Photochemical & Photobiological Sciences* **2011**, *10*, 1420.

(88) Bohne, C. In *Supramolecular Photochemistry*; John Wiley & Sons, Inc.: 2011, p 1.

(89) Weiss, R. G.; Térech, P. In *Molecular Gels: Materials with Self-Assembled Fibrillar Networks*; Weiss, R. G., Terech, P., Eds.; Springer Netherlands: Dordrecht, 2006, p 1.

(90) Hildebrand, A.; Neubert, R.; Garidel, P.; Blume, A. *Langmuir* **2002**, *18*, 2836.

(91) In *Principles of Fluorescence Spectroscopy*; Lakowicz, J. R., Ed.; Springer US: Boston, MA, 2006, p 797.

(92) Koynov, K.; Butt, H.-J. *Current Opinion in Colloid & Interface Science* **2012**, *17*, 377.

(93) Brito-Silva, A. M.; Sobral-Filho, R. G.; Barbosa-Silva, R.; de Araújo, C. B.; Galembeck, A.; Brolo, A. G. *Langmuir* **2013**, *29*, 4366.

(94) Brinker, C. J.; Scherer, G. W. *Sol-gel Science: The Physics and Chemistry of Sol-gel Processing*; Gulf Professional Publishing, 1990.

(95) Hess, S. T.; Huang, S.; Heikal, A. A.; Webb, W. W. *Biochemistry* **2002**, *41*, 697.

(96) Yu, J.; Lammi, R.; Gesquiere, A. J.; Barbara, P. F. *Journal of Physical Chemistry B* **2005**, *109*, 10025.

(97) Widengren, J.; Schwille, P. *Journal of Physical Chemistry A* **2000**, *104*, 6416.

(98) Good, R. J.; Koo, M. N. *Journal of Colloid and Interface Science* **1979**, *71*, 283.

(99) Zhou, Y.-N.; Li, J.-J.; Zhang, Q.; Luo, Z.-H. *AIChE Journal* **2014**, *60*, 4211.

(100) Otsuka, T.; Maeda, T.; Hotta, A. *Journal of Physical Chemistry B* **2014**, *118*, 11537.

(101) Collins, K. D.; Washabaugh, M. W. *Quarterly Reviews of Biophysics* **1985**, *18*, 323.

(102) Lo Nostro, P.; Ninham, B. W. *Chemical Reviews* **2012**, *112*, 2286.

(103) Lo Nostro, P.; Ninham, B. W.; Milani, S.; Lo Nostro, A.; Pesavento, G.; Baglioni, P. *Biophysical Chemistry* **2006**, *124*, 208.

(104) Becker, T.; Yong Goh, C.; Jones, F.; McIldowie, M. J.; Mocerino, M.; Ogden, M. I. *Chemical Communications* **2008**, 3900.

(105) Nebot, V. J.; Ojeda-Flores, J. J.; Smets, J.; Fernández-Prieto, S.; Escuder, B.; Miravet, J. F. *Chemistry – A European Journal* **2014**, *20*, 14465.

(106) Roy, S.; Javid, N.; Frederix, P. W. J. M.; Lamprou, D. A.; Urquhart, A. J.; Hunt, N. T.; Halling, P. J.; Ulijn, R. V. *Chemistry – A European Journal* **2012**, *18*, 11723.

(107) Ganong, W. F.; Barrett, K. E. *Review of medical physiology*; Appleton & Lange Norwalk, CT, 1995.

(108) Watkins, A. R. *The Journal of Physical Chemistry* **1974**, *78*, 2555.

(109) Collins, K. D. *Biophysical Journal* **1997**, *72*, 65.

(110) Haynes, W. M. In *CRC Handbook of Chemistry and Physics, 94th Edition*; CRC Press: 2013, p 2668.

(111) Gu, J. J.; Hofmann, A. F.; Ton-Nu, H. T.; Schteingart, C. D.; Mysels, K. J. *Journal of Lipid Research* **1992**, *33*, 635.

(112) In *Principles of Fluorescence Spectroscopy*; Lakowicz, J. R., Ed.; Springer US: Boston, MA, 2006, p 277.

(113) Li, R.; Carpentier, E.; Newell, E. D.; Olague, L. M.; Heafey, E.; Yihwa, C.; Bohne, C. *Langmuir* **2009**, *25*, 13800.